

**TOTAL DISC REPLACEMENT:
Periprosthetic Wear Debris and Biological Responses**

A Dissertation

Submitted to the Faculty of

Drexel University

By

Sai Y. Veruva

In Partial Fulfillment of the

Requirements for the degree of

Doctor of Philosophy

January 2016

© Copyright 2016.

Sai Y. Veruva. All Rights Reserved.

Dedication

To my engineering role models,

My father, Eswar Rao Veruva

And my grandfather, Sesa Rao Katragadda

Acknowledgements

I would like to express my immense gratitude to my academic co-advisors, Dr. Steven M. Kurtz and Dr. Marla J. Steinbeck. Dr. Kurtz, through his depth of expertise and reach in the orthopedics research community, provided me with invaluable mentorship and opened doors to connect me with the greatest and finest in the field of clinical orthopedics. I'm indebted to his wisdom and his definitive approach to helping me on my formative scientific journey. Dr. Steinbeck, who is also extremely knowledgeable in this field and beyond, complimented this experience with exceptional guidance, care and patience, all while conveying the spirit of adventure in regard to research and scholarship. I'm grateful for her fierce belief in me and nurturing my work to near perfection and unwittingly kicking the novice idea out of my head that I could have been done with this dissertation 6 months early. Without their supervision, constant help, and push to strive for achieving high level research, this dissertation would just not have been possible.

I would also like to acknowledge and express my deep appreciation to my committee members, Dr. Fred Allen, Dr. Theresa Freeman, Dr. Uri Hershberg and Dr. Kara Spiller, for their many intellectual contributions, guidance and resources to perform innovative and insightful research. I am fortunate to have such a dedicated group encouraging and enabling me to explore new techniques and conduct quality work.

Special thanks to the participating clinicians and surgeons, particularly Dr. Jorge Isaza and Dr. Todd Lanman, whose collaborations with the Implant Research

Center were instrumental in procuring the implants and tissues required to perform this research.

I am also grateful to my peers and lab mates for the stimulating discussions, constructively challenging my ideas, the sleepless nights of working together before deadlines, and all the fun we have had over the years.

Last, but certainly not the least, I would like to thank my largest pillar of strength: my family. My parents, Eswar and Durga Veruva, and my sister and brother-in-law, Teju and Rajiv Shukla, have showered me with unconditional love and support, and kept me sane through what initially seemed like an endless journey. At the end of this journey, Nikita Mathur, you deserve a special mention and a big thank you for always having a smile for me and keeping the “quantum of solace” even when I have been missing in action on many an occasion on the account of this dissertation.

“Somewhere, something incredible is waiting to be known.”

— Carl Edward Sagan

TABLE OF CONTENTS

	Page
List of Tables	xiv
List of Figures	xvi
List of Abbreviations.....	xxiii
ABSTRACT	1
 CHAPTER 1: Introduction & Background	
1.1 Low Back Pain & Surgical Fusion	4
1.2 Total Disc Replacement: An Alternative for DDD?	5
1.3 The Historical CHARITÉ Disc Design & Early Retrieval Studies	6
1.4 The Modern TDR: ProDisc-L & the new CHARITÉ	8
1.5 TDR Complications & Neuropathic Pain	9
1.6 What We Know About Lumbar Pain from the Degenerative Disc	11
1.7 Overview of Thesis & Specific Aims	15
1.7.1 Aim I	16
1.7.2 Aim II	17
1.7.3 Aim III.....	18

1.8	References	19
-----	------------------	----

**CHAPTER 2: A Systematic Review of Design & Biomaterial Factors Affecting
the Clinical Wear Performance of Total Disc Replacements**

2.1	Abstract	28
2.2	Introduction	29
2.3	Search Strategy & Criteria	31
2.4	Results	38
	2.4.1. Lumbar Total Disc Replacement	38
	2.4.2. Cervical Total Disc Replacement	39
2.5	Discussion	41
2.6	Limitations	48
2.7	References	49

**CHAPTER 3: Retrieval Analyses of Contemporary Lumbar TDRs &
Periprosthetic Tissue Responses**

3.1	Abstract	52
3.2	Introduction	53
3.3	Materials & Methods	56
	3.3.1 Tissue Collection & Patient Clinical Information	56

3.3.2 Implant Retrieval Analysis	59
3.3.3 Tissue Preparation and Histological Analysis	59
3.3.4 Wear Particle Characterization	61
3.3.5 Statistical Analysis	63
3.4 Results	64
3.4.1 Device Retrieval Analysis for Contemporary L-TDRs	64
3.4.2 UHMWPE Wear Debris from Contemporary L-TDRs & Biological Tissue Responses	67
3.4.3 Wear Particle Number, Size & Shape for Contemporary L-TDRs ...	72
3.4.4 Comparison of Particle Characteristics to MoP Historical L-TDRs.	76
3.5 Discussion	76
3.6 Limitations	82
3.7 References	83

CHAPTER 4: Periprosthetic Immune Response to UHMWPE Wear Particles and Inflammatory Factor Production in the Lumbar Spine

4.1 Abstract	87
4.2 Introduction	88
4.3 Materials & Methods	90

4.3.1 Tissue Collection & Patient Information	91
4.3.2 Tissue Preparation	91
4.3.3 Wear Particle Analysis	93
4.3.4 Immunohistochemistry	93
4.3.5 Imaging & Analysis	94
4.3.6 Statistical Analysis	96
4.4 Results	96
4.4.1 Mean Inflammatory Factor Expression in Patient Tissues	96
4.4.2 Mean Inflammatory Factor Expression in Tissues from TDR Patients and Associations with Patient Clinical and Implant Factors	98
4.4.3 Correlations between the Amount of Wear Debris Amount and Inflammatory Factors in TDR Tissues.....	100
4.4.4 Correlations between Wear Debris Characteristics and Inflammatory Factors in TDR Tissues.....	102
4.4.5 Correlations between Wear Debris, Inflammatory Factors and the Number of Macrophages	104
4.4.6 Correlations of NGF and Substance P with Other Factors	107
4.5 Discussion	108
4.6 References	112

CHAPTER 5: Investigations into the Pathogenesis of Inflammatory Particle Disease in the Lumbar Spine based on Localized Changes in Vascularization & Innervation

5.1	Abstract	116
5.2	Introduction	117
5.3	Materials & Methods	119
5.3.1	Tissue Selection & Patient Information	119
5.3.2	Tissue Preparation & Immunohistochemistry	120
5.3.3	Imaging & Analysis	121
5.3.4	Statistical Analysis	123
5.4	Results	123
5.4.1	Correlations between the Total Number of Blood Vessels and Inflammatory-Mediated Pain Factors in TDR Tissues	123
5.4.2	Co-localization of Factors with Blood Vessels	126
5.4.3	Correlations for Blood Vessel Number with Inflammatory-mediated Pain Factor Expression and Macrophages in Tissues with Varying Levels of Vascularity	127
5.5	Discussion	130

5.6	References	132
-----	------------------	-----

CHAPTER 6: Rare and Abnormal Biological Complications of Osteolysis after

Total Disc Replacement: A Case Series

6.1	Abstract	136
6.2	Introduction	137
6.3	Materials & Methods	139
6.3.1	Patients and Clinical Information	139
6.3.2	Implant Retrieval Analysis	139
6.3.3	Tissue Preparation and Histological Analysis	139
6.4	Case 1	140
6.4.1	Device Retrieval Analysis	143
6.4.2	Tissue Analysis	144
6.5	Case 2	145
6.5.1	Device Retrieval Analysis	147
6.5.2	Tissue Analysis	148
6.6	Discussion	150
6.7	References	153

CHAPTER 7: Conclusions & Future Directions

7.1	Conclusions	155
7.2	Implications & Future Directions	158
7.2.1	Therapeutic Strategies for Treatment	158
7.2.2	Cervical Total Disc Replacement	162
7.3	References	163
Appendix	166
1.	MATLAB Scripts	166
2.	ImageJ Macros	168
3.	Image-Pro Plus Macro	170

LIST OF TABLES

Table	Page
Table 2-1. Summary of contemporary lumbar total disc replacements	32
Table 2-2. Summary of contemporary cervical total disc replacements	33
Table 2-3. Summary of findings from 14 published studies of retrieved implants, tissues, & fluids from lumbar total disc replacements	43
Table 2-4. Summary of findings from eight published studies of retrieved implants and tissues from cervical total disc replacements	44
Table 3-1. Clinical information of MoP L-TDR retrievals	58
Table 3-2. Modified Oxford scoring criteria for grading biological responses in periprosthetic tissues of L-TDRs	61
Table 3-3. Histologic evaluation and mean scores of retrieved tissues with wear debris	69
Table 3-4. Histologic evaluation & mean scores of retrieved tissues w/out wear	73
Table 3-5. UHMWPE particle number and characteristics from tissues with wear debris	75
Table 3-6. Comparing UHMWPE particle number and characteristics in patients with wear debris	75
Table 4-1. Clinical Information of Patient Cohorts	92

Table 5-1. Tissue Selection and Clinical Information for TDR Patients	120
Table 6-1. Clinical information for the hybrid case 1 & non-hybrid case 2	142
Table 6-2. An overview of tissue morphology for the two cases.....	146

LIST OF FIGURES

Figure	Page
Figure 1-1. (A) Anteroposterior and (B) lateral radiographs of a successfully implanted CHARITÉ TDR in the lumbosacral spine	7
Figure 1-2. (A) CHARITÉ mobile-bearing artificial disc; (B) ProDisc-L fixed-bearing artificial disc	9
Figure 2-1. A flow diagram demonstrates the systematic review protocol	37
Figure 3-1. Tissues are harvested from annular regions during L-TDR revision surgery	56
Figure 3-2. Sagittal CT scan illustrating implant subsidence at the L4 level on the right side of the vertebra from a fixed-bearing L-TDR patient (BHSP023)	57
Figure 3-3. Representative images of L-TDR periprosthetic tissues with wear particles under polarized light (left) followed by thresholding for UHMWPE particles in MATLAB (right)	62
Figure 3-4. Patient tissues with detectable wear debris had a heterogeneous distribution of particles as illustrated by significant debris in the lateral tissue from patient BHSP027 (left), but no debris in other regions of same tissue (right)	64
Figure 3-5. Representative fixed-bearing L-TDR retrieval components (top). All fixed-bearing UHMWPE cores showed evidence of burnishing (green arrow) and	

mild abrasive scratching (blue arrow). Impingement was noted in two patients and the respective components evidenced plastic deformation (red arrow) 65

Figure 3-6. Representative fixed-bearing retrieval with impinged regions on both endplates (black arrows). SEM images showed the impinged region on the metallic plate (lower right) has a smooth surface compared to the unimpinged region (upper right) 66

Figure 3-7. Representative mobile-bearing L-TDR retrieval components (top). Two of four patients with mobile-bearing UHMWPE cores showed evidence of burnishing, pitting (green arrow). Minor unidirectional scratches were noted on endplates from all patients (red arrow) 67

Figure 3-8. Transmitted light images (left) and polarized microscopy (middle) of tissue sections revealed the presence of UHMWPE wear and corresponding macrophage infiltration; particles were characterized using a MATLAB threshold (right) 68

Figure 3-9. Wright Giemsa and Prussian blue stains were used to identify inflammatory cells and hemosiderin deposits, respectively. There were macrophages, plasma cells, and lymphocytes with hemosiderin deposits in tissues around fixed-bearing L-TDRs (left), but only macrophages in mobile-bearing L-TDR tissues (middle). There was no inflammation or hemosiderin present in control tissue (right) obtained from primary surgery (Original magnification x 400; inset, x 1000) 70

Figure 3-10. Representative fixed-bearing L-TDR tissue images showed increased vascularization (top left) in tissues with wear debris and necrosis (bottom left) in tissues without wear debris. Mobile-bearing L-TDR tissues had lower vascularization (top right) in tissues with wear debris and a mix of moderate vascularization and isolated necrosis (bottom right) in tissues without wear debris (Original magnification, x 400)	72
Figure 3-11. Equivalent circular diameter size distribution for wear particles in fixed- and mobile-bearing L-TDR tissues	74
Figure 3-12. Aspect ratio distribution for wear particles in fixed- and mobile-bearing L-TDR tissues	74
Figure 3-13. Circularity distribution for wear particles in fixed- and mobile-bearing L-TDR tissues	74
Figure 4-1. Representative image of a tissue with DAB deposition after immunohistochemistry (left) followed by thresholding for DAB-stained pixels in MATLAB (right)	95
Figure 4-2. Mean expression of inflammatory factors in tissues for TDR, DDD and normal IVD patients	97
Figure 4-3. Mean expression of inflammatory factors in TDR tissues with (n=14) and without (n=16) wear debris, DDD and normal patient tissues	97
Figure 4-4. Gender (A) and implant complications (B) showed no significant association with inflammatory factors	99

Figure 4-5. Implantation time showed no significant association to factor expression	99
Figure 4-6. Representative tissue sections with wear debris (left, polarized light) and TNF α immunostaining (right). The blue arrows indicate wear particles and the red arrow a macrophage surrounded by TNF α expressing fibroblasts	100
Figure 4-7. UHMWPE wear debris correlated with TNF α & IL-1 β	101
Figure 4-8. UHMWPE wear debris correlated with VEGF	101
Figure 4-9. UHMWPE wear debris correlated with NGF and SP	102
Figure 4-10A. Particle ECD means did not correlate to any factor expression.....	103
Figure 4-10B. Particle aspect ratio means correlated with TNF α but no other factors.....	103
Figure 4-10C Particle circularity means did not correlate to any factor expression	103
Figure 4-11. Representative tissue sections with wear debris (left) and CD68+ macrophages (right). The blue arrows indicate wear particles and the red arrows macrophage	104
Figure 4-12. UHMWPE wear debris strongly correlated with CD68+ macrophages	105
Figure 4-13. CD68+ cells correlated with TNF α and IL-1 β	105
Figure 4-14. CD68+ cells correlated with VEGF, but not PDGFbb	106
Figure 4-15. CD68+ cells correlated with NGF and substance P	106

Figure 4-16. Representative inflamed tissue samples from serial sections immunostained for NGF and substance P (left) that matched proportionally with inflammatory and vascularization factors (right). The red arrows indicate a macrophage positive for the respective immunostain	107
Figure 4-17. Spearman Rho correlations for NGF & SP	108
Figure 5-1. Blood vessel number correlated with VEGF and PDGFbb	124
Figure 5-2. Blood vessel number correlated with TNF α and IL-1 β	125
Figure 5-3. Blood vessel number correlated with NGF and substance P	125
Figure 5-4. Representative images of TDR tissues immunostained for PDGFbb (left), NGF (middle) and substance P (right) illustrating co-localization of all three factors to blood vessels (black arrows)	126
Figure 5-5. Percentage decrease of all six factors in periprosthetic tissues when blood vessels were masked	127
Figure 5-6. Blood vessel number and factor expression per image in (A) low and (B) highly vascularized patient tissues	128
Figure 5-7. Blood vessel number and macrophage number per image in low vascularized (A) and highly vascularized (B) patient tissues	129
Figure 6-1. Sagittal (A) and axial (B) CT scans from case 1 illustrating discogenic herniation and osteolytic cysts at inferior L4 and superior L5. The axial scan also	

shows that there may be facet osteophytes and nerve root compression at the
foramen 141

Figure 6-2. Retrieved ProDisc-L TDR, 5 years after insertion. The device was
damaged during explantation. While it is unclear as to whether the polyethylene
core was damaged in-vivo, there is no evidence of wear mechanisms on the end-
plates 143

Figure 6-3. Bony tissue from case 1 stained with H&E (100X) showed necrotic bone
with empty osteocyte lacunae (arrow) and necrotic marrow 144

Figure 6-4. Sagittal (A) and axial (B) CT scans from case 2 showing L4 subsidence
on the right side of the vertebra and one large osteolytic cyst in L5. Smaller
osteolytic formations are also evident at superior L5 145

Figure 6-5. Retrieved ProDisc-L TDR, 3 years after insertion. Note the signs of
impingement on both endplates (arrows). The impinged region on the metallic
plate (lower right) has a smooth surface compared to the unimpinged region
(upper right) 147

Figure 6-6. Histology of inner-cyst tissue with H/E stain showing mixed
inflammation throughout. Inset A shows presence of macrophage-ingested metallic
debris (H/E, 400X). Inset B shows presence of lymphocytes in the tissue (Wright-
Giemsa, 400X) 148

Figure 6-7. Titanium alloy and cobalt-chrome particles (arrows) were confirmed
by use of backscatter scanning electron microscopy with elemental dispersive

spectroscopy. Analysis of a region of interest (square) evidenced cobalt as the most abundant metal visualized by scanning electron microscopy 149

Figure 6-8. An H/E stained region of left-cyst tissue was stained with Wright-Giemsa (A, 1000X) and observed under polarized light (B, 1000X), showing evidence of mixed inflammation and polyethylene particles, respectively 150

LIST OF ABBREVIATIONS

ASD	Adjacent Segment Disease
C-TDR	Cervical total disc replacement
CoCr	Cobalt-Chromium
DDD	Disc Degenerative Disease
DOF	Degrees of freedom
ESEM	Environmental scanning electron microscope
FDA	US Food and Drug Administration
FTIR	Fourier transform infrared spectroscopy
GUR	Granular, UHMWPE and Ruhrchemie
IL-1 β	Interleukin-1 β
IVD	Intervertebral Disc
L-TDR	Lumbar total disc replacement
MOM	Metal-on-metal
MOP	Metal-on-polyethylene
NO	Nitric Oxide
NGF	Nerve Growth Factor
PCU	Polycarbonate-urethane

PDGFbb	Platelet-derived growth factor-BB
PEEK	Polyether ether ketone
ROM	Range of motion
SEM	Scanning electron microscope
TDR	Total disc replacement
THR	Total hip replacement
Ti	Titanium
TJR	Total joint replacement
TKR	Total knee replacement
TNF α	Tumor necrosis factor alpha
UHMWPE	Ultra-high-molecular-weight polyethylene
VEGF	Vascular endothelial growth factor

ABSTRACT

Total disc replacement (TDR) was clinically introduced as an alternative to spinal fusion to relieve back pain, maintain mobility of the spine and eliminate the adverse side effects of fusion. More recently, gamma-inert-sterilized ultra-high molecular weight polyethylene (UHMWPE) TDR cores were introduced to replace historical gamma-air-sterilized cores in an effort to reduce UHMWPE wear debris and inflammation. In this study, both implant and periprosthetic tissue retrievals from patients with gamma-inert-sterilized TDRs were evaluated for *in vivo* performance and biological responses, respectively. As pain was the primary revision reason for all patients, the contributions of implant-related damage and tissue responses to the development of pain were also a focus of this investigation.

After analyzing implants and tissues for 11 TDR patients, detectable UHMWPE wear debris was identified with corresponding macrophage infiltration in six patients with associated implant damage. Neither damage nor TDR bearing design, fixed vs mobile, influenced the amount, size and shape characteristics of wear particles. However, comparisons to a retrieval study of historical devices indicated that the number of UHMWPE particles generated from gamma-inert-sterilized devices were decreased by 99% ($p=0.003$) and were 50% rounder ($p=0.003$), confirming the improved wear resistance of the newer devices. Accordingly, periprosthetic tissue reactions were also substantially reduced.

Prospective immunohistochemical investigations for these devices showed, for the first time, that UHMWPE wear-debris induced tissue reactions in the human

lumbar spine can be linked to inflammation. First, inflammatory factors were elevated in TDR periprosthetic tissues (n=30) when compared to disc degenerative disease (DDD) patient tissues (n=3) from primary surgery and disc tissues (n=4) from normal autopsy patients with no history of lower back pain. The mean percent area of production for vascular endothelial growth factor (VEGF) (p=0.04), interleukin-1beta (IL-1 β), (p=0.01) and substance P (p=0.01) were significantly higher in TDR tissues when compared to tissues obtained from DDD patients. Although platelet derived growth factor-bb (PDGFbb) p=0.14), tumor necrosis factor-alpha (TNF α) (p=0.06) and nerve growth factor (NGF) (p=0.19) were also increased in the TDR patient tissues, these increases were not significant. Compared to normal disc tissues, the mean percent area for all six factors was statistically increased in TDR tissues (at least p<0.05). Interestingly, no statistical differences were observed between DDD and normal disc tissues. Next, our studies showed that TNF α , IL-1 β , VEGF, NGF and substance P strongly correlated with the number of wear particles and also the number of macrophages for the TDR patient group (at least p<0.05 for all). Finally, the pro-inflammatory/pain factors, TNF α and IL-1 β , and the vascularization factors, VEGF and PDGFbb, significantly correlated with the presence of the neural innervation and hypersensitization agents, NGF and substance P (p<0.01 for all). These findings suggest not only the presence of inflammatory reactions, but the presence of factors that can directly and indirectly contribute to the pain sensitivity.

In addition to wear-debris and subsequent inflammation, increased vascularization was another key histomorphological change observed in the TDR tissues that may be involved in the pathogenesis of particle disease. In brief, the

ingrowth of blood vessels may be providing a conduit for nociceptive innervation. Studying vascularity in revision tissues showed the total number of blood vessels was significantly associated with $\text{TNF}\alpha$, $\text{IL-1}\beta$, VEGF, PDGFbb, NGF and substance P (at least $p < 0.05$ for all), suggesting an interrelation between vascular changes and inflammatory-mediated responses. Furthermore, analysis at the local level revealed the innervation/pain factors, NGF and substance P, were predominantly localized to vascular channels, suggestive of nerve ingrowth and potential neural-maladaptive plasticity at periprosthetic sites. Lastly, comparing blood vessel number with factor expression and macrophage number in individual images obtained from tissue sections with low and high vascularity suggested a temporal link between $\text{TNF}\alpha$, macrophages and angiogenesis. Taken together, elucidating the pathogenesis of inflammatory particle disease will provide information needed to identify potential therapeutic targets and treatment strategies to mitigate pain.

CHAPTER 1

Introduction & Background

1.1 Low Back Pain & Surgical Fusion

Low back pain is reported to be the leading cause of disability worldwide according to the 2010 Global Burden of Disease Study [48]. It is also the leading cause of activity limitation and work absence, resulting in a heavy economic burden on individuals, communities and governments [2, 74]. Degenerative disc disease (DDD) is one pathology known to result in chronic back pain due to the biomechanical instability caused by loss of disc height, disc dehydration and/or annular tears [18, 24, 82]. When conservative treatments such as pain medications and physical therapy fail, discectomy or surgical fusion are implemented to mitigate pain for patients with DDD. The number of spinal fusions performed each year is continually increasing [14], with an estimated 380,000 thoracolumbar fusions performed in 2013 according to the 2013 Spinal Surgery Update by the Millennium Research Group. However, the clinical success rate of lumbar fusion is variable ranging from 16-95%, as long-term results are poor due to increased risk of complications [7, 18, 80]. One noteworthy and common complication is adjacent segment disease (ASD) [23, 54]. ASD is the associated degeneration of adjacent intervertebral discs (IVDs) due to abnormal loading and increased mobility of IVDs

above or below the fused degenerated disc. Definitive treatment for this complication is a topic of continuing research, but disc replacement has been regarded as a potential solution [87].

1.2 Total Disc Replacement: An Alternative Treatment for DDD?

Following the encouraging short term results of Fernstrom implantation of a steel ball in place of an IVD in the 1960s [15], total disc replacement (TDR) was conceived as an alternative to spinal fusion and its resulting complications. TDR involves the removal of a damaged or degenerating IVD and replacement with an artificial device. In theory, implantation of a mobile and potentially shock-absorbing component to replace a degenerating disc will not only restore disc height and alleviate pain, but also preserve spinal segmental motion and transmit/absorb load between vertebral bodies. In contrast to fusion, this preservation of mobility has been speculated to prevent ASD since excess strain at adjacent vertebral levels is theoretically diminished [18, 46]. In addition, other complications that may arise from fusion such as the morbidity associated with bone graft harvest, stiffening of the lumbar spine, sagittal balance misalignment, and nonunion are all avoided with disc arthroplasty [33, 47, 62].

Several studies have demonstrated clinical success of disc arthroplasty in comparison to fusion for short and mid-term results [46, 82, 93]. Despite this evidence, fusion is still regarded as the “gold standard” for surgical treatment of DDD, and only 24,579 cervical and lumbar disc replacements were performed in 2013 (Millennium Research Group). Roughly 10 years have passed since TDRs were

approved by the Food and Drug Administration (FDA) for use in the US, but the excitement surrounding TDR technology has been tempered due to limited long-term data, which is needed to convince insurance companies to cover the increased cost of this surgery. Thus, it is crucial to pin-point any long-term pitfalls of motion preservation surgery and understand successful features as well as failure modes of both contemporary and emerging designs of artificial discs to further improve the technology.

1.3 The Historical CHARITÉ Disc Design & Early Retrieval Studies of Wear Debris

While Fernstrom's steel spheres and many early artificial disc designs receded from clinical use soon after their introduction, the CHARITÉ artificial disc design has been used extensively since its development in the 1980s, with few changes to design and biomaterials over the past 2 decades [34]. The SB CHARITÉ III was the third iteration of the original device that became commercialized in 1987 by Waldemar Link GmbH & Co. The lumbar TDR (L-TDR) design adapted biomaterials and design principles based on successful total joint replacement (TJR) designs. The original L-TDR incorporated two cobalt-chromium (CoCr) metallic endplates that were fixed to the superior/inferior vertebrae, and articulated against a mobile polymer core made of ultra-high molecular weight polyethylene (UHMWPE), which was gamma-air-sterilized. The design features were iconic for "historical" metal-on-polyethylene (MOP) L-TDRs. The clinical performance of this

disc design was reported to result in good to excellent clinical outcomes based on the alleviation pain and preservation of motion (Figure 1-1) [13, 39, 46, 66].

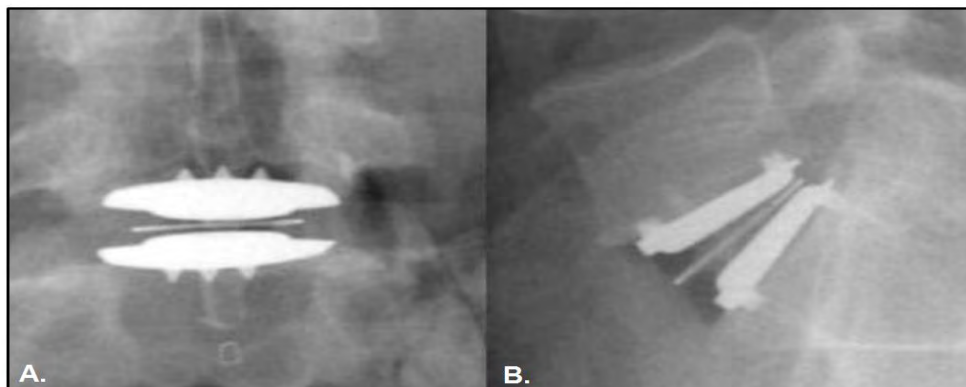


Figure 1-1. (A) Anteroposterior and (B) lateral radiographs of a successfully implanted CHARITÉ TDR in the lumbosacral spine.

While MOP designs have proven to be relatively successful in TJR, UHMWPE prosthetic wear debris generation is a clinically relevant complication that can ultimately result in osteolysis and aseptic loosening [28, 29]. Wear debris generation and osteolysis were initially thought to be negligible in anterior column of the lumbar spine due to the decreased sliding distance in MOP TDRs compared to total hip and total knee arthroplasty [40, 41]. However, retrieval studies of original/historical TDRs with gamma-air-sterilized UHMWPE cores demonstrated wear of the UHMWPE core, along with three rare cases of osteolysis in the lumbar spine [37, 78, 85]. Additionally, both submicron (0.05-2.0 μm) and large UHMWPE wear particles ($\geq 2.05 \mu\text{m}$) were present in periprosthetic tissues from historical TDRs, and these particles were associated with a chronic innate inflammatory response [57, 58]. TDR wear particles had a size range that was similar to that observed in revision tissues from total knee replacements (TKRs), however the majority were smaller than 6 μm as seen in revision tissues from total

hip replacements (THRs) [57]. Furthermore, the extent of impingement of the implant positively correlated with increased submicron wear debris and biological/inflammatory activity of these particles [4]. Collectively, these studies and others have established the clinically relevant complication of UHMWPE core wear for the historical TDRs [36, 38, 56, 83, 84], which served as an impetus for improving TDR bearing surface materials and designs.

1.4 The Modern TDR: ProDisc-L & the new CHARITÉ

The growing field of artificial disc replacement includes a broad range of designs and a heterogeneous assortment of biomaterials, but the most commonly employed L-TDRs have relied on developing better MOP devices [86]. Modern MOP devices, such as the ProDisc-L and CHARITÉ (re-modeled in 2004), incorporate conventional polyethylene cores which are fabricated with gamma-inert-sterilized UHMWPE GUR 1020 resin, designed to improve oxidation resistance and thus enhance the wear performance of the cores. While both devices were approved by the FDA and in clinical use for several years, the CHARITÉ was discontinued in 2011 as their manufacturer, Synthes, was acquired by the ProDisc-L developer, DePuy. Today, the ProDisc-L remains as the only lumbar TDR in the present US market, however there is an extensive clinical history database for both devices as tens of thousands of people have received these devices.

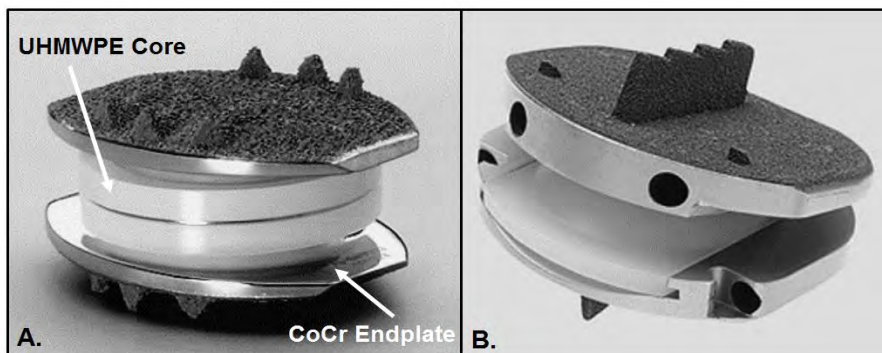


Figure 1-2. (A) CHARITÉ mobile-bearing artificial disc; (B) ProDisc-L fixed-bearing artificial disc.

The biomaterials used in the fabrication of the ProDisc-L prosthesis are quite similar to the CHARITÉ, specifically a conventional UHMWPE core and two CoCr endplates, plasma-coated on the outside with titanium. However, unlike the mobile-bearing CHARITÉ, the core of ProDisc-L is fixed via a locking mechanism into the inferior endplate, thus allowing relative motion only between the core and the superior endplate (Figure 1.2) [34]. To the author's knowledge, no studies have evaluated implant wear or periprosthetic tissue reactions for contemporary MOP L-TDRs. Additionally, it remains unclear whether TDR design will influence the generation of UHMWPE particles and the associated chronic inflammatory response.

1.5 TDR Revision, Complications & Pain

TDR revision surgery can be a dangerous procedure due to the difficulty that is involved in retrieving the prosthesis that is adhered or in close proximity to great vessels and nerve plexus [82]. Nevertheless, revision cases are growing as TDRs are becoming more widely used. While TDR technology provides an alternative treatment approach to fusion, new operative techniques unfortunately mean new complications. However, many complications arising from TDRs that require

revision surgery result from iatrogenic causes such as inappropriate indications, poor implantation technique and malpositioning of the implant [5]. Implant subsidence into the vertebral body is a common problem that could potentially result from inadequate determination of preoperative bone quality as TDR contraindications include osteophenic/osteoporotic bones [26]. Other complications of poor implantation that result in revision surgeries include device migration, extrusion, or dislodgement that may ultimately result in spinal cord compression, causing nerve irritation or vascular impedance. A malpositioned prosthesis can cause foraminal narrowing and compromise the dorsal root ganglion or nerve root, thereby resulting in radiculopathy and excruciating pain. Adding to these complications, positional changes of the implant *in vivo* can also lead to wear debris generation from unintended contact between device components.

Pain is the primary reason for TDR revision, but iatrogenic damage is not always the cause. Periprosthetic wear debris generation in artificial disc replacement has recently emerged as a clinically relevant complication that may lead to a painful inflammatory response similar to what has been observed for some TJRs [20, 22]. Studies suggest there may be a functional link between the innate immune response, and neurological changes that ultimately result in the generation of peripheral pain [75, 94]. Specifically, activated macrophages have been reported to contribute to experimental pain states by releasing factors such as tumor necrosis factor- α (TNF α), interleukin-1 β (IL-1 β), IL-8, nerve growth factor (NGF), nitric oxide (NO) and prostanoids [43, 64, 76]. However, the role of wear-debris-induced inflammation and subsequent mediation of pain post-spinal arthroplasty remains

unknown. Thus, investigating wear debris and the resulting biological responses will be invaluable in understanding some of the underlying mechanisms of pain, which can then be targeted to preserve or extend the life-time of the implant.

1.6 What We Know About Lumbar Pain from the Degenerative Disc

Much of what is known about the pathological states that can contribute to the mediation of pain in the lumbar spine is derived from the large body of research comparing the normal disc to degenerative states. The normal intervertebral disc is comprised of three regions that are morphologically distinct: the inner gelatinous nucleus pulposus (NP), the outer annulus fibrosis (AF) and cartilaginous endplates. While the adult human NP is completely avascular and aneural, a relatively low number of small blood vessels and nerve fibers are found in the very outer regions of the AF and endplates [11, 63, 67, 92]. The capillaries present in these regions provide nutrients to cells within the disc through diffusion-facilitated fluid transport that occurs from normal movements. During movement compressive loading causes water in the NP to extrude metabolic waste products from cells towards the blood vessels and the osmotic potential of the nucleus draws back nutrients into the inner disc. However, the distance between NP cells and the nearest blood vessel can be as much as 8 mm, resulting in a nutrient- and oxygen- poor environment [30, 81]; this hostile environment is reflected in significantly lower cell densities and metabolic activities than other cartilaginous tissues. The small existing body of NP cells regulate homeostatic turnover of the extracellular matrix and any imbalance in the

degradative/synthetic processes can contribute to loss of tissue integrity and degenerative conditions.

Disc degeneration is characterized by not only the overall breakdown of the extracellular matrix, but also changes in resident cell number, phenotype and behavior. These changes can contribute to inflammatory-mediated discogenic pain (inflammatory changes in the disc that influence the nervous system by stimulation of nociceptors in the AF) and/or pain caused by the physical biomechanical instability of the spine leading to disc herniation and impingement of nerve roots [8, 21, 91]. The loss of proteoglycans and overall breakdown of matrix is reflected in the poor reparative capacity of the disc. The breakdown of the matrix surrounding the cells ultimately results in inflammation, the replacement of NP with disorganized scar and granulated tissue [55]. The reparative effort of AF cells in response to matrix degeneration and tears/fissures also causes inflammation, scarring and promotes neovascularization [16, 17]. This process has been associated with an infiltration of inflammatory cells, as resident macrophages are not present [6, 17]. Koike and colleagues have found correlations that suggest progressive degeneration is accompanied by angiogenesis and that newly formed vessels play an important role as a passage for macrophages to enter the disc space [31]. Interestingly, an immunohistochemical study on human autopsy degenerative discs also showed the presence of CD68-positive (pan-macrophage marker) cells in the NP, and suggested these cells were transformed resident cells rather than invading monocytes [50]. While more substantiative evidence is necessary to determine whether the degenerative pathology enables a microenvironment

conducive to transdifferentiation of resident NP cells towards a macrophage-like phenotype, the presence of transformed cells or infiltrated inflammatory cells both have the potential to mediate pain.

Inflammatory cells in the degenerated disc and AF secrete proinflammatory cytokines such as TNF α and IL-1 β that can directly and/or indirectly mediate pain sensitization [21, 53, 89, 91]. Both cytokines can directly exert algescic effects by binding to pain-associated receptors on the synapses of sensory neurons (which then respond by sending signals to the brain, initiating the perception of pain) [75, 94]. These cytokines also have the potential to induce neural ingrowth into the disc and mediate hypersensitization by upregulating the expression of factors like NGF and substance P, both of which are also found to be upregulated or increased in the outer AF of degenerated disc [1, 21, 60]. Furthermore, TNF α and IL-1 β have been shown to induce blood vessel ingrowth by stimulating the release of factors like vascular endothelial growth factor (VEGF) [6, 79]. Activated fibroblasts and macrophages in close proximity to existing blood vessels can coordinate signals with endothelial cells (ECs) and other stromal cells to stimulate angiogenesis [10, 27].

Angiogenesis is a crucial component in the pain-associated pathogenesis of disc degeneration and herniation. An immunohistochemical study of 50 herniated discs showed 88% and 78% immunopositivity for the angiogenic growth factors, VEGF and platelet-derived growth factor (PDGFbb), respectively; both factors were predominantly observed in tissue capillaries, but also present in disc cells and

fibroblasts [77]. The presence of these factors in degenerated and herniated discs has been associated with neovascularization of the poorly vascular AF and avascular NP [6, 12]. This is a very noteworthy morphological change for two reasons. First, the newly formed blood vessels branch out to form a network of smaller vessels that provide a venue for monocyte infiltration into the disc tissue via post-capillary venules; this process can then induce further inflammation and vascularization in the disc space [31, 51]. Second, vascularization also contributes to pathological innervation into the disc space: blood vessels extend through the AF towards the degenerating NP and this process can be accompanied by ingrowing nerve fibers [16, 17]. On the basis that these nerve fibers originate from the dorsal root ganglia, they are nociceptive [3, 9, 19, 52]. Importantly, these nerve fibers can also become hypersensitized due the inflammatory conditions in the degenerated disc, thereby contributing to discogenic pain [19]. Gruber and colleagues (2012) proposed nerve ingrowth into the inner AF of degenerative discs encounter a proinflammatory cytokine-rich milieu that promotes hyperalgesia and exacerbates pain [21]. To complicate an already complex phenomenon in the degenerating disc, both ECs and nerve cells, in addition to inflammatory cells, produce proinflammatory cytokines, vascularization factors, neurotrophins or neuropeptides [51, 65, 70, 75, 91]. Taken together, inflammation and the vascularization/innervation process work in synergy to mediate discogenic pain. Although it is still not clear which comes first, both processes involve potential targets for therapeutic intervention to mitigate pain.

TDR is a surgical procedure that involves the removal of the degenerated disc in its entirety to alleviate back pain. Thus, in theory, the majority of the pathological disc is discarded, with the exception of outer-most portions of the AF. However, since the AF can be involved in the pathogenesis of discogenic pain, it raises the interesting question of how pain is developing in patients revised for TDRs. This present body of research aims to not only evaluate the wear performance of TDRs in patients that were originally indicated for DDD, but also study any overlaps in pain-associated pathologies, since the primary reason for TDR revision surgery is pain.

1.7 Overview of Thesis & Specific Aims

This thesis presents extensive work reviewing artificial disc implant designs and biomaterials, followed by studying TDR retrievals, wear debris generation from these devices and the biological responses to the debris. The field of artificial disc replacement includes a broad range of designs as well as heterogeneous assortment of biomaterials for lumbar and cervical regions of the spine. Chapter 2 provides a systematic review evaluating the design and material factors that are associated with differences in clinical wear performance of lumbar and cervical TDRs. The rest of the thesis details experimental research evaluating the wear performance and biocompatibility of lumbar TDRs comprised specifically of the 2-piece, metal-on-polyethylene (MOP) design. Chapter 3 describes the retrieval analyses of contemporary MOP lumbar device components and periprosthetic tissue responses (*see Aim I below*). Chapter 4 investigates the immune responses to polyethylene wear particles and the involvement of inflammatory factors known to play both a

direct and indirect role in inflammatory-mediated pain (*see Aim II below*). Chapter 5 evaluates the relationship between inflammation, vascularization and innervation in the periprosthetic lumbar spine to elucidate the wear-debris-induced pathogenesis based on localized tissue/cellular responses (*see Aim III below*). Chapter 6 provides more information on the biological responses that led to the rare case of osteolysis noted in two TDR revision patients. Lastly, Chapter 7 summarizes the findings from the above body of research, along with implications of this work and future directions.

1.7.1 Aim I: Retrieval Analyses of Contemporary MOP L-TDR Device Components & Periprosthetic Tissue Responses

Modern L-TDR designs incorporate gamma-inert-sterilized or conventional ultra-high-molecular-weight polyethylene (UHMWPE) cores to improve wear resistance, minimize wear debris generation and reduce the risk of revision surgery [35]. Whether this contemporary material or the type of TDR design (mobile vs fixed) will influence UHMWPE wear debris and the subsequent tissue reactions in the spine remain unanswered questions. The hypothesis was that conventional UHMWPE cores used in contemporary TDR designs will decrease wear damage and periprosthetic tissue reactions compared to historical designs. *The goals were to determine whether: (1) periprosthetic UHMWPE wear debris and biological tissue responses are present in tissues from revised contemporary MOP L-TDRs; (2) there is an influence of bearing design (i.e. fully mobile vs. fixed designs) on wear particle*

number, size and shape; and (3) wear particles characteristics from contemporary MOP L-TDRs differ from historical MOP L-TDRs and conventional THR.

1.7.2 Aim II: Investigate the Immune Response to UHMWPE Wear Particles and the Involvement of Inflammatory Factors known to Play Both a Direct and Indirect Role in Inflammatory-mediated Pain

Pain is the primary reason for revision of artificial discs. However, whether pain is mediated or exacerbated as a biological consequence of wear debris remains unclear. Hip and knee arthroplasty and *in vitro* studies have revealed that UHMWPE wear debris stimulate resident and recruited macrophages to secrete a number of inflammatory cytokines, chemokines, reactive oxygen species and reactive nitrogen species [25, 32, 44, 45, 59, 61, 68, 69, 71, 73, 88]. These factors are predominantly associated with the induction of bone resorption in TJAs, which can lead to the development of osteolysis and implant loosening [73]. However, their presence, quantity and role in the clinical failure of contemporary TDR designs have not been determined, where pain rather than osteolysis is the central reason for revision. Interestingly many of the aforementioned biological factors produced in response to wear debris in TJR have also been implicated in nociceptive pain mediation [90, 94]. Based on preliminary data from TDR wear debris and tissue analyses performed in Aim I, it was hypothesized that biological reactions to wear debris in the spine are unique, in that the production and interplay between key inflammatory mediators may be contributing to abnormal or enhanced pain sensitization. To test this hypothesis and better understand the biological responses in TDR patient tissues

with and without detectable wear debris, *the second specific aim of this study was to analyze periprosthetic tissues from revised artificial discs using immunohistochemistry to quantify the levels of select inflammatory factors that are known to play both direct and indirect roles in the mediation of pain.*

1.7.3 Aim III: Evaluate the Relationship between Inflammation, Vascularization and Innervation in the Periprosthetic Lumbar Spine to Elucidate the Wear-Debris-Induced Pathogenesis based on Localized Tissue/Cellular Responses

As a part of Aim II, we reported an association for the angiogenic factor, VEGF with the neutrophin, NGF and the neuropeptide, Substance P. Associations for these factors have been previously reported, specifically at the sites of neovascularization, where infiltrating vessels are thought to physically provide a route for nerves to form and grow [6, 17, 42, 49]. Interestingly, inflammation and the production of the proinflammatory cytokines TNF α and IL-1 β were also associated with these neovascular changes. Taken together, these findings raise an important question: what is the significance of increased vascularization in TDR patient tissues and could the number of vessels independently serve as a pathogenic indicator and therapeutic target for pain-associated ‘particle disease’ in these individuals? To answer this question, macrophage, inflammatory factor and blood vessel and nerve cell contributions to the adverse reactions in TDR tissues needed to be systematically evaluated. We hypothesized that while inflammation is the driving force, increased vascularization may be a key histomorphological change

leading to nociception. Therefore, *the final and prospective specific aim was to elucidate the wear-debris-induced inflammatory pathogenesis in TDR tissues based on vascular density and NGF and substance P production at the localized level.*

1.8 References

1. Abe Y, Akeda K, An HS, Aoki Y, Pichika R, Muehleman C, Kimura T, Masuda K. Proinflammatory cytokines stimulate the expression of nerve growth factor by human intervertebral disc cells. *Spine (Phila Pa 1976)*. 2007;32:635-642.
2. Andersson GBJ. The Epidemiology of Spinal Disorders. *The Adult Spine: Principles and Practice*. Philadelphia: Lippincott-Raven; 1997:93-141.
3. Ashton IK, Roberts S, Jaffray DC, Polak JM, Eisenstein SM. Neuropeptides in the human intervertebral disc. *Journal of orthopaedic research : official publication of the Orthopaedic Research Society*. 1994;12:186-192.
4. Baxter RM, Macdonald DW, Kurtz SM, Steinbeck MJ. Severe impingement of lumbar disc replacements increases the functional biological activity of polyethylene wear debris. *The Journal of bone and joint surgery. American volume*. 2013;95:e751-759.
5. Bertagnoli R, Zigler J, Karg A, Voigt S. Complications and strategies for revision surgery in total disc replacement. *The Orthopedic clinics of North America*. 2005;36:389-395.
6. Binch AL, Cole AA, Breakwell LM, Michael AL, Chiverton N, Cross AK, Le Maitre CL. Expression and regulation of neurotrophic and angiogenic factors during human intervertebral disc degeneration. *Arthritis research & therapy*. 2014;16:416.
7. Blumenthal S, McAfee PC, Guyer RD, Hochschuler SH, Geisler FH, Holt RT, Garcia R, Jr., Regan JJ, Ohnmeiss DD. A prospective, randomized, multicenter Food and Drug Administration investigational device exemptions study of lumbar total disc replacement with the CHARITE artificial disc versus lumbar fusion: part I: evaluation of clinical outcomes. *Spine (Phila Pa 1976)*. 2005;30:1565-1575; discussion E1387-1591.
8. Boos N, Weissbach S, Rohrbach H, Weiler C, Spratt KF, Nerlich AG. Classification of age-related changes in lumbar intervertebral discs: 2002 Volvo Award in basic science. *Spine (Phila Pa 1976)*. 2002;27:2631-2644.
9. Brown MF, Hukkanen MV, McCarthy ID, Redfern DR, Batten JJ, Crock HV, Hughes SP, Polak JM. Sensory and sympathetic innervation of the vertebral endplate in patients with degenerative disc disease. *The Journal of bone and joint surgery. British volume*. 1997;79:147-153.
10. Carmeliet P, Jain RK. Molecular mechanisms and clinical applications of angiogenesis. *Nature*. 2011;473:298-307.
11. Choi YS. Pathophysiology of Degenerative Disc Disease. *Asian Spine Journal*. 2009;3:39-44.

12. David G. Angiogenesis in the degeneration of the lumbar intervertebral disc. 2010;3:154-161.
13. David T. Long-term results of one-level lumbar arthroplasty: minimum 10-year follow-up of the CHARITE artificial disc in 106 patients. *Spine (Phila Pa 1976)*. 2007;32:661-666.
14. de Kleuver M, Oner FC, Jacobs WC. Total disc replacement for chronic low back pain: background and a systematic review of the literature. *European spine journal : official publication of the European Spine Society, the European Spinal Deformity Society, and the European Section of the Cervical Spine Research Society*. 2003;12:108-116.
15. Fernstrom U. Arthroplasty with intercorporal endoprosthesis in herniated disc and in painful disc. *Acta chirurgica Scandinavica. Supplementum*. 1966;357:154-159.
16. Freemont AJ, Peacock TE, Goupille P, Hoyland JA, O'Brien J, Jayson MI. Nerve ingrowth into diseased intervertebral disc in chronic back pain. *Lancet*. 1997;350:178-181.
17. Freemont AJ, Watkins A, Le Maitre C, Baird P, Jeziorska M, Knight MT, Ross ER, O'Brien JP, Hoyland JA. Nerve growth factor expression and innervation of the painful intervertebral disc. *The Journal of pathology*. 2002;197:286-292.
18. Frelinghuysen P, Huang RC, Girardi FP, Cammisa FP, Jr. Lumbar total disc replacement part I: rationale, biomechanics, and implant types. *The Orthopedic clinics of North America*. 2005;36:293-299.
19. Garcia-Cosamalon J, del Valle ME, Calavia MG, Garcia-Suarez O, Lopez-Muniz A, Otero J, Vega JA. Intervertebral disc, sensory nerves and neurotrophins: who is who in discogenic pain? *Journal of anatomy*. 2010;217:1-15.
20. Grammatopoulos G, Pandit H, Kamali A, Maggiani F, Glyn-Jones S, Gill HS, Murray DW, Athanasou N. The correlation of wear with histological features after failed hip resurfacing arthroplasty. *The Journal of bone and joint surgery. American volume*. 2013;95:e81.
21. Gruber HE, Hoelscher GL, Ingram JA, Hanley EN, Jr. Genome-wide analysis of pain-, nerve- and neurotrophin -related gene expression in the degenerating human annulus. *Molecular pain*. 2012;8:63.
22. Hallab N, Cunningham B, Jacobs JJ. Spinal implant debris-induced osteolysis. *Spine (Phila Pa 1976)*. 2003;28:S125-138.
23. Hilibrand AS, Robbins M. Adjacent segment degeneration and adjacent segment disease: the consequences of spinal fusion? *Spine J*. 2004;4:190s-194s.
24. Hochschuler SH, Ohnmeiss DD, Guyer RD, Blumenthal SL. Artificial disc: preliminary results of a prospective study in the United States. *European spine journal : official publication of the European Spine Society, the European Spinal Deformity Society, and the European Section of the Cervical Spine Research Society*. 2002;11 Suppl 2:S106-110.
25. Horowitz SM, Gonzales JB. Effects of polyethylene on macrophages. *Journal of orthopaedic research : official publication of the Orthopaedic Research Society*. 1997;15:50-56.

26. Huang RC, Lim MR, Girardi FP, Cammisa FP, Jr. The prevalence of contraindications to total disc replacement in a cohort of lumbar surgical patients. *Spine (Phila Pa 1976)*. 2004;29:2538-2541.
27. Hughes CC. Endothelial-stromal interactions in angiogenesis. *Current opinion in hematology*. 2008;15:204-209.
28. Ingham E, Fisher J. Biological reactions to wear debris in total joint replacement. *Proceedings of the Institution of Mechanical Engineers. Part H, Journal of engineering in medicine*. 2000;214:21-37.
29. Ingham E, Fisher J. The role of macrophages in osteolysis of total joint replacement. *Biomaterials*. 2005;26:1271-1286.
30. Katz MM, Hargens AR, Garfin SR. Intervertebral disc nutrition. Diffusion versus convection. *Clinical orthopaedics and related research*. 1986:243-245.
31. Koike Y, Uzuki M, Kokubun S, Sawai T. Angiogenesis and inflammatory cell infiltration in lumbar disc herniation. *Spine (Phila Pa 1976)*. 2003;28:1928-1933.
32. Koulouvaris P, Ly K, Ivashkiv LB, Bostrom MP, Nestor BJ, Sculco TP, Purdue PE. Expression profiling reveals alternative macrophage activation and impaired osteogenesis in periprosthetic osteolysis. *Journal of orthopaedic research : official publication of the Orthopaedic Research Society*. 2008;26:106-116.
33. Kumar MN, Baklanov A, Chopin D. Correlation between sagittal plane changes and adjacent segment degeneration following lumbar spine fusion. *European spine journal : official publication of the European Spine Society, the European Spinal Deformity Society, and the European Section of the Cervical Spine Research Society*. 2001;10:314-319.
34. Kurtz SM. *The UHMWPE Biomaterials Handbook*. Burlington, MA: Academic Press; 2009.
35. Kurtz SM, MacDonald D, Ianuzzi A, van Ooij A, Isaza J, Ross ER, Regan J. The natural history of polyethylene oxidation in total disc replacement. *Spine (Phila Pa 1976)*. 2009;34:2369-2377.
36. Kurtz SM, Patwardhan A, MacDonald D, Ciccarelli L, van Ooij A, Lorenz M, Zindrick M, O'Leary P, Isaza J, Ross R. What is the correlation of in vivo wear and damage patterns with in vitro TDR motion response? *Spine*. 2008;33:481-489.
37. Kurtz SM, Toth JM, Siskey R, Ciccarelli L, Macdonald D, Isaza J, Lanman T, Punt I, Steinbeck M, Goffin J, van Ooij A. The Latest Lessons Learned from Retrieval Analyses of Ultra-High Molecular Weight Polyethylene, Metal-on-Metal, and Alternative Bearing Total Disc Replacements. *Seminars in spine surgery*. 2012;24:57-70.
38. Kurtz SM, van Ooij A, Ross R, de Waal Malefijt J, Pelozo J, Ciccarelli L, Villarraga ML. Polyethylene wear and rim fracture in total disc arthroplasty. *Spine J*. 2007;7:12-21.
39. Lemaire JP, Carrier H, Sariali el H, Skalli W, Lavaste F. Clinical and radiological outcomes with the Charite artificial disc: a 10-year minimum follow-up. *Journal of spinal disorders & techniques*. 2005;18:353-359.

40. Link HD, Keller A. Biomechanics of Total Disc Replacement. In: Buttner-Janzen K, Hochschuler SH, McAfee PC, ed. *The Artificial Disc*. Berlin: Springer Berlin Heidelberg; 2003:33-52.
41. Link HD, McAfee PC, Pimenta L. Choosing a cervical disc replacement. *Spine J*. 2004;4:294S-302S.
42. Malinsky J. The ontogenetic development of nerve terminations in the intervertebral discs of man. (Histology of intervertebral discs, 11th communication). *Acta anatomica*. 1959;38:96-113.
43. Marchand F, Perretti M, McMahon SB. Role of the immune system in chronic pain. *Nature reviews. Neuroscience*. 2005;6:521-532.
44. Matthews JB, Besong AA, Green TR, Stone MH, Wroblewski BM, Fisher J, Ingham E. Evaluation of the response of primary human peripheral blood mononuclear phagocytes to challenge with in vitro generated clinically relevant UHMWPE particles of known size and dose. *Journal of biomedical materials research*. 2000;52:296-307.
45. Matthews JB, Green TR, Stone MH, Wroblewski BM, Fisher J, Ingham E. Comparison of the response of primary human peripheral blood mononuclear phagocytes from different donors to challenge with model polyethylene particles of known size and dose. *Biomaterials*. 2000;21:2033-2044.
46. McAfee PC, Cunningham B, Holsapple G, Adams K, Blumenthal S, Guyer RD, Dmietriev A, Maxwell JH, Regan JJ, Isaza J. A prospective, randomized, multicenter Food and Drug Administration investigational device exemption study of lumbar total disc replacement with the CHARITE artificial disc versus lumbar fusion: part II: evaluation of radiographic outcomes and correlation of surgical technique accuracy with clinical outcomes. *Spine (Phila Pa 1976)*. 2005;30:1576-1583; discussion E1388-1590.
47. Moore KR, Pinto MR, Butler LM. Degenerative disc disease treated with combined anterior and posterior arthrodesis and posterior instrumentation. *Spine (Phila Pa 1976)*. 2002;27:1680-1686.
48. Murray CJ, Vos T, Lozano R, Naghavi M, Flaxman AD, Michaud C, Ezzati M, Shibuya K, Salomon JA, Abdalla S, Aboyans V, Abraham J, Ackerman I, Aggarwal R, Ahn SY, Ali MK, Alvarado M, Anderson HR, Anderson LM, Andrews KG, Atkinson C, Baddour LM, Bahalim AN, Barker-Collo S, Barrero LH, Bartels DH, Basanez MG, Baxter A, Bell ML, Benjamin EJ, Bennett D, Bernabe E, Bhalla K, Bhandari B, Bikbov B, Bin Abdulhak A, Birbeck G, Black JA, Blencowe H, Blore JD, Blyth F, Bolliger I, Bonaventure A, Boufous S, Bourne R, Boussinesq M, Braithwaite T, Brayne C, Bridgett L, Brooker S, Brooks P, Brugha TS, Bryan-Hancock C, Bucello C, Buchbinder R, Buckle G, Budke CM, Burch M, Burney P, Burstein R, Calabria B, Campbell B, Canter CE, Carabin H, Carapetis J, Carmona L, Cella C, Charlson F, Chen H, Cheng AT, Chou D, Chugh SS, Coffeng LE, Colan SD, Colquhoun S, Colson KE, Condon J, Connor MD, Cooper LT, Corriere M, Cortinovis M, de Vaccaro KC, Couser W, Cowie BC, Criqui MH, Cross M, Dabhadkar KC, Dahiya M, Dahodwala N, Damsere-Derry J, Danaei G, Davis A, De Leo D, Degenhardt L, Dellavalle R, Delossantos A, Denenberg J, Derrett S, Des Jarlais DC, Dharmaratne SD,

- Dherani M, Diaz-Torne C, Dolk H, Dorsey ER, Driscoll T, Duber H, Ebel B, Edmond K, Elbaz A, Ali SE, Erskine H, Erwin PJ, Espindola P, Ewoigbokhan SE, Farzadfar F, Feigin V, Felson DT, Ferrari A, Ferri CP, Fevre EM, Finucane MM, Flaxman S, Flood L, Foreman K, Forouzanfar MH, Fowkes FG, Fransen M, Freeman MK, Gabbe BJ, Gabriel SE, Gakidou E, Ganatra HA, Garcia B, Gaspari F, Gillum RF, Gmel G, Gonzalez-Medina D, Gosselin R, Grainger R, Grant B, Groeger J, Guillemin F, Gunnell D, Gupta R, Haagsma J, Hagan H, Halasa YA, Hall W, Haring D, Haro JM, Harrison JE, Havmoeller R, Hay RJ, Higashi H, Hill C, Hoen B, Hoffman H, Hotez PJ, Hoy D, Huang JJ, Ibeanusi SE, Jacobsen KH, James SL, Jarvis D, Jasrasaria R, Jayaraman S, Johns N, Jonas JB, Karthikeyan G, Kassebaum N, Kawakami N, Keren A, Khoo JP, King CH, Knowlton LM, Kobusingye O, Koranteng A, Krishnamurthi R, Laden F, Lalloo R, Laslett LL, Lathlean T, Leasher JL, Lee YY, Leigh J, Levinson D, Lim SS, Limb E, Lin JK, Lipnick M, Lipshultz SE, Liu W, Loane M, Ohno SL, Lyons R, Mabweijano J, MacIntyre MF, Malekzadeh R, Mallinger L, Manivannan S, Marcenes W, March L, Margolis DJ, Marks GB, Marks R, Matsumori A, Matzopoulos R, Mayosi BM, McAnulty JH, McDermott MM, McGill N, McGrath J, Medina-Mora ME, Meltzer M, Mensah GA, Merriman TR, Meyer AC, Miglioli V, Miller M, Miller TR, Mitchell PB, Mock C, Mocumbi AO, Moffitt TE, Mokdad AA, Monasta L, Montico M, Moradi-Lakeh M, Moran A, Morawska L, Mori R, Murdoch ME, Mwaniki MK, Naidoo K, Nair MN, Naldi L, Narayan KM, Nelson PK, Nelson RG, Nevitt MC, Newton CR, Nolte S, Norman P, Norman R, O'Donnell M, O'Hanlon S, Olives C, Omer SB, Ortblad K, Osborne R, Ozgediz D, Page A, Pahari B, Pandian JD, Rivero AP, Patten SB, Pearce N, Padilla RP, Perez-Ruiz F, Perico N, Pesudovs K, Phillips D, Phillips MR, Pierce K, Pion S, Polanczyk GV, Polinder S, Pope CA, 3rd, Popova S, Porrini E, Pourmalek F, Prince M, Pullan RL, Ramaiah KD, Ranganathan D, Razavi H, Regan M, Rehm JT, Rein DB, Remuzzi G, Richardson K, Rivara FP, Roberts T, Robinson C, De Leon FR, Ronfani L, Room R, Rosenfeld LC, Rushton L, Sacco RL, Saha S, Sampson U, Sanchez-Riera L, Sanman E, Schwebel DC, Scott JG, Segui-Gomez M, Shahrzad S, Shepard DS, Shin H, Shivakoti R, Singh D, Singh GM, Singh JA, Singleton J, Sleet DA, Sliwa K, Smith E, Smith JL, Stapelberg NJ, Steer A, Steiner T, Stolk WA, Stovner LJ, Sudfeld C, Syed S, Tamburlini G, Tavakkoli M, Taylor HR, Taylor JA, Taylor WJ, Thomas B, Thomson WM, Thurston GD, Tleyjeh IM, Tonelli M, Towbin JA, Truelsen T, Tsilimbaris MK, Ubeda C, Undurraga EA, van der Werf MJ, van Os J, Vavilala MS, Venketasubramanian N, Wang M, Wang W, Watt K, Weatherall DJ, Weinstock MA, Weintraub R, Weisskopf MG, Weissman MM, White RA, Whiteford H, Wiebe N, Wiersma ST, Wilkinson JD, Williams HC, Williams SR, Witt E, Wolfe F, Woolf AD, Wulf S, Yeh PH, Zaidi AK, Zheng ZJ, Zonies D, Lopez AD, AlMazroa MA, Memish ZA. Disability-adjusted life years (DALYs) for 291 diseases and injuries in 21 regions, 1990-2010: a systematic analysis for the Global Burden of Disease Study 2010. *Lancet*. 2012;380:2197-2223.
49. Nerlich AG, Schaaf R, Walchli B, Boos N. Temporo-spatial distribution of blood vessels in human lumbar intervertebral discs. *European spine journal : official publication of the European Spine Society, the European Spinal*

- Deformity Society, and the European Section of the Cervical Spine Research Society.* 2007;16:547-555.
50. Nerlich AG, Weiler C, Zipperer J, Narozny M, Boos N. Immunolocalization of phagocytic cells in normal and degenerated intervertebral discs. *Spine (Phila Pa 1976)*. 2002;27:2484-2490.
 51. Newman AC, Hughes CC. Macrophages and angiogenesis: a role for Wnt signaling. *Vascular cell*. 2012;4:13.
 52. Ohtori S, Takahashi K, Chiba T, Yamagata M, Sameda H, Moriya H. Substance P and calcitonin gene-related peptide immunoreactive sensory DRG neurons innervating the lumbar intervertebral discs in rats. *Annals of anatomy = Anatomischer Anzeiger : official organ of the Anatomische Gesellschaft*. 2002;184:235-240.
 53. Park JY, Kuh SU, Park HS, Kim KS. Comparative expression of matrix-associated genes and inflammatory cytokines-associated genes according to disc degeneration: analysis of living human nucleus pulposus. *Journal of spinal disorders & techniques*. 2011;24:352-357.
 54. Park P, Garton HJ, Gala VC, Hoff JT, McGillicuddy JE. Adjacent segment disease after lumbar or lumbosacral fusion: review of the literature. *Spine (Phila Pa 1976)*. 2004;29:1938-1944.
 55. Peng B, Hao J, Hou S, Wu W, Jiang D, Fu X, Yang Y. Possible pathogenesis of painful intervertebral disc degeneration. *Spine (Phila Pa 1976)*. 2006;31:560-566.
 56. Punt I, Baxter R, van Ooij A, Willems P, van Rhijn L, Kurtz S, Steinbeck M. Submicron sized ultra-high molecular weight polyethylene wear particle analysis from revised SB Charite III total disc replacements. *Acta biomaterialia*. 2011;7:3404-3411.
 57. Punt IM, Austen S, Cleutjens JP, Kurtz SM, ten Broeke RH, van Rhijn LW, Willems PC, van Ooij A. Are periprosthetic tissue reactions observed after revision of total disc replacement comparable to the reactions observed after total hip or knee revision surgery? *Spine (Phila Pa 1976)*. 2012;37:150-159.
 58. Punt IM, Cleutjens JP, de Bruin T, Willems PC, Kurtz SM, van Rhijn LW, Schurink GW, van Ooij A. Periprosthetic tissue reactions observed at revision of total intervertebral disc arthroplasty. *Biomaterials*. 2009;30:2079-2084.
 59. Purdue PE, Koulouvaris P, Potter HG, Nestor BJ, Sculco TP. The cellular and molecular biology of periprosthetic osteolysis. *Clinical orthopaedics and related research*. 2007;454:251-261.
 60. Purmessur D, Freemont AJ, Hoyland JA. Expression and regulation of neurotrophins in the nondegenerate and degenerate human intervertebral disc. *Arthritis research & therapy*. 2008;10:R99.
 61. Puskas BL, Menke NE, Huie P, Song Y, Ecklund K, Trindade MC, Smith RL, Goodman SB. Expression of nitric oxide, peroxynitrite, and apoptosis in loose total hip replacements. *Journal of biomedical materials research. Part A*. 2003;66:541-549.
 62. Rao RD, David KS, Wang M. Biomechanical changes at adjacent segments following anterior lumbar interbody fusion using tapered cages. *Spine (Phila Pa 1976)*. 2005;30:2772-2776.

63. Repanti M, Korovessis PG, Stamatakis MV, Spastris P, Kosti P. Evolution of disc degeneration in lumbar spine: a comparative histological study between herniated and postmortem retrieved disc specimens. *Journal of spinal disorders*. 1998;11:41-45.
64. Ribeiro RA, Vale ML, Thomazzi SM, Paschoalato AB, Poole S, Ferreira SH, Cunha FQ. Involvement of resident macrophages and mast cells in the writhing nociceptive response induced by zymosan and acetic acid in mice. *European journal of pharmacology*. 2000;387:111-118.
65. Risbud MV, Shapiro IM. Role of Cytokines in Intervertebral Disc Degeneration: Pain and Disc-content. *Nature reviews. Rheumatology*. 2014;10:44-56.
66. Ross R, Mirza AH, Norris HE, Khatri M. Survival and clinical outcome of SB Charite III disc replacement for back pain. *The Journal of bone and joint surgery. British volume*. 2007;89:785-789.
67. Roughley PJ. Biology of intervertebral disc aging and degeneration: involvement of the extracellular matrix. *Spine (Phila Pa 1976)*. 2004;29:2691-2699.
68. Shanbhag AS, Jacobs JJ, Black J, Galante JO, Glant TT. Human monocyte response to particulate biomaterials generated in vivo and in vitro. *Journal of orthopaedic research : official publication of the Orthopaedic Research Society*. 1995;13:792-801.
69. Shanbhag AS, Kaufman AM, Hayata K, Rubash HE. Assessing osteolysis with use of high-throughput protein chips. *The Journal of bone and joint surgery. American volume*. 2007;89:1081-1089.
70. Shubayev VI, Kato K, Myers RR. *Cytokines in Pain*. Boca Raton, FL: CRC Press/Taylor & Francis; 2010.
71. Stea S, Visentin M, Donati ME, Granchi D, Ciapetti G, Sudanese A, Toni A. Nitric oxide synthase in tissues around failed hip prostheses. *Biomaterials*. 2002;23:4833-4838.
72. Steinbeck M, Veruva SY. Pathophysiologic Reactions to UHMWPE Wear Particles. In: Kurtz SM, ed. *UHMWPE Biomaterials Handbook: Ultra High Molecular Weight Polyethylene in Total Joint Replacement and Medical Devices*: William Andrew; 2015.
73. Steinbeck MJ, Jablonowski LJ, Parvizi J, Freeman TA. The role of oxidative stress in aseptic loosening of total hip arthroplasties. *The Journal of arthroplasty*. 2014;29:843-849.
74. Taimela S, Kujala UM, Salminen JJ, Viljanen T. The prevalence of low back pain among children and adolescents. A nationwide, cohort-based questionnaire survey in Finland. *Spine (Phila Pa 1976)*. 1997;22:1132-1136.
75. Thacker MA, Clark AK, Marchand F, McMahon SB. Pathophysiology of peripheral neuropathic pain: immune cells and molecules. *Anesthesia and analgesia*. 2007;105:838-847.
76. Thomazzi SM, Ribeiro RA, Campos DI, Cunha FQ, Ferreira SH. Tumor necrosis factor, interleukin-1 and interleukin-8 mediate the nociceptive activity of the supernatant of LPS-stimulated macrophages. *Mediators of inflammation*. 1997;6:195-200.

77. Tolonen J, Gronblad M, Virri J, Seitsalo S, Rytomaa T, Karaharju EO. Platelet-derived growth factor and vascular endothelial growth factor expression in disc herniation tissue: and immunohistochemical study. *European spine journal : official publication of the European Spine Society, the European Spinal Deformity Society, and the European Section of the Cervical Spine Research Society*. 1997;6:63-69.
78. Tumialan LM, Gluf WM. Progressive vertebral body osteolysis after cervical disc arthroplasty. *Spine (Phila Pa 1976)*. 2011;36:E973-978.
79. Tunyogi-Csapo M, Koreny T, Vermes C, Galante JO, Jacobs JJ, Glant TT. Role of fibroblasts and fibroblast-derived growth factors in periprosthetic angiogenesis. *Journal of orthopaedic research : official publication of the Orthopaedic Research Society*. 2007;25:1378-1388.
80. Turner JA, Ersek M, Herron L, Deyo R. Surgery for lumbar spinal stenosis. Attempted meta-analysis of the literature. *Spine (Phila Pa 1976)*. 1992;17:1-8.
81. Urban JP, Holm S, Maroudas A, Nachemson A. Nutrition of the intervertebral disc: effect of fluid flow on solute transport. *Clinical orthopaedics and related research*. 1982:296-302.
82. van den Eerenbeemt KD, Ostelo RW, van Royen BJ, Peul WC, van Tulder MW. Total disc replacement surgery for symptomatic degenerative lumbar disc disease: a systematic review of the literature. *European spine journal : official publication of the European Spine Society, the European Spinal Deformity Society, and the European Section of the Cervical Spine Research Society*. 2010;19:1262-1280.
83. van Ooij A, Kurtz SM, Stessels F, Noten H, van Rhijn L. Polyethylene wear debris and long-term clinical failure of the Charite disc prosthesis: a study of 4 patients. *Spine (Phila Pa 1976)*. 2007;32:223-229.
84. van Ooij A, Oner FC, Verbout AJ. Complications of artificial disc replacement: a report of 27 patients with the SB Charite disc. *Journal of spinal disorders & techniques*. 2003;16:369-383.
85. Veruva SY, Lanman TH, Hanzlik JA, Kurtz SM, Steinbeck MJ. Rare complications of osteolysis and periprosthetic tissue reactions after hybrid and non-hybrid total disc replacement. *European spine journal : official publication of the European Spine Society, the European Spinal Deformity Society, and the European Section of the Cervical Spine Research Society*. 2014.
86. Veruva SY, Steinbeck MJ, Toth J, Alexander DD, Kurtz SM. Which design and biomaterial factors affect clinical wear performance of total disc replacements? A systematic review. *Clinical orthopaedics and related research*. 2014;472:3759-3769.
87. Virk SS, Niedermeier S, Yu E, Khan SN. Adjacent segment disease. *Orthopedics*. 2014;37:547-555.
88. Wang ML, Hauschka PV, Tuan RS, Steinbeck MJ. Exposure to particles stimulates superoxide production by human THP-1 macrophages and avian HD-11EM osteoclasts activated by tumor necrosis factor-alpha and PMA. *The Journal of arthroplasty*. 2002;17:335-346.

89. Weiler C, Nerlich AG, Bachmeier BE, Boos N. Expression and distribution of tumor necrosis factor alpha in human lumbar intervertebral discs: a study in surgical specimen and autopsy controls. *Spine (Phila Pa 1976)*. 2005;30:44-53; discussion 54.
90. Winrow VR, Winyard PG, Morris CJ, Blake DR. Free radicals in inflammation: second messengers and mediators of tissue destruction. *British medical bulletin*. 1993;49:506-522.
91. Wuertz K, Haglund L. Inflammatory Mediators in Intervertebral Disk Degeneration and Discogenic Pain. *Global Spine Journal*. 2013;3:175-184.
92. Yasuma T, Arai K, Yamauchi Y. The histology of lumbar intervertebral disc herniation. The significance of small blood vessels in the extruded tissue. *Spine (Phila Pa 1976)*. 1993;18:1761-1765.
93. Zechmeister I, Winkler R, Mad P. Artificial total disc replacement versus fusion for the cervical spine: a systematic review. *European spine journal : official publication of the European Spine Society, the European Spinal Deformity Society, and the European Section of the Cervical Spine Research Society*. 2011;20:177-184.
94. Zhang JM, An J. Cytokines, inflammation, and pain. *International anesthesiology clinics*. 2007;45:27-37.

CHAPTER 2

A Systematic Review of Design & Biomaterial Factors Affecting the Clinical Wear Performance of Total Disc Replacements[†]

2.1 Abstract

Total disc replacement was clinically introduced to reduce pain and preserve segmental motion of the lumbar and cervical spine. Previous case studies have reported implant wear and adverse local tissue reactions around artificial prostheses, but it is unclear how design and biomaterials affect clinical outcomes. In this study, we asked which design and material factors are associated with differences in clinical wear performance (implant wear and periprosthetic tissue response) of (1) lumbar and (2) cervical total disc replacements?

To research the literature for publications related to TDR implant wear and periprosthetic tissue response, we performed a systematic review using an advanced search in MEDLINE and Scopus electronic databases. Of the 340 references identified, 33 were retrieved for full-text evaluation, from which 16 papers met the inclusion criteria, which were semi-quantitative analysis of wear and adverse local tissue reactions along with a description of the implanted device. The 16 papers included 12 on lumbar disc replacement and five on cervical disc replacement; one of the included studies reported on both lumbar and cervical disc replacement. An additional three papers were found by searching bibliographies of

[†]The content of this chapter was published in the journal of Clinical Orthopaedics and Related Research: Veruva, S.Y., Steinbeck, M.J., Toth, J., Alexander, D.D. and Kurtz, S.M. *Which design and biomaterial factors affect clinical wear performance of total disc replacements? A systematic review.* Clin Orthop Relat Res, 2014. **472**(12): p. 3759-69.

the original articles, bringing the total to 19 papers (14 lumbar and 7 cervical studies). There were seven case reports, three case series, two case-control studies, and seven analytical studies. The Methodological Index for Non-randomized Studies (MINORS) Scale was used to score case series and case-control studies, which yielded mean scores of 10.3 of 16 and 17.5 of 24, respectively. In general, the case series (3) and case-control (2) studies were of good quality. In lumbar regions, metal-on-polymer devices with mobile-bearing designs consistently generated small and large polymeric wear debris, triggering periprosthetic tissue activation of macrophages and the formation of giant cells, respectively. In the cervical regions, metal-on-polymer devices with fixed-bearing designs had similar outcomes. Information on lumbar fixed-bearing devices and cervical mobile-bearing devices was limited. All metal-on-metal constructs, of both lumbar and cervical constructs, tended to generate small metallic wear debris, which typically triggered an adaptive immune response of predominantly activated lymphocytes. There were no retrieval studies on one-piece prostheses.

This review provides evidence that design and biomaterials affect the type of wear and inflammation. However, clinical study design, follow-up, and analytical techniques differ among investigations, preventing us from drawing firm conclusions about the relationship between implant design and wear performance for both cervical and lumbar total disc replacement.

2.2 Introduction

Total disc replacement (TDR) was clinically introduced as an alternative to fusion to reduce pain and preserve segmental motion of the cervical and lumbar spine. TDR designs currently on the market may be classified as either fixed- or mobile-bearing analogous to total knee replacements. Of these designs, the most widely used in the market today include metallic endplates, which are fixed to the adjacent vertebral bodies and one or more articulations that involve either metal-on-polymer or metal-on-metal bearing surfaces. The most commonly used lumbar disc replacements have relied on either cobalt-chromium (CoCr) alloy endplates articulating with a polymer core of ultrahigh-molecular-weight polyethylene (hereafter polyethylene) or metal-on-metal (MoM) bearings fabricated from CoCr alloys. In the cervical spine, a broader range of biomaterials have been used, including polyethylene, CoCr alloys, stainless steel, titanium (Ti) alloys, polyurethanes, polyetheretherketone, and Ti alloy-ceramic composites. In addition to the fixed- and mobile-bearing designs, a third “one-piece” classification of artificial disc design, in which an elastomeric polymer disc is fixed to metallic endplates, is currently undergoing clinical investigation. Thus, the field of artificial disc replacement includes a broad range of designs as well as heterogeneous assortment of biomaterials for lumbar (Table 2-1) and cervical regions of the spine (Table 2-2).

Although the early developers of disc arthroplasty argued that the release of wear debris would not be a clinically relevant issue [1], case studies have emerged in the literature over the past decade that illustrate the potential for not only wear debris-induced osteolysis with metal-on-polymer (MoP) TDRs, but also adverse local tissue reactions for MoM TDRs [2]. Compared with THAs and TKAs, little is known about the clinical damage modes for TDRs because the surgery to remove a

malfunctioning artificial disc can be challenging, or even life-threatening, especially for the lumbar spine [3]. There has been one systematic review of complications in cervical disc arthroplasty [4] and previous (nonsystematic) surveys of retrieved total disc replacements [5, 6], but the authors are not aware of a previous systematic approach to examine the effects of design and material selection on wear, corrosion, and tissue response of revised TDRs. Because the biomechanical requirements for TDRs differ for the cervical and lumbar spine and are reflected in both the TDR design and material selection, studies on TDRs for each region of the spine should be considered separately.

We therefore performed a systematic review to evaluate which design and material factors are associated with differences in clinical wear performance (implant wear and periprosthetic tissue response) of (1) lumbar and (2) cervical total disc replacements.

2.3 Search Strategy & Criteria

This systematic review used guidelines from the Cochrane handbook during the development of the study protocol and report [7]. To address the research questions posed in this review, studies were identified by searching the MEDLINE and Scopus electronic databases. An advanced search was performed in MEDLINE through PubMed by querying spine and arthroplasty MeSH terms along with title, abstract, and text word fields in the database. The following precise syntax was used for the search: (((((((corrosion[tw] OR wear[tw] OR deform*[tw] OR degra*[tw] OR fracture[tw]))) OR (((adverse[tw] AND effects[tw]))))) AND (((spin

Table 2-1. Summary of contemporary lumbar total disc replacements

Device	Manufacturer	Classification	Biomaterials	Bearing design	IDE trial status (www.clinicaltrials.gov)	Current regulatory status
CHARITÉ	DePuy Synthes Spine, Raynham, MA	MoP	CoCr-UHMWPE	Mobile	Completed	FDA-approved but withdrawn from US/OUS market after DePuy Synthes merger, 2012
ProDisc-L	DePuy Synthes Spine, West Chester, PA	MoP	CoCr-UHMWPE	Fixed	Completed	FDA-approved, available US/OUS
Activ-L	Aesculap AG, Tuttlingen, Germany	MoP	CoCr-UHMWPE	Mobile	Active; not recruiting	Available OUS
Mobidisc	LDR Spine, Troyes, France	MoP	CoCr-UHMWPE	Mobile	Terminated	Withdrawn
Maverick	Medtronic, Memphis, TN	MOM	CoCr-CoCr	Fixed	Completed	Available OUS
Kineflex	Spinal Motion Inc, Mountainview, CA	MoP	CoCr-CoCr	Mobile	Terminated	Withdrawn
Flexicore	Stryker Spine, Allendale, NJ	MoP	CoCr-CoCr	Constrained	Not registered	Withdrawn
Baguera L	Spineart, Geneva, Switzerland	MoP	Diamolith-coated Ti-UHMWPE	Fixed	Not registered	Available OUS
CADisc-L	Ranier Technology, Cambridge, UK	1P	1-piece polyurethane	One-piece	Completed	Available OUS
Freedom	AxioMed, Garfield, OH	1P	Ti plates and elastomer core	One-piece	Recruiting	Available OUS
eDisc	Integra Spine, Vista, CA	1P	Ti plates and elastomer core	One-piece	Not registered	Available OUS
Physio-L	Nexgen Spine, Whippany, NJ	1P	Ti plates and elastomer core	One-piece	Not registered	Available OUS
M6-L	Spinal Kinetics Sunnyvale, CA	1P	Ti plates and polyurethane- UHMWPE fiber core	One-piece	Withdrawn	NA

IDE = Investigational Device Exemption; MoP = metal-on-polyethylene; 1P = one-piece; CoCr = cobalt-chromium; Ti = titanium; OUS = outside United States; NA = not available.

Table 2-2. Summary of contemporary cervical total disc replacements

Device	Manufacturer	Classification	Biomaterials	Bearing design	IDE trial status	Current regulatory status
Prestige ST	Medtronic, Memphis, TN	MoM	Stainless steel-stainless steel	Fixed	Completed	FDA-approved, available US/OUS
Bryan	Medtronic, Memphis, TN	MoP	Ti-PCU	Mobile	Completed	FDA-approved, available US/OUS
Prodisc-C	DePuy Synthes Spine, West Chester, PA	MoP	CoCr-UHMWPE	Fixed	Completed	FDA-approved, available US/OUS
PCM	Nu Vasive, San Diego, CA	MoP	CoCr-UHMWPE	Fixed	Completed	FDA-approved, available US/OUS
Mobi-C	LDR Spine, Troyes, France	MoP	CoCr-UHMWPE	Mobile	Completed	FDA-approved, available US/OUS
SECURE-C	Globus Medical, Audubon, PA	MoP	CoCr-UHMWPE	Mobile	Active; not recruiting	FDA-approved, available US/OUS
Activ C	Aesculap AG, Tuttlingen, Germany	MoP	CoCr-UHMWPE	Mobile	Unknown	Available OUS
Kineflex/C	Spinal Motion Inc, Mountainview, CA	MoM	CoCr-CoCr	Mobile	Terminated	Withdrawn
CerviCore	Stryker Spine, Allendale, NJ	MoM	CoCr-CoCr	Constrained	Not registered	Withdrawn
DISCOVER	DePuy Synthes Spine, West Chester, PA	MoP	Ti-UHMWPE	Fixed	Active; not recruiting	Available OUS
Baguera C	Spineart, Geneva, Switzerland	MoP	Diamolith-coated Ti-UHMWPE	Fixed	Not registered	Available OUS
Prestige LP	Medtronic, Memphis, TN	CoC	Ti-ceramic composite	Fixed	Active; not recruiting	Available OUS
NUNEC	Pioneer Surgical Technology, Marquette, MI	PoP	PEEK-PEEK	Fixed	Recruiting	Available OUS
Freedom	AxioMed, Garfield, OH	1P	Ti plates and polymer core	One-piece	Recruiting	Available OUS
NeoDisc	Nu Vasive, San Diego, CA	1P	Silicone elastomer and textile	One-piece	Completed	Available OUS
CADisc-C	Ranier Technology, Cambridge, UK	1P	1-piece polyurethane	One-piece	Not registered	Available OUS
Discocerv	Alphatec Spine Inc, Carlsbad, CA	CoC	Ceramic-ceramic	Fixed	Terminated	Available OUS
ALTIA	Amedica, Salt Lake City, UT	CoC	Ceramic-ceramic (silicon nitride)	Fixed	Not registered	Available OUS
CerPass	Nu Vasive, San Diego, CA	CoM	Ceramic-ceramic	Fixed	Terminated	NA
M6-C	Spinal Kinetics Sunnyvale, CA	1P	Ti plates & PCU-UHMWPE fiber core	One-piece	Withdrawn	NA

IDE = Investigational Device Exemption; MoM = metal-on-metal; MoP = metal-on-polymer; CoC = ceramic-on-ceramic; PoP = polymer-on-polymer; 1P = one-piece; CoM = ceramic-on-metal; Ti = titanium; PCU = poly(carbonate urethane); CoCr = cobalt-chromium; PEEK = polyether ether ketone; OUS = outside United States; NA = not available.

e[mh]) OR ((Spinal[tw] OR disc[tw] OR disk[tw])) AND (((((((artificial[tw] AND prosthesis*[tw])) OR (((disc[tw] AND arthroplasty*[tw]) OR (Disc[tw] AND implant) OR (Disc[tw] AND replace*) OR (Disc[tw] AND prosthesis*)))) OR posterior fusion[tw]) OR (stabilization[tw])))) AND ((peek[tw] OR polyethylene[tw] OR polycarbonate urethane[tw] OR cobalt chromium[tw] OR prodisc[tw] OR freedom[tw] OR charite[tw] OR maverick[tw] OR kineflex[tw] OR activ[tw] OR mobidisc[tw] OR flexicore[tw] OR xl[tw] OR bryan[tw] OR prestige[tw] OR cadisc[tw] OR nubac[tw] OR secure[tw] OR discover[tw] OR nunec[tw] OR pcm[tw] OR dynesys[tw])))))) NOT (finite element[tiab] OR biomechanical analysis[tiab] OR biomechanics*[ti] OR model[tiab] OR MRI[tiab] OR clinical outcome*[ti] OR ossification[ti]) AND "humans"[mh] AND ("2000/01/01"[pdat] : "2013/12/31"[pdat]) AND "English"[la]. The search was streamlined to specifically identify reports of wear, corrosion, and periprosthetic tissue response after spinal arthroplasty. Terms in the latter portion of the code were chosen based on the brand names of motion preservation devices currently in active use or under investigation. Lastly, the search code excluded papers centrally themed around finite element analysis, biomechanical modeling, or strict clinical outcomes. PubMed filters further restricted results to human studies and reports published in English. Using the aforementioned criteria, 160 articles were obtained from MEDLINE published between January 1, 2001, and April 30, 2014. The same search strategy and filters were used for the Scopus database, yielding 180 articles, many of which overlapped the search results from MEDLINE. The following precise syntax was

used in Scopus: ((((((TITLE-ABS-KEY(corrosion) OR TITLE-ABS-KEY(wear) OR TITLE-ABS-KEY(deform*) OR TITLE-ABS-KEY(degra*) OR TITLE-ABS-KEY(fracture))) OR (((TITLE-ABS-KEY(adverse) AND TITLE-ABS-KEY(effects)))))) AND ((((((TITLE-ABS-KEY(spine) OR TITLE-ABS-KEY(spinal) OR TITLE-ABS-KEY(disc) OR TITLE-ABS-KEY(disk))) AND ((((((TITLE-ABS-KEY(artificial) AND TITLE-ABS-KEY(prosthe*)) OR (((TITLE-ABS-KEY(disc) AND TITLE-ABS-KEY(arthroplast*) OR (TITLE-ABS-KEY(disc) AND TITLE-ABS-KEY(implant)) OR (TITLE-ABS-KEY(disc) AND TITLE-ABS-KEY(replace*)) OR (TITLE-ABS-KEY(disc) AND TITLE-ABS-KEY(prosthe*))))) OR TITLE-ABS-KEY(fusion)) OR (TITLE-ABS-KEY(stabilization)))))) AND ((TITLE-ABS-KEY(peek) OR TITLE-ABS-KEY(polyethylene) OR TITLE-ABS-KEY(polycarbonate urethane) OR TITLE-ABS-KEY(cobalt chromium) OR TITLE-ABS-KEY(prodisc) OR TITLE-ABS-KEY(freedom) OR TITLE-ABS-KEY(charite) OR TITLE-ABS-KEY(maverick) OR TITLE-ABS-KEY(kineflex) OR TITLE-ABS-KEY(activ) OR TITLE-ABS-KEY(mobidisc) OR TITLE-ABS-KEY(flexicore) OR TITLE-ABS-KEY(xl) OR TITLE-ABS-KEY(bryan) OR TITLE-ABS-KEY(prestige) OR TITLE-ABS-KEY(cadisc) OR TITLE-ABS-KEY(nubac) OR TITLE-ABS-KEY(secure) OR TITLE-ABS-KEY(discover) OR TITLE-ABS-KEY(nunec) OR TITLE-ABS-KEY(pcm) OR TITLE-ABS-KEY(dynesys)))))))))) AND NOT (TITLE-ABS-KEY(finite element) OR TITLE-ABS-KEY(biomechanical analysis) OR TITLE-ABS-KEY(biomech*) OR TITLE-ABS-KEY(model) OR TITLE-ABS-KEY(mri) OR TITLE-ABS-KEY(clinical outcome*) OR TITLE-ABS-KEY(ossification))) AND (PUBYEAR > 1999 AND PUBYEAR < 2015) AND (LIMIT-TO(LANGUAGE,"English")).

Of the 340 papers obtained using the search strategies, duplicates were removed and studies were then screened and assessed for eligibility to be included in the systematic review (Figure 2-1). Screening of titles and abstracts revealed 55 articles with potential relevance for this review. Next, *in vitro* studies and review articles were excluded, narrowing the number of eligible papers for inclusion to 33. An additional three studies were located by searching bibliographies of key articles and identifying full-text articles by hand search. Further full-text assessment for eligibility led to the exclusion of papers without any semiquantitative analyses of wear, corrosion, osteolysis, or adverse local tissue reactions; this left 19 articles meeting the inclusion criteria, of which 14 were lumbar and seven were cervical TDR studies (with one overlapping study). The majority of clinical research was low-level evidence [8] and included a total of seven Level V case reports, three Level IV case series, and two Level III case-control studies. Case series and case-control studies, in general, were good-quality studies with mean scores of 10.3 of 16.0 and 17.5 of 24.0, respectively, on the Methodological Index for Non-randomized Studies (MINORS) Scale [9]. The main limitations to these studies included the lack of unbiased assessments, sufficiently long follow-up implantation times, and prospective calculations of study size. We did not grade study quality for the seven analytical reports because a suitable tool for this purpose is not available.

Each study was reviewed in detail by three authors (SYV, MJS, SMK). Data were extracted using a standardized form, which included study design, number of patients, patient demographic information, implant type, design, biomaterials, and

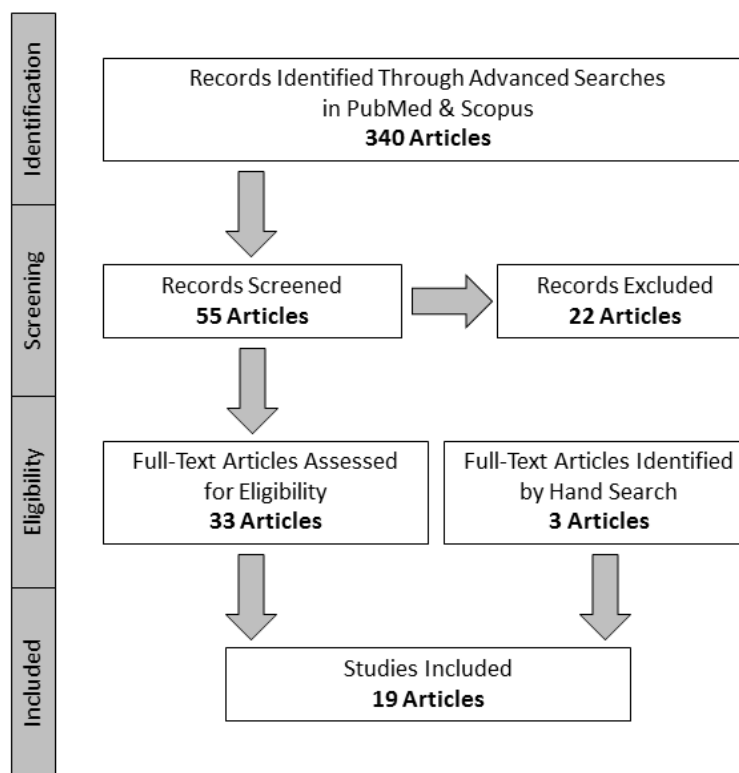


Figure 2-1. A flow diagram demonstrates the systematic review protocol.

outcome measures for device damage, wear, corrosion, metal ion levels, histology, and osteolysis. Some overlapping studies involving the same patients were included if the authors reported on larger patient pools in prospective retrieval studies or if authors evaluated varying durations of follow-up in clinical metal-ion investigations.

For the systematic review, we summarized the authors' assessments of the removed artificial disc wear, corrosion, and/or periprosthetic tissue responses. We then classified these damage factors as absent or present in the patient cohorts to evaluate the impact of implant design and biomaterials on wear and corrosion performance. Given the methodological and analytical heterogeneity (ie, between-

study variation) between the studies included in this systematic review, the retrospective nature of the clinical series, and the absence of control groups in many of the studies, we were unable to combine data across studies to perform a quantitative meta-analysis. Instead we sought to examine each study to obtain the desired information concerning clinical performance outcomes based on implant design, wear performance, and local tissue reactions in light of each study's strengths and limitations.

2.4 Results

2.4.1 Lumbar Total Disc Replacement

In MoP studies, the mobile-bearing designs, CHARITÉ (Depuy Synthes Spine, Raynham, MA, USA), Activ-L (Aesculap AG, Tuttlingen, Germany), and Mobidisc (LDR Spine, Troyes, France), demonstrated evidence of polyethylene surface damage, polyethylene wear debris, and innate periprosthetic inflammation; fixed-bearing ProDisc-L (DePuy Synthes Spine, West Chester, PA, USA) devices evidenced a high frequency of endplate impingement and metal wear debris (Table 2-3). A total of 49 mobile-bearing MoP retrievals with gamma-air-sterilized polyethylene were evaluated in two studies (48 from one report and one from a case study) [10, 11]. Impingement, typically between the polyethylene core and the metallic endplate, was observed in 34 of 49 (69%) of the retrievals in those two studies. Two separate studies analyzed periprosthetic tissues from 22 of the 48 retrievals and reported polyethylene wear and inflammation in 16 of 22 (73%) patients [12]. A direct association was observed for severe or moderate impingement, wear debris,

and inflammation for 11 of the 34 impinged devices [13]. Despite the high incidence of polyethylene wear, osteolysis was only reported in one of 48 (2.1%) implants [10]. For mobile-bearing designs with conventional or gamma-inert-sterilized cores, a single report on three retrievals found wear particle generation was two orders less when compared to gamma-air-sterilized cores [14]. Nevertheless, impingement, wear debris, and innate inflammation were observed in all three retrievals. For fixed-bearing designs, one study reported burnishing in 11 of 19 (58%) and another reported the same wear mechanism in one of one retrieval [15, 16]. In a separate case report for a prosthesis removed as a result of migration, the presence of metallic debris was observed on the polyethylene core [17].

In MoM studies, both mobile-bearing Kineflex (Spinal Motion Inc, Mountainview, CA, USA) and fixed-bearing Maverick (Medtronic, Memphis, TN, USA) devices generated metallic debris accompanied by a mixed innate and adaptive immune response. Based on a case report of two mobile-bearing retrievals, implant damage in one was negligible and unreported in the second; however, tissues from both devices contained metallic debris [18]. Similarly, fixed-bearing implant analysis of tissues from two separate case studies [18, 19] reported metallic debris. Furthermore, all tissue retrievals showed mixed inflammation. Two independent studies looking at systemic metal ions found elevated serum Co and Cr ion levels postoperatively between 0.25 and 49.4 years [20, 21].

2.4.2 Cervical Total Disc Replacement

In MoP studies, there were no reports on mobile-bearing designs; the fixed-bearing designs, ProDisc-C (DePuy Synthes Spine, West Chester, PA, USA) and Bryan Cervical Disc (Medtronic, Memphis, TN, USA), showed a high frequency of endplate impingement with polymeric wear debris and mixed inflammation (Table 2-4). As observed in lumbar fixed-bearing designs, burnishing was consistent with metallic endplate impingement in 24 of 30 (80%) retrievals [22]. A separate case report noted a rare incidence of osteolysis [23]. In another study, impingement was observed in nine of 30 (30%) retrievals [5]. Tissues obtained from 15 of these 30 devices showed polymeric debris. Similarly, a separate case study reported polymeric debris [24]. Metallic debris was infrequent to negligible in all but one of the cases [25]. An innate immune response was predominant in all tissues, although a few isolated regions of lymphocytic infiltration were noted [5]. In MoM studies, impingement was observed in one case study of a mobile-bearing Kineflex/C (Spinal Motion Inc, Mountainview, CA, USA) device; fixed-bearing Prestige Cervical Disc (Medtronic, Memphis, TN, USA) devices evidenced impingement, metallic debris, and mixed inflammation.

A case study on one mobile-bearing device reported no evidence of metal particles in tissues, but visual evidence of metallosis within the joint tissue was pronounced [18]. In devices with fixed-bearing designs, impingement was evident in 11 of 16 (68.8%) retrievals, typically in anterior regions [5]. In addition, screw hole fretting and fretting adjacent to bone screws were detected. Metallosis was observed in all 15 (100%) patients with tissue retrievals and metallic debris within the tissue was noted, but in both cases its distribution was not uniform and was

described as focal. A separate study with an unreported bearing design also reported the presence of metallic debris in tissue retrievals [26]. Mixed inflammation was observed in all tissues for both mobile- and fixed-bearing designs.

2.5 Discussion

Although benefits of treating degenerative disc conditions with TDR include preservation of motion and limiting stress at adjacent vertebra, potential complications associated with wear debris remain a concern. The aim of this study was to systematically review reports of wear, corrosion, and subsequent biological responses for lumbar and cervical TDR. Additionally, we sought to determine whether design and material issues were associated with the wear and corrosion behavior of these motion-preserving spinal devices. After analyzing reports from 14 lumbar and seven cervical studies (in 19 papers), we found that wear-associated complications may be specific to the biomaterial used for TDR in both regions of the spine. Specifically, MoP devices typically produced polymeric wear debris, which was usually accompanied by an innate inflammatory response. On the other hand, MoM constructs tended to generate small metallic wear debris and metal ions, which activated an adaptive immune mechanism leading to adverse local tissue reactions in some patients.

As of the time of this writing, for the one lumbar and five cervical disc artificial disc designs that have been approved by the FDA, only one is a MoM cervical device fabricated from stainless steel (Table 2). MoM prostheses have been under heavy scrutiny by researchers/regulators given the high-profile concern of

previous recall and warnings of THA devices with Co-based alloy MoM bearings [27]. Metallosis and subsequent soft tissue reactions and pseudotumors have been reported in patients with CoCr MoM articulations, in which some cases showed aseptic lymphocyte-dominated vasculitis-associated lesion response associated with normal implant wear rates [2, 18]. Metal hypersensitivity is also an issue with CoCr designs [26], although the relationship between delayed hypersensitivity and metallic debris remains unclear. Adverse host responses may also be triggered by metal tribochemical reactions *in vivo*, but to our knowledge, there have been no direct and standardized measurements of implant corrosion in TDRs. Although fretting and corrosion products were observed in some cervical MoM TDRs [5, 24], the extent of corrosive removal of metal in these devices remains unclear. Serum assays after lumbar TDR have revealed an elevation in Co and Cr ions, thereby inferring corrosion, but it was later concluded that these levels were similar to those observed for successful MoM THAs [20, 21, 28]. Despite these biomaterial issues, using MoM designs has its benefits, for example, these devices are theoretically designed to achieve lower volumetric wear (mainly as a result of lower friction) in comparison to traditional MoP designs, which potentially would reduce local inflammation and osteolysis. Also, it is worth noting that adverse local tissue reactions have been reported with all implant designs; thus, the small number of case reports for MoM studies exhibit important risks/complications of the technology. Further long-term follow-up studies are necessary to better understand the impact of such designs/materials on long-term wear rates.

Table 2-3. Summary of findings from 14 published studies of retrieved implants, tissues, & fluids from lumbar total disc replacements

Classification	Bearing design	Device	Study	Mean implantation time (years)	Impingement	Periprosthetic debris		Inflammation		Osteolysis	Systemic metal ions measured (# of patients)
						Polymeric	Metallic	Innate	Adaptive		
MoP	Mobile	CHARITÉ	David, 2005 [9]	9.5	0/1	NR	NR	NR	NR	0/1	NR
MoP	Fixed	ProDisc-L	Stieber and Donald, 2006 [37]	0.1	NR	NR	1/1	NR	NR	NR	NR
MoP	Mobile	CHARITÉ	van Ooij et al, 2007 [40]	9.4	5/5	5/5	0/5	Y	N	1/5	NR
MoP	Mobile	CHARITÉ	Kurtz et al, 2009 [21]	8.50	34/48*	NR	NR	NR	NR	1/48*	NR
MoP	Fixed	ProDisc-L	Choma et al, 2009 [5]	1.2	1/1	1/1	0/1	N	N	NR	NR
MoP	Mobile	Activ-L; Mobidisc	Austen et al, 2012 [2]	1.9	3/3	3/3	0/3	Y	N	NR	NR
MoP	Mobile	CHARITÉ	Punt et al, 2012 [34]	10.0	NR	21/22	0/22	Y	N	NR	NR
MoP	Fixed	ProDisc-L	Lebl et al, 2012 [26]	1.1	11/19	NR	NR	NR	NR	NR	NR
MoP	Mobile	CHARITÉ	Baxter et al, 2013 [3]	9.7	NR	11/11	0/11	Y	N	NR	NR
MoM	Fixed	Maverick	Francois et al, 2007 [12]	1.2	NR	NA	1/1	Y	Y	NR	NR
MoM	Fixed	Maverick	Zeh et al, 2009 [42]†	3.1	NR	NA	NA	NA	NA	NA	15/15
MoM	Mobile	Kineflex	Guyer et al, 2011 [17]	1.7	NR	NA	2/2	Y	Y	NR	NR
MoM	Fixed	Maverick	Guyer et al, 2011 [17]	3.1	NR	NA	1/1	Y	Y	NR	NR
MoM	Fixed	Maverick	Kurtz et al, 2012 [24]	1.3	2/7	NA	1/1	Y	Y	NR	NR
MoM	Fixed	Maverick	Gornet et al, 2013 [16]†	3	NR	NR	NR	NR	NR	NR	24/24

*This cohort includes retrievals from study performed by van Ooij et al [40]; †these are metal ion clinical studies, not retrieval studies; MoP = metal-on-polyethylene; MoM = metal-on-metal; NR = not reported; Y = yes; N = no; NA = not applicable.

Table 2-4. Summary of findings from eight published studies of retrieved implants and tissues from cervical total disc replacements

Classification	Bearing design	Device	Study	Mean implantation time (years)	Impingement	Periprosthetic debris		Inflammation		Osteolysis
						Polymeric	Metallic	Innate	Adaptive	
MoP	Fixed	Bryan	Anderson et al, 2004 [1]	1.0	NR	2/2	0/2	Y	N	NR
MoP	Fixed	ProDisc-C	Tumailan and Gluf, 2011 [38]	1.3	NR	NR	NR	NR	NR	1/1
MoP	Fixed	Bryan	Fan et al, 2012 [11]	8.0	NR	1/1	1/1	NR	NR	NR
MoP	Fixed	Bryan	Kurtz et al, 2012 [24]	3.2	9/30	15/15	~0/15	Y	Y	NR
MoP	Fixed	ProDisc-C	Lebl et al, 2012 [27]	1.0	24/30	NR	NR	NR	NR	NR
MoM	Fixed	Prestige	Anderson et al, 2004 [1]	2.4	0/2	NA	2/2	Y	Y	NR
MoM	Mobile	Kineflex/C	Cavanaugh et al, 2009 [4]	~0.6	NR	NA	1/1	Y	Y	NR
MoM	Mobile	Kineflex/C	Guyer et al, 2011 [17]	1.2	1/1	NA	0/1	Y	Y	NR
MoM	Fixed	Prestige	Kurtz et al, 2012 [24]	2.0	11/16	NA	15/15	Y	Y	NR

MoP = metal-on-polyethylene; MoM = metal-on-metal; NR = not reported; Y = yes; N = no; NA = not applicable.

Unlike MoM devices, the central concern with the use of MoP devices is the generation of polymeric wear debris from bearing surfaces and the subsequent innate inflammatory response. Recent studies on MoP TDRs have revealed that tissue responses resulting from wear-related damage are indeed comparable to responses seen in total joint arthroplasties (TJAs) [12]. However, for THAs, polyethylene wear activates an innate inflammatory response that is associated with osteolysis and aseptic loosening, which is a fundamental cause of clinical failure [29, 30]. Vertebral osteolysis, on the other hand, appears to be a rare phenomenon in the spine and has only been reported in one patient with lumbar mobile-bearing TDR and one patient with cervical fixed-bearing TDR in the retrieval studies [23, 31] included in this review. Explanations for the relatively low frequency of osteolysis may include the low ranges of motion in the anterior column of the lumbar spine and an absence of resident macrophages and synovium compared with the hip and knee [1]. Furthermore, the reduced particle concentration/number, degree of inflammation and/or cytokine levels may be too low to directly cause osteolysis [14]. Reduced cytokine levels and/or local cellular responses to these factors is of particular interest since similar cytokines which include tumor necrosis factor- α , interleukin-1, and interleukin-6 are released by macrophages and giant cells in both tissue types; however, osteoclastogenesis is observed in THAs and neuroinflammatory pain in TDRs [32, 33]. For these reasons, the presence of wear remains a critical concern in the spine.

This review consisted primarily of papers reporting on wear performance of MoP retrievals with fixed- or mobile-bearing designs; collectively, these reports

indicated that wear damage mechanisms may be linked to the bearing design. Mobile-bearing retrievals tended to have characteristic multidirectional scratches with adhesive/abrasive wear mechanisms at the dome (much like THAs) and microadhesive/microabrasive wear mechanisms at the rim (much like TKAs) [34]. Although several fixed-bearing retrievals also had signs of scratches in the dome regions, a large percentage had characteristic metallic and endplate burnishing typically in the posterior region associated with impingement [15]. Also, fatigue-related rim damage and radial crack formation were only reported in gamma-air-sterilized cores of historical mobile-bearing retrievals, attributable to oxidative degradation [10, 11]. This was not evident in gamma-inert sterilized fixed-bearing designs and it is possible that the fixture of the core in designs may contribute to these wear mechanisms. The increased mobility and abnormalities in ROMs in mobile-bearing designs can influence the number and type of wear debris generation. Although flexion/extension ROM was restored to physiological ranges by both designs [35-37], mobile-bearing devices provide higher degrees of freedom (i.e., CHARITÉ; 5 DOF) compared with fixed bearings (i.e., ProDisc-L; 3 DOF). The long-term consequences of the differing kinematics on wear debris generation and subsequent inflammation remain unclear.

For the papers identified by the systematic search, there were no studies of wear for one-piece spine retrievals, thereby highlighting a need for research on nonball-and-socket type designs to evaluate their effectiveness and resistance to wear/corrosion. Ball-and-socket articulating bearings were originally modeled from total joint arthroplasties, which raises the question whether they replicate the

biomechanics of the intervertebral disc. Ball-and-socket designs are typically rigid in the axial direction and are not designed to resist moments in bending or rotation forces like the natural and deformable spinal disc, which may lead to altered ROM, segmental lordosis, or overloading of facet joints [38-41]. One-piece designs typically incorporate compliant elastomer biomaterials to mimic the physiological six degrees of freedom [42, 43]. Although the first one-piece model, known as the Acroflex (DePuy-AcroMed, Inc., Raynham, MA) discs, was abandoned as a result of failure of elastic rubber [44], newer designs have developed to improve the technology, including solving the issue of bonding elastic components to titanium endplates. Long-term follow-up studies are required to better understand the wear performance for these devices.

In summary, current TDRs have been developed using total joint arthroplasty models and thus comparable biomaterial issues have been observed. MoP devices raise a concern for the production of polymeric wear debris that initiates innate inflammation. MoM devices present the risk of generating small metallic debris, metal ion release, adaptive host responses, metal hypersensitive reactions, and pseudotumor formation. Increases in systemic metal ion levels have also been detected, raising the likelihood of responses in other tissues. Design factors such as mobile- and fixed-bearing or one-piece constructs may also influence wear performance of TDRs, but more research is necessary to better understand which models truly mimic the natural motions of the spine while minimizing wear. Additional analytical studies with standardized cohort and case-control based observations would augment the existing body of literature and facilitate a more

formal quantitative assessment of TDR material and design. In addition, future studies need to address how design and wear of the various biomaterials impact neuroinflammation in the spine, considering pain is the primary reason for revision of both lumbar and cervical TDRs.

2.6 Study Limitations

Limitations of this review included the number limited number of studies and the mixed quality of the research, of which only a small number of case-control studies scored well on the MINORS quality scale. Furthermore, in the application of our inclusion and exclusion criteria, studies that did not report at least semiquantitative measures of wear were excluded, thus potentially eliminating studies with some important clinical information and patient outcomes in response to the use of certain implant designs/biomaterials. It is also important to note that all the studies that were included involved cases in which the primary revision reason was pain rather than an association with wear, and tissue evaluations of wear debris and inflammatory responses were limited. Nevertheless, these criteria were necessary to report common endpoints and measurable findings that could be summarized and evaluated. Finally, variability in the reporting of wear and related damage mechanisms made it difficult to synthesize results as did the inclusion of data from case reports, which lack a representative comparison group. Standardized test methods for retrieval analysis of TDRs have only recently been developed [5]; thus, older studies included in this review typically relied on visual characterization of wear.

2.7 References

1. Link, H.D. and A. Keller, *Biomechanics of Total Disc Replacement*, in *The Artificial Disc*, K. Buttner-Janz, S.H. Hochschuler, and P.C. McAfee, Editors. 2003, Springer Berlin Heidelberg: Berlin. p. 33-52.
2. Golish, S.R. and P.A. Anderson, *Bearing surfaces for total disc arthroplasty: metal-on-metal versus metal-on-polyethylene and other biomaterials*. Spine J, 2012. **12**(8): p. 693-701.
3. van Ooij, A., F.C. Oner, and A.J. Verbout, *Complications of artificial disc replacement: a report of 27 patients with the SB Charite disc*. J Spinal Disord Tech, 2003. **16**(4): p. 369-83.
4. Lehman, R., et al., *A systematic review of cervical artificial disc replacement wear characteristics and durability*. Evid Based Spine Care J, 2012. **3**(S1): p. 31-8.
5. Kurtz, S.M., et al., *The Latest Lessons Learned from Retrieval Analyses of Ultra-High Molecular Weight Polyethylene, Metal-on-Metal, and Alternative Bearing Total Disc Replacements*. Semin Spine Surg, 2012. **24**(1): p. 57-70.
6. Kurtz, S., et al., *Retrieval analysis of motion preserving spinal devices and periprosthetic tissues*. SAS, 2009. **3**(4): p. 161-177.
7. *Cochrane Handbook for Systematic Reviews of Interventions*. The Cochrane Collaboration 2013/01/01]; Available from: <http://www.cochrane.org/training/cochrane-handbook>.
8. Hujoel, P., *Grading the evidence: the core of EBD*. J Evid Based Dent Pract, 2009. **9**(3): p. 122-4.
9. Slim, K., et al., *Methodological index for non-randomized studies (minors): development and validation of a new instrument*. ANZ J Surg, 2003. **73**(9): p. 712-6.
10. Kurtz, S.M., et al., *The natural history of polyethylene oxidation in total disc replacement*. Spine (Phila Pa 1976), 2009. **34**(22): p. 2369-77.
11. David, T., *Revision of a Charite artificial disc 9.5 years in vivo to a new Charite artificial disc: case report and explant analysis*. Eur Spine J, 2005. **14**(5): p. 507-11.
12. Punt, I.M., et al., *Are periprosthetic tissue reactions observed after revision of total disc replacement comparable to the reactions observed after total hip or knee revision surgery?* Spine (Phila Pa 1976), 2012. **37**(2): p. 150-9.
13. Baxter, R.M., et al., *Severe impingement of lumbar disc replacements increases the functional biological activity of polyethylene wear debris*. J Bone Joint Surg Am, 2013. **95**(11): p. e751-9.
14. Austen, S., et al., *Clinical, radiological, histological and retrieval findings of Activ-L and Mobidisc total disc replacements: a study of two patients*. Eur Spine J, 2012. **21 Suppl 4**: p. S513-20.
15. Lebl, D.R., et al., *In vivo functional performance of failed Prodisc-L devices: retrieval analysis of lumbar total disc replacements*. Spine (Phila Pa 1976), 2012. **37**(19): p. E1209-17.

16. Choma, T.J., et al., *Retrieval analysis of a ProDisc-L total disc replacement*. J Spinal Disord Tech, 2009. **22**(4): p. 290-6.
17. Stieber, J.R. and G.D. Donald III, *Early Failure of Lumbar Disc Replacement Case Report and Review of the Literature*. J Spinal Disord Tech, 2006. **19**(1): p. 55-60.
18. Guyer, R.D., et al., *Early failure of metal-on-metal artificial disc prostheses associated with lymphocytic reaction: diagnosis and treatment experience in four cases*. Spine (Phila Pa 1976), 2011. **36**(7): p. E492-497.
19. Francois, J., R. Coessens, and P. Lauweryns, *Early removal of a Maverick disc prosthesis: surgical findings and morphological changes*. Acta Orthop Belg., 2007. **73**(1): p. 122-127.
20. Gornet, M.F., et al., *Prospective study on serum metal levels in patients with metal-on-metal lumbar disc arthroplasty*. Eur Spine J, 2013. **22**: p. 741-746.
21. Zeh, A., et al., *Time-dependent release of cobalt and chromium ions into the serum following implantation of the metal-on-metal Maverick type artificial lumbar disc (Medtronic Sofamor Danek)*. Arch Orthop Trauma Surg, 2009. **129**(6): p. 741-6.
22. Lebl, D.R., et al., *The mechanical performance of cervical total disc replacements in vivo: prospective retrieval analysis of prodisc-C devices*. Spine (Phila Pa 1976), 2012. **37**(26): p. 2151-60.
23. Tumialan, L.M. and W.M. Gluf, *Progressive vertebral body osteolysis after cervical disc arthroplasty*. Spine (Phila Pa 1976), 2011. **36**(14): p. E973-8.
24. Anderson, P.A., et al., *A comparison of simulator-tested and -retrieved cervical disc prostheses. Invited submission from the Joint Section Meeting on Disorders of the Spine and Peripheral Nerves, March 2004*. J Neurosurg Spine, 2004. **1**(2): p. 202-210.
25. Fan, H., et al., *Implant failure of Bryan cervical disc due to broken polyurethane sheath: a case report*. Spine (Phila Pa 1976), 2012. **37**(13): p. E814-6.
26. Cavanaugh, D.A., et al., *Delayed hyper-reactivity to metal ions after cervical disc arthroplasty: a case report and literature review*. Spine (Phila Pa 1976), 2009. **34**(7): p. E262-265.
27. *Metal-on-Metal Hip Implants*. Medical Devices 2013/01/01]; Available from: <http://www.fda.gov/medicaldevices/productsandmedicalprocedures/implantsandprosthetics/metalonmetalhipimplants/default.htm>.
28. Zeh, A., et al., *Release of cobalt and chromium ions into the serum following implantation of the metal-on-metal Maverick-type artificial lumbar disc (Medtronic Sofamor Danek)*. Spine (Phila Pa 1976), 2007. **32**(3): p. 348-52.
29. Kurtz, S.M., *The UHMWPE Biomaterials Handbook*. 2 ed. Ultra-High Molecular Weight Polyethylene in Total Joint Replacement and Medical Devices. 2009, Burlington, MA: Academic Press.
30. Jacobs, J.J., et al., *Wear Particles*. J Bone Joint Surg Am, 2006. **88**(suppl 2): p. 99-102.
31. van Ooij, A., et al., *Polyethylene wear debris and long-term clinical failure of the Charite disc prosthesis: a study of 4 patients*. Spine (Phila Pa 1976), 2007. **32**(2): p. 223-9.

32. Gallo, J., et al., *Bone remodeling, particle disease and individual susceptibility to periprosthetic osteolysis*. *Physiol Res*, 2008. **57**(3): p. 339-49.
33. Scholz, J. and C.J. Woolf, *The neuropathic pain triad: neurons, immune cells and glia*. *Nat Neurosci*, 2007. **10**(11): p. 1361-8.
34. Punt, I., et al., *Submicron sized ultra-high molecular weight polyethylene wear particle analysis from revised SB Charite III total disc replacements*. *Acta Biomater*, 2011. **7**(9): p. 3404-11.
35. Zigler, J., et al., *Results of the prospective, randomized, multicenter Food and Drug Administration investigational device exemption study of the ProDisc-L total disc replacement versus circumferential fusion for the treatment of 1-level degenerative disc disease*. *Spine (Phila Pa 1976)*, 2007. **32**(11): p. 1155-62; discussion 1163.
36. Gornet, M.F., et al., *Lumbar disc arthroplasty with Maverick disc versus stand-alone interbody fusion: a prospective, randomized, controlled, multicenter investigational device exemption trial*. *Spine (Phila Pa 1976)*, 2011. **36**(25): p. E1600-11.
37. McAfee, P.C., et al., *A prospective, randomized, multicenter Food and Drug Administration investigational device exemption study of lumbar total disc replacement with the CHARITE artificial disc versus lumbar fusion: part II: evaluation of radiographic outcomes and correlation of surgical technique accuracy with clinical outcomes*. *Spine (Phila Pa 1976)*, 2005. **30**(14): p. 1576-83; discussion E388-90.
38. van den Broek, P.R., et al., *Design of next generation total disk replacements*. *J Biomech*, 2012. **45**(1): p. 134-40.
39. Cunningham, B.W., et al., *General principles of total disc replacement arthroplasty: seventeen cases in a nonhuman primate model*. *Spine (Phila Pa 1976)*, 2003. **28**(20): p. S118-24.
40. O'Leary, P., et al., *Response of Charite total disc replacement under physiologic loads: prosthesis component motion patterns*. *Spine J*, 2005. **5**(6): p. 590-9.
41. Chung, S.K., Y.E. Kim, and K.C. Wang, *Biomechanical effect of constraint in lumbar total disc replacement: a study with finite element analysis*. *Spine (Phila Pa 1976)*, 2009. **34**(12): p. 1281-6.
42. Heuer, F., et al., *Stepwise reduction of functional spinal structures increase range of motion and change lordosis angle*. *J Biomech*, 2007. **40**(2): p. 271-80.
43. Lazennec, J.-Y., et al., *Clinical outcomes, radiologic kinematics, and effects on sagittal balance of the 6-degrees-of-freedom LP-ESP® lumbar disc prosthesis*. *The Spine Journal*, (0).
44. Devin, C.J., T.G. Myers, and J.D. Kang, *Chronic failure of a lumbar total disc replacement with osteolysis. Report of a case with nineteen-year follow-up*. *J Bone Joint Surg Am*, 2008. **90**(10): p. 2230-4.

CHAPTER 3

Retrieval Analyses of Contemporary Lumbar TDRs & Periprosthetic Tissue Responses[†]

3.1 Abstract

Lumbar total disc replacement (L-TDR) is a procedure used to relieve lower back pain and maintain mobility. Contemporary metal-on-polyethylene (MoP) L-TDRs were developed to address wear performance concerns about historical designs, but wear debris generation and periprosthetic tissue reactions for these newer implants have not been determined. The purpose of this study was to determine (1) whether periprosthetic ultrahigh-molecular-weight polyethylene (UHMWPE) wear debris and biological responses were present in tissues from revised contemporary MoP L-TDRs that contain conventional cores fabricated from γ -inert-sterilized UHMWPE; (2) how fixed- versus mobile-bearing design affected UHMWPE wear particle number, shape, and size; and (3) how these wear particle characteristics compare with historical MoP L-TDRs that contain cores fabricated from γ -air-sterilized UHMWPE. We evaluated implant retrievals and periprosthetic tissues from 11 patients who received eight fixed-bearing ProDisc-L and four mobile-bearing CHARITÉ contemporary L-TDRs with a mean implantation time of 4.1 and 2.7 years, respectively. Implants were first examined for wear and surface damage. Histologic analysis of tissues was then performed to assess biological responses and polarized light microscopy was used to quantify number and

[†]The content of this chapter was published in the journal of Clinical Orthopaedics and Related Research: Veruva SY, Lanman TH, Isaza JE, MacDonald DW, Kurtz SM, Steinbeck MJ. UHMWPE Wear Debris and Tissue Reactions Are Reduced for Contemporary Designs of Lumbar Total Disc Replacements. *Clinical orthopaedics and related research*. 2015;473:987-998.

size/shape characteristics of UHMWPE wear particles. Comparisons were made to previously reported particle data for historical L-TDRs. All fixed-bearing (100%) and two of four mobile-bearing (50%) implant component retrievals indicated wear damage. Five of seven (71%) fixed-bearing and one of four mobile-bearing L-TDR patient tissues contained at least 4 particles/mm² wear with associated macrophage infiltration. Tissues with wear debris were highly vascularized, whereas those without debris were more necrotic. Given the samples available, the tissue around mobile-bearing L-TDR was observed to contain 87% more, 11% rounder, and 11% less-elongated wear debris compared to tissues around fixed-bearing devices; however, there were no significant differences. Compared to historical L-TDRs, UHMWPE particle number and circularity for contemporary L-TDRs were 99% less ($p = 0.003$) and 50% rounder ($p = 0.003$). In this study, short-term results suggest there was no significant influence of fixed- or mobile-bearing design on wear particle characteristics of contemporary L-TDRs, but conventional UHMWPE has notably improved the wear resistance of these devices compared to historical UHMWPE.

3.2 Introduction

Lumbar total disc replacement (L-TDR) is an established alternative to spinal fusion for degenerative disc disease and its associated lower back and leg pain. With the goal to preserve natural segmental motion in the spine, commonly used implant designs incorporate cobalt-chromium (CoCr) metallic endplates, which are fixed to the adjacent vertebral bodies, articulating against a polymer core made of ultrahigh-

molecular-weight polyethylene (UHMWPE). As a result of the decreased sliding distance in metal-on-polyethylene (MoP) L-TDRs compared with THA and TKA, wear and osteolysis of L-TDRs were originally thought to be negligible in the anterior column of the lumbar spine [24, 25]. However, studies of historical L-TDRs with γ -air-sterilized UHMWPE cores have demonstrated wear of the UHMWPE core along with rare cases of osteolysis in the lumbar spine [21, 44]. Additionally, both submicron (0.05-2 μm) and large UHMWPE wear particles ($\geq 2 \mu\text{m}$) were present in periprosthetic tissues from historical TDRs [33, 34]. The presence of wear debris was associated with an innate inflammatory response and in one case contributed to osteolysis. The particle shapes were comparable to those observed in revision tissues from THA and generally round to oval in morphology, whereas the TKA particles were more needle-shaped [33]. The mean particle numbers were similar and ranged from 0 to 1002 particles/ mm^2 [33]. Additionally, the extent of impingement of the implant positively correlated with increased submicron wear debris and thus, biological activity of the particles [5]. Collectively, these studies and others have established the clinically relevant complication of UHMWPE core wear for historical L-TDRs [20, 22, 32, 42, 43] and served as an impetus for improving bearing surface materials and designs.

Contemporary L-TDR designs incorporate γ -inert-sterilized (conventional) UHMWPE cores and air-impermeable packaging to improve oxidation resistance and thus enhance the wear performance of the cores [19, 45]. The ProDisc-L (DePuy Synthes Spine, West Chester, PA, USA) and CHARITÉ (originally Waldemar Link, Hamburg, Germany, later fabricated by DePuy Spine, Raynham, MA, USA, and

currently discontinued) are two established contemporary designs. The biomaterials used in the fabrication of the ProDisc-L prosthesis are quite similar to the CHARITÉ as they both consist of two CoCr alloy endplates articulating against a conventional UHMWPE core component. Although the materials used in these L-TDRs are similar, there are differences in the design of these implants. Unlike the mobile-bearing design of the CHARITÉ, the core of ProDisc-L is fixed through a locking mechanism into the inferior endplate, thus allowing relative motion only between the core and the superior endplate [18]. Other contemporary L-TDRs designs currently in clinical use are the Mobidisc (LDR Spine, Troyes, France) and Activ-L (Aesculap AG, Tuttlingen, Germany), which use similar biomaterials in fabrication but differ specifically from the CHARITÉ in the amount of constraint presented by the bearing. To our knowledge, only one case report has evaluated retrievals of Mobidisc and Activ-L from two patients [2], and there is still limited understanding of implant wear or periprosthetic tissue reactions for contemporary MoP L-TDRs. Additionally, it remains unclear whether the L-TDR design will influence the generation of UHMWPE particles and their associated biologic response.

In this study, we analyzed retrievals of two contemporary designs of fixed-bearing and mobile-bearing L-TDRs to evaluate γ -inert-sterilized UHMWPE performance *in vivo* and to compare design differences. We asked: (1) are periprosthetic UHMWPE wear debris and associated biological responses present in tissues from revised contemporary MoP L-TDRs that contain cores fabricated from γ -inert sterilized UHMWPE; (2) what is the influence of bearing design (i.e., fully

mobile versus fixed designs) on wear particle number, size, and shape; and (3) how do the detectable wear UHMWPE particles from contemporary MoP L-TDRs compare with historical MoP L-TDRs that contain cores fabricated from γ -air-sterilized UHMWPE?

3.3 Materials & Methods

3.3.1 Tissue Collection & Patient Clinical Information

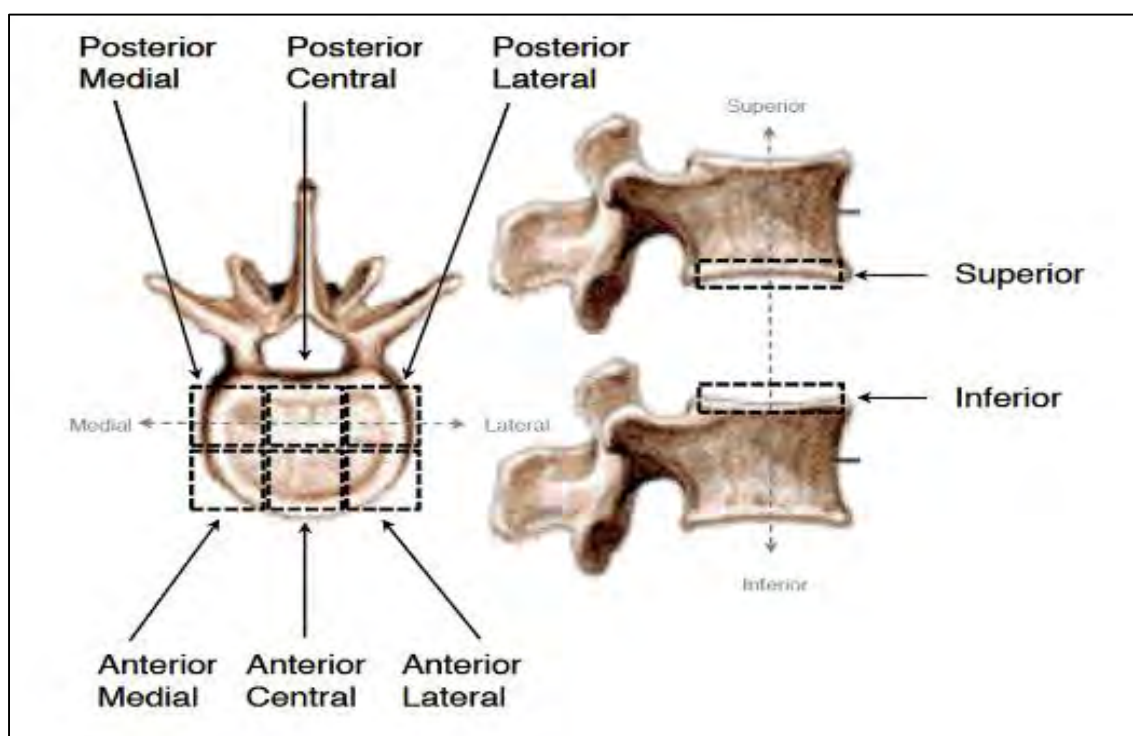


Figure 3-1. Tissues are harvested from annular regions during L-TDR revision surgery.

Spine tissues from regions adjacent to the implanted device were obtained at the time of revision surgery (Figure 3-1). Tissues, along with their respective devices, were collected as part of a public, multicenter retrieval research program initiated in 2004 [17, 22]. Contemporary TDRs were classified as modern device designs incorporating components made of γ -inert-sterilized UHMWPE GUR 1020 resin; this

study investigated tissue retrievals from around two contemporary lumbar designs: the fixed-bearing ProDisc-L and mobile-bearing CHARITÉ. The fixed-bearing L-TDR cohort included seven patients and eight implants (implantation time, 1-6 years; mean, 4.1 years), whereas the mobile-bearing cohort included four patients and four implants (implantation time, 2-3 years; mean, 2.7 years). All were primarily revised for persistent back and/or leg pain and, for two of the patients, osteolysis was observed (Table 3-1). Implant subsidence or migration was a complication noted in three patients with fixed-bearing and one patient with mobile-bearing L-TDRs (Figure 3-2). Primary surgical tissues were obtained from other L-TDR patients and served as controls. Quantitative findings on particle number and were compared to our previous findings for 16 patient tissue responses from revised historical TDRs, SB CHARITÉ III, in which the core was either γ -air-sterilized UHMWPE GUR 412 resin or γ -inert-sterilized UHMWPE GUR 1020 resin with polymer barrier packing that allowed exposure to air [32].



Figure 3-2. Sagittal CT scan illustrating implant subsidence at the L4 level on the right side of the vertebra from a fixed-bearing L-TDR patient (BHSP023).

Table 3-1. Clinical information of MoP L-TDR retrievals

Patient ID	Device	Bearing design	Patient sex	Age at implantation (years)	Primary diagnosis	Level	Year of index surgery	Year of removal surgery	Implantation time (years)	Revision reason(s)	Complications	Osteolysis
BHSP 022	ProDisc-L	Fixed	Male	41	Herniated disc; lumbar pain/radiculopathy	L4-L5	2007	2012	5.0	Right L4-L5 arthropathy; facet pain; progressive degeneration; radiculopathy		Yes
BHSP 023	ProDisc-L	Fixed	Male	56	Herniated disc; lumbar pain/radiculopathy	L4-L5	2009	2012	3.0	Increasing pain in the back, lower back and left quad	Subsidence	Yes
BHSP 025a BHSP 025b	ProDisc-L ProDisc-L	Fixed Fixed	Male	49	Disc degeneration; discogenic back pain	L4-L5; L5-S1	2009	2013	4.0	Severe pain	Posterior migration; compressing nerve roots	No
BHSP 026	ProDisc-L	Fixed	Female	N/A	N/A	L5-S1	N/A	2012	N/A	Persistent pain		No
BHSP 027	ProDisc-L	Fixed	Female	33	Herniated disc w/degeneration; back pain	L4-L5	2008	2013	5.0	Lumbar pain; radiculopathy		No
BHSP 0032	ProDisc-L	Fixed	Male	46	N/A	L5-S1	2008	2014	6.0	Severe lower back pain; L4-L5 disc injury; radiculopathy	Subsidence; upper level degeneration	No
PDL 004	ProDisc-L	Fixed	Female	27	Unremitting lower back pain	L5-S1	2008	2009	1.3	Pain; ventral encroachment into spinal canal	Partial dissociation	No
BRSP 003	CHARITÉ	Mobile	Male	28	Disc degeneration	L4-L5	2006	2008	1.5	Discogenic pain		No
BRSP 004	CHARITÉ	Mobile	Female	22	Disc degeneration	L5-S1	2004	2008	3.3	Discogenic pain		No
BRSP 006	CHARITÉ	Mobile	N/A	N/A	Disc degeneration	L4-L5	2005	2008	2.7	Painful instrumentation	Subsidence; scarring in disc space	No
BRSP 007	CHARITÉ	Mobile	N/A	N/A	Painful retained hardware	L5-S1	2005	2008	3.3	Pain	Periprosthetic scarring	No

MoP = metal-on-polyethylene; L-TDR = lumbar total disc replacement; N/A = not available

3.3.2 Implant Retrieval Analysis

All implants were cleaned with 10% bleach and examined under a stereomicroscope equipped with a digital camera (Leica DFC490, Wetzlar, Germany) to assess surface damage and gross fracture. All components were inspected to identify surface damage mechanisms (plastic deformation, scratching, burnishing, pitting, and embedded debris). Select implant components with macroscopic surface damage were further analyzed using scanning electron microscopy (SEM; Supra 50 VP, Zeiss Peabody, Massachusetts) to identify specific wearing patterns and distinguish any iatrogenic damage introduced by the surgeon during the retrieval process. Lastly, Energy-dispersive X-ray spectroscopy (EDS) was utilized to detect and identify any abnormal surface deposits on implant components, whereas x-ray fluorescence (XRF) was used to conduct elemental analysis on the interior of the metallic endplates to ensure they met the American Society for Testing and Materials (ASTM) weight standards.

3.3.3 Tissue Preparation and Histological Analysis

Tissues collected from revision and primary surgeries were fixed in either formalin or Universal Molecular Fixative (UMFIX; Sakura Finetek USA, Inc, Torrance, CA, USA). One to two 4-mm punches from each tissue, considering variations in color, texture, and size of specimen, were embedded in paraffin blocks, and 6- μ m serial sections were mounted onto ProbeOnPlus (Fischer Scientific Co, Pittsburgh, PA, USA) slides. Slides were dewaxed, rehydrated, and stained with hematoxylin,

and eosin (H&E) (ThermoFisher Scientific, Waltham, MA) to visualize the nucleic acids, extracellular matrix and other proteins in the tissue sections. The alcian blue stain (Electron Microscopy Sciences, Hatfield, PA) was also used in conjunction with H/E to detect cartilaginous regions. Subsequently, Wright-Giemsa (Electron Microscopy Sciences, Hatfield, PA) and Prussian blue (Electron Microscopy Sciences, Hatfield, PA) stains were used for further in-depth histological evaluation when inflammation was present to facilitate the differentiation of leukocytes and identify hemosiderin deposits, respectively. Transmitted and polarized light images were captured using an Olympus BX50 microscope (Olympus, Melville, NY, USA) equipped with a stepper motor-controlled stage, an elliptically polarized light imaging system, and a Jenoptik ProgRes Speed XT Core5 camera (Jenoptik, Jena, Germany). A 36-image (200X magnification) composite, that spanned the entire tissue section, was created for each section under transmitted light to grade tissue reactions by at least two individuals (SYV, MJS) using a scoring system scaled from 0 to 3 (Table 3-2). The scoring criteria were based on the Oxford method that is presently used for grading total joint arthroplasty tissues for macrophage and lymphocyte inflammation, aseptic lymphocyte-dominated vasculitis associated lesion (ALVAL), and necrosis [8, 31], but modified to exclude ALVAL responses to metal wear debris and include hemosiderin deposition and vascularization, which are more predominant in spine tissue. This criteria allowed us to make semi-quantitative comparisons to previous research using similar grading scales for periprosthetic inflammatory responses.

Table 3-2. Modified Oxford scoring criteria for grading biological responses in periprosthetic tissues of L-TDRs

Score	Necrosis	Hemosiderin	Innate Inflammation		Vascularization	
	Tissue Percent Area	Tissue Percent Area	Number of Cells	Tissue Percent Area	Number of Blood Vessels	Tissue Percent Area
0+	0	0	0	0	0	0
1+	Scattered or Isolated	< 10	1-9	< 10	< 10	< 10
2+	< 25	10-50	10-50	10-50	10-50	10-25
3+	> 25	> 50	> 50	> 50	> 50	> 25

3.3.4 Wear Particle Characterization

For UHMWPE particle analysis, a 36-image (200X magnification) composite was created from each tissue section under polarized light that corresponded to the transmitted light tissue composites. Our polarized light microscopy enabled us to detect particles as small as 0.34 μm . In each individual image, UHMWPE wear particle number, size, and shape were determined by first using a customized image threshold operation programmed in MATLAB® (MathWorks Inc, Natick, MA, USA) followed by counting/measuring particles using NIH ImageJ (National Institutes of Health, Bethesda, MD, USA) (Figure 3-3). In brief, polarized light images were split into three eight-bit channels (red, green, and blue). Signal from blue channels were converted into masks based on a threshold value relative to the average signal intensity of each image. All images were visually reviewed to ensure that false-



Figure 3-3. Representative images of L-TDR periprosthetic tissues with wear particles under polarized light (left) followed by thresholding for UHMWPE particles in MATLAB (right).

positive signals from birefringent collagen or dust did not contribute to particle counts. The resulting particle number was then converted to number/mm² area of tissue using a measured conversion factor of 3.887 $\mu\text{m}/\text{pixel}$. Initial validation of this technique was performed using an environmental scanning electron microscope (ESEM) to study histomorphologic changes and wear debris in periprosthetic tissues of THAs [3]. Particle size and shape were characterized by calculating the equivalent circular diameter (ECD) (Equation 3-1), aspect ratio (Equation 3-2) and perimeter-based-circularity (Equation 3-3); the use of these measurements for particle analysis was validated in an earlier study by Baxter et al [4] and compared to ASTM guidelines for particle characterization [1].

$$ECD = \sqrt{4 \times A(p) / \pi}$$

Equation 3-1. Equivalent circular diameter (ECD) (μm), where $A(p)$ is the area of the particle, represents the diameter of a circle that occupies the same two dimensional surface area as the particle. ECD provides a standardized measure of particle size [30].

$$AR = \frac{L(p)}{W(p)}$$

Equation 3-2. Aspect ratio (AR) (unitless), where L(p) is the particle length and W(p) is the particle breadth, represents the proportional relationship between length and breadth. AR provides a standardized measure to classify the general form of particles (e.g. equant, acicular or fibrous) [30].

$$C = \frac{4 \times \pi \times A(p)}{P^2}$$

Equation 3-3. Circularity (C) (unitless), where A(p) is the area of the particle and P is the perimeter, represents the degree (from 0 to 1) to which the particle is similar to a circle based on the smoothness of the perimeter. C provides a measure for both particle form and roughness [30].

3.3.5 Statistical Analysis

Descriptive statistics were used for evaluating wear debris-induced tissue responses, which were semi-quantitatively compared based on histology/tissue scores. When quantifying UHMWPE particle numbers, the total number of particles in all tissue sections for each patient was normalized to total tissue sectional area, minimizing the effect of region-specific heterogeneity of particle distribution (Figure 3-4). Size and shape measurements of particles were averaged for each patient when detectable wear debris was present. To statistically compare UHMWPE particle number, ECD, perimeter, circularity, and aspect ratio between the two different bearing designs, the Mann-Whitney U-test was employed using IBM SPSS Statistics V22 software package (IBM Corporation, Armonk, NY, USA). Significance was based on $p < 0.05$. Because we were unable to detect statistical differences in particle measurements between the two bearing designs, fixed- and mobile-bearing patients were combined into a single contemporary L-TDR cohort before comparing it with the historical L-TDR cohort. To compare these two groups,

the Mann-Whitney U-test was used to test differences in UHMWPE particle number, circularity, and aspect ratio. Particle size measurements of ECD (mean, $2.71\mu\text{m} \pm 4.29$) and perimeter (mean, $11.07\mu\text{m} \pm 27.54$) were not statistically analyzed because particles larger than $2\mu\text{m}$ were not evaluated in the historical L-TDR cohort.

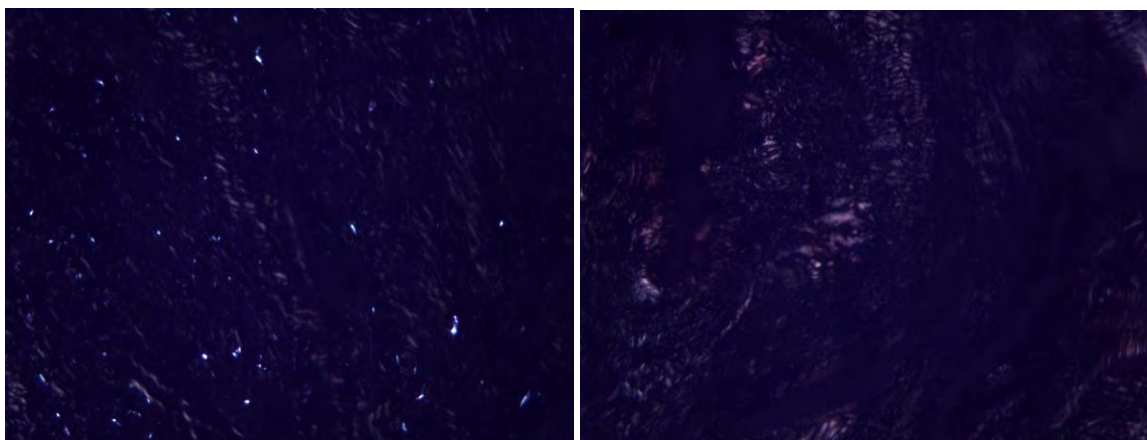


Figure 3-4. Patient tissues with detectable wear debris had a heterogeneous distribution of particles as illustrated by significant debris in the lateral tissue from patient BHSP027 (left, 200X), but no debris in other regions of same tissue (right).

3.4 Results

3.4.1 Device Retrieval Analysis for Contemporary L-TDRs

The eight fixed-bearing L-TDRs (implantation time, 1-6 years; mean, 4.1 years) exhibited minor to moderate signs of implant damage after discounting iatrogenic markings that were induced inadvertently by the surgeon. All eight cores from the seven patients (100%) showed evidence of burnishing and mild abrasive scratching on the bearing surfaces (Figure 3-5). In addition, impingement was noted in two of eight implants (25%) from two different patients with malpositioning, and the respective components evidenced plastic deformation (Figure 3-5). Microscopic scratches of fan-shaped pattern were found on the interior of these metallic plates



Figure 3-5. Representative fixed-bearing L-TDR retrieval components (top). All fixed-bearing UHMWPE cores showed evidence of burnishing (green arrow) and mild abrasive scratching (blue arrow). Impingement was noted in two patients and the respective components evidenced plastic deformation (red arrow).

and a glossy appearance on the polyethylene core, respectively. SEM images of the impinged regions showed a polished appearance in comparison to the as-manufactured texture seen in non-impinged regions of the metallic plate (Figure 3-6). The unidirectional and circumferential wear patterns seen on the endplates suggest the wear may have occurred during axial rotation and/or lateral bending of

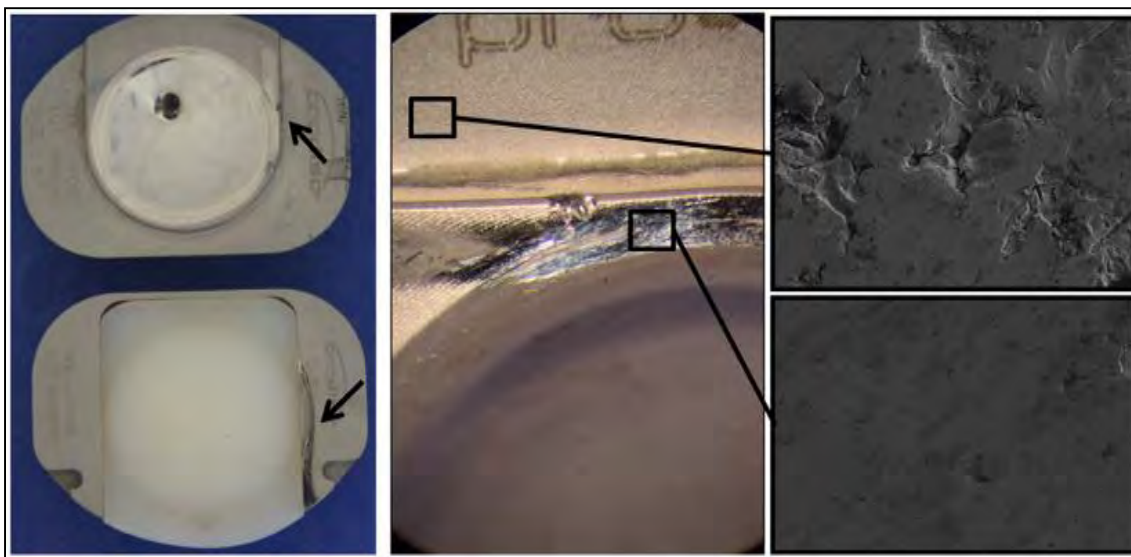


Figure 3-6. Representative fixed-bearing retrieval with impinged regions on both endplates (black arrows). SEM images showed the impinged region on the metallic plate (lower right) had a smooth surface compared to the unimpinged region (upper right).

the articulating surfaces. Lastly, all fixed-bearing retrievals showed no indications of fatigue wear or fracture of the polyethylene core. No abnormal surface deposits were observed by SEM/EDS analysis. XRF scans showed the metallic surface-constituents on the interior of the endplates consistently matched CoCr ratios seen in ASTM F-75 cobalt alloy standards, and the exterior of plates consisted of weight compositions seen in commercially pure titanium.

The four mobile-bearing L-TDRs (implantation time, 2-3 years; mean, 2.7 years) exhibited minor signs of implant damage after discounting iatrogenic markings. Two of four mobile bearing cores showed signs of burnishing, pitting and mild scratching (Figure 3-7). Minor unidirectional scratches were present on the endplates from all patients. There were no obvious signs of impingement on the metallic endplates. Analysis using SEM and EDS revealed no abnormal surface deposits on the metallic endplates. As expected, XRF scans consistently detected cobalt-chromium ratios matching ASTM F-75 cobalt alloy weight-standards in the interior of the endplates.



Figure 3-7. Representative mobile-bearing L-TDR retrieval components (top). Two of four patients with mobile-bearing UHMWPE cores showed evidence of burnishing, pitting (green arrow). Minor unidirectional scratches were noted on endplates from all patients (red arrow).

3.4.2 UHMWPE Wear Debris from Contemporary L-TDRs & Biological Tissue Responses

Periprosthetic UHMWPE wear debris with corresponding macrophage infiltration was observed in five of seven patients with a fixed-bearing L-TDR and one of four patients with a mobile-bearing L-TDR. Generally, detectable wear debris was associated with low to moderate biological tissue responses as compared to tissues (controls) from L-TDR patients undergoing primary surgery (Figure 3-8). For the fixed-bearing L-TDR revisions, tissues from three of seven (43%) patients

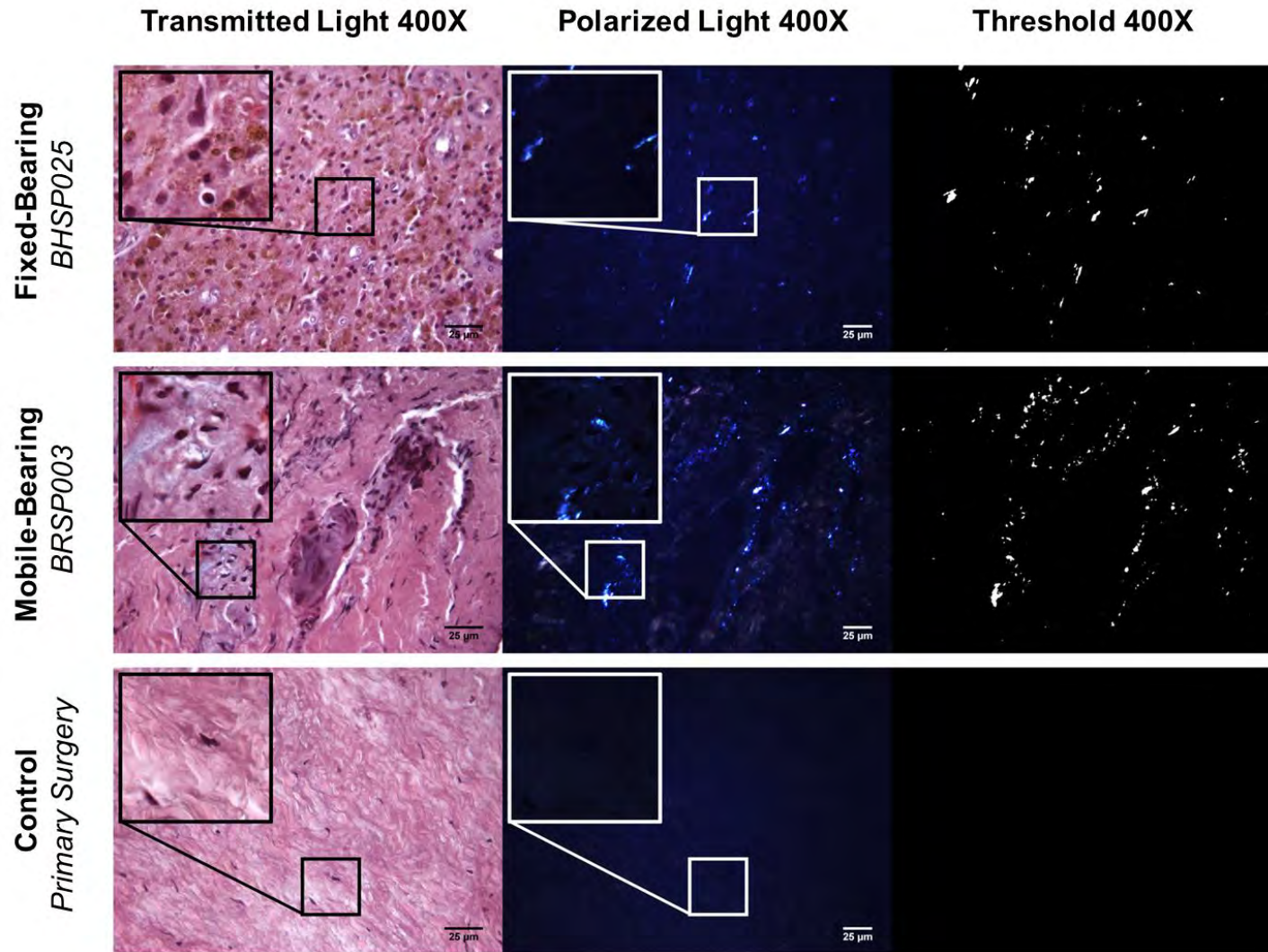


Figure 3-8. Transmitted light images (left) and polarized microscopy (middle) of tissue sections revealed the presence of UHMWPE wear and corresponding macrophage infiltration; particles were characterized using a MATLAB threshold (right).

Table 3-3. Histologic evaluation and mean scores of retrieved tissues with wear debris

Patient ID	Implant bearing design	Tissue samples with wear debris	UHMWPE wear debris (particles/mm ²)	Metal wear debris	Inflammation (macrophages)	Type of inflammatory cells	Necrosis	Hemosiderin	Vascularization
BHSP 022	Fixed	2/4	4.27	No	0.5	Macrophages	1.0	0.5	0
BHSP 023	Fixed	6/14	4.78	Yes	1.7	Predominantly macrophages with lymphocytes and plasma cells	0.9	1.2	1.3
BHSP 025a	Fixed	2/6	21.82	Yes	2.0	Predominantly macrophages with lymphocytes and plasma cells	1.5	2.0	2
BHSP 025b	Fixed	6/12	1.74	Yes	1.8	Predominantly macrophages with lymphocytes and plasma cells	0.0	1.7	2.5
BHSP 027	Fixed	3/6	29.12	No	1.7	Macrophages	0.5	0.0	1.5
BHSP 0032	Fixed	1/1	15.03	Yes	1.5	Predominantly macrophages with lymphocytes	1.0	0.0	2.5
PDL 004	Fixed	1/3	20.91	No	0.0	None	1.0	0.0	0
BRSP 003	Mobile	1/4	107.33	No	3.0	Macrophages	1.0	0.0	1

Inflammation, necrosis, hemosiderin, and vascularization scores on a 0-3 scale.

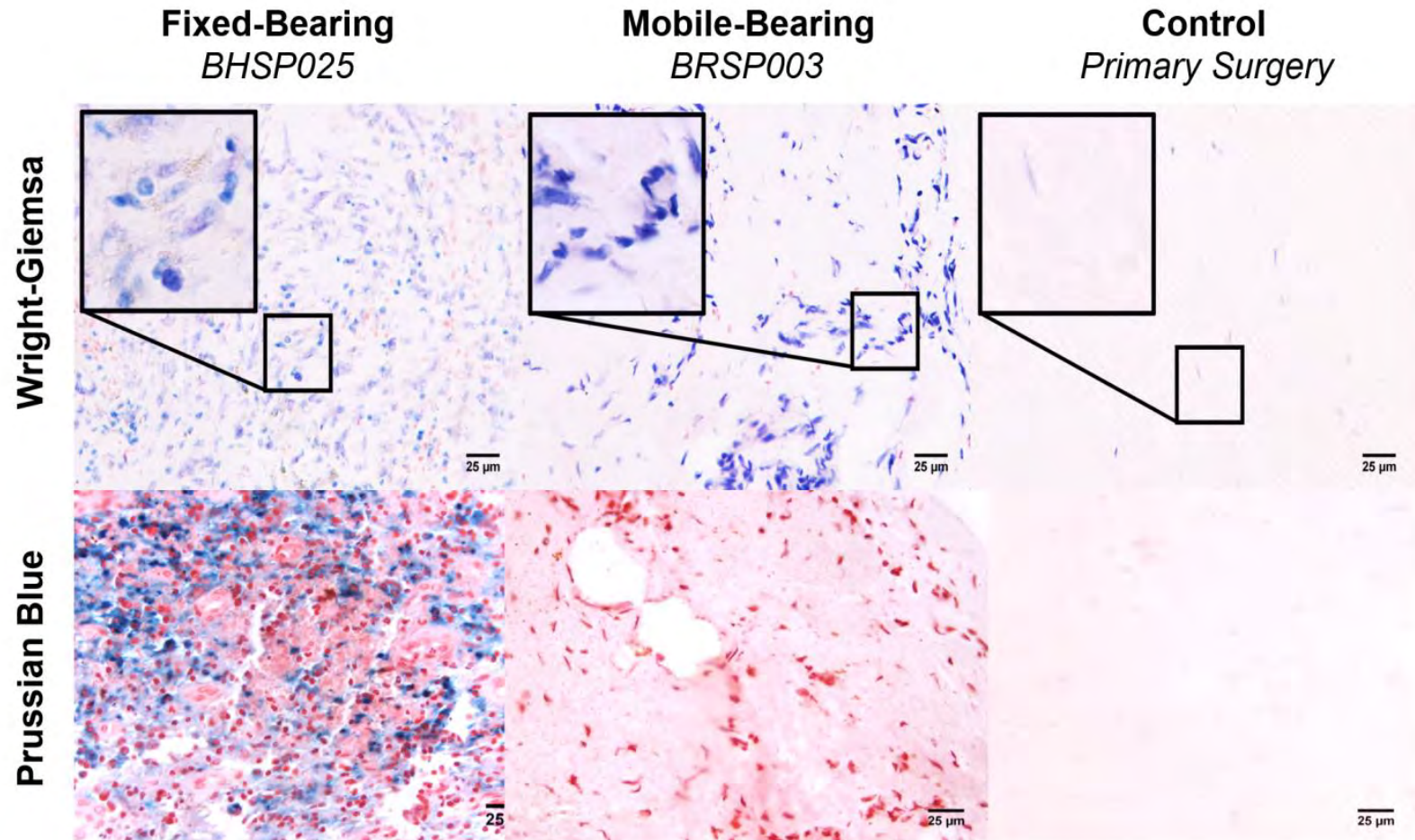


Figure 3-9. Wright Giemsa and Prussian blue stains were used to identify inflammatory cells and hemosiderin deposits, respectively. Both fixed-bearing (left) and mobile-bearing (middle) tissues showed inflammatory infiltrates, but hemosiderin deposits were also found in fixed-bearing cohorts. There was no inflammation or hemosiderin present in control tissue (right) obtained from primary surgery (Original magnification x 400; inset, x 1000).

contained at least 15 UHMWPE particles/mm² with an associated macrophage infiltration score > 1.5 (Table 3-3). Tissues from the two other patients (29%) contained < 5 UHMWPE particles/mm² and a variable macrophage infiltration (0.5 and 2). Tissues with UHMWPE wear debris from patients BHSP 023 and BHSP 025, who had their implants revised for malpositioning and device impingement, also had some isolated regions containing metal wear debris, lymphocytes, plasma cells, and hemosiderin that occupied > 10% of the total tissue area (Figure 3-9). Another tissue with UHMWPE wear debris from patient BHSP 0032 also contained metal particles and lymphocytes but no hemosiderin deposits. Patient PDL 004 had one tissue sample with an isolated area containing 21 UHMWPE particles/mm² but no detectable inflammation. For the mobile-bearing L-TDR cohort, tissue that contained detectable UHMWPE wear debris (> 0.34 μ m) was found in only one of four patients. None of the tissues associated with the mobile-bearing devices contained metallic debris, and none of the implants exhibited rim impingement. A tissue sample from patient BRSP 003 contained 107 UHMWPE wear particles/mm² and it had a high macrophage infiltration score (3.0). For the fixed-bearing cohort, tissues with wear debris were consistently more vascularized with mean scores as high as 3 (range, 0-3), whereas necrotic/acellular regions were scarce (Figure 3-10). In contrast, the majority of tissue samples around the devices that did not contain detectable wear debris had low vascularity and more prominent regions of necrosis (mean necrosis score, 2) (Table 3-4). Tissues around mobile-bearing devices, with or without detectable wear, were moderately vascularized with isolated necrotic regions.

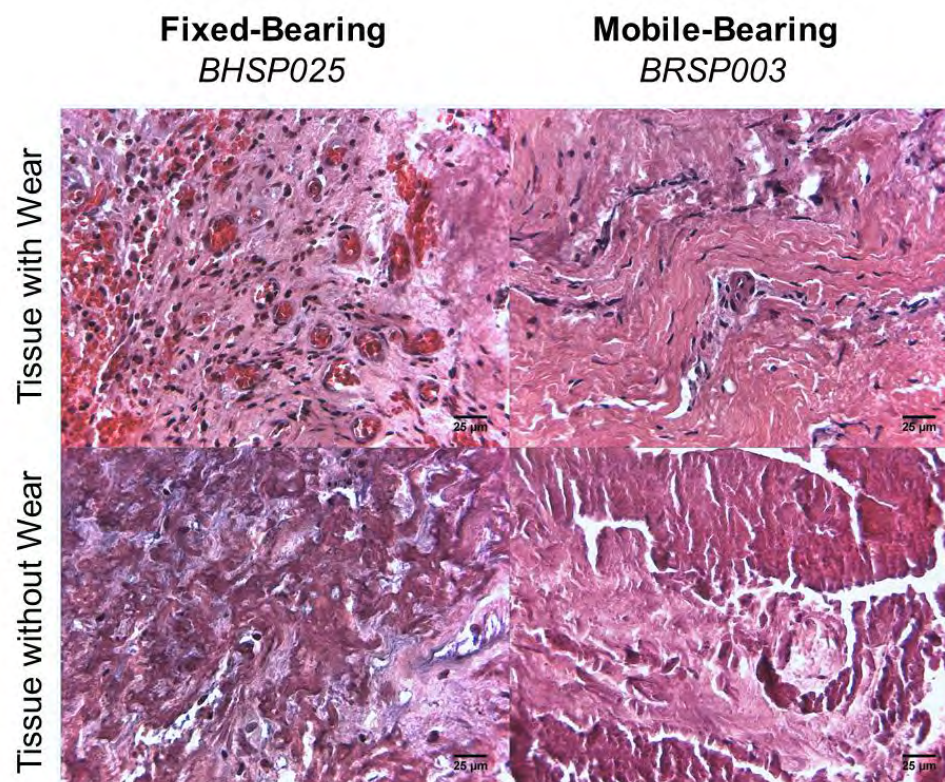


Figure 3-10. Representative fixed-bearing L-TDR tissue images showed increased vascularization (top left) in tissues with wear debris and regions of necrosis (bottom left) in tissues without wear debris. Mobile-bearing L-TDR tissues had lower vascularization (top right) in tissues with wear debris and a mix of moderate vascularization and isolated necrosis (bottom right) in tissues without wear debris (Original magnification, x 400).

3.4.3 Wear Particle Number, Size & Shape for Contemporary L-TDRs

In general, L-TDRs patient tissues collectively had limited wear debris and the majority were small ($< 10 \mu\text{m}$) with low aspect ratio and high circularity (Figures 3-11, 3-12, 3-13). For the mobile-bearing L-TDR patient tissue with UHMWPE wear debris, particle number was increased by 87% compared to fixed-bearing patient tissues, and the particles were 11% rounder and 11% less elongated (Table 3-5), but, with the number of samples available, these differences were not significant. Qualitative observations revealed the area percentage or amount of

Table 3-4. Histologic evaluation & mean scores of retrieved tissues without wear

Patient ID	Implant bearing design	Tissue samples without wear debris	Necrosis	Hemosiderin	Vascularization
BHSP 022	Fixed	2/4	0.5	0.5	0.0
BHSP 023	Fixed	8/14	1.2	0.8	0.8
BHSP 025a	Fixed	4/6	2.0	0.0	0.0
BHSP 025b	Fixed	6/12	1.0	1.0	1.2
BHSP 026	Fixed	4/4	0.8	0.8	1.0
BHSP 027	Fixed	3/6	1.5	0.0	0.0
PDL 004	Fixed	2/3	1.0	0.0	0.0
BRSP 003	Mobile	3/4	0.7	0.0	1.0
BRSP 004	Mobile	4/4	0.5	0.0	1.5
BRSP 006	Mobile	6/6	0.7	0.0	1.3
BRSP 007	Mobile	2/2	0.0	0.0	0.0

Note: Necrosis, hemosiderin, and vascularization scores on a 0-3 scale.

tissue occupied by particles from the mobile-bearing device was more extensive than the particles from fixed-bearing devices with the exception of tissues from patient BHSP 022, which contained large ($> 10 \mu\text{m}$) particles (highest ECD and perimeter values). Nonetheless, the overall distribution of particle sizes was similar for both cohorts. The majority of the particles were between 1 and $10 \mu\text{m}$ (75% and 83% for the fixed-bearing and mobile-bearing L-TDR cohorts, respectively). Submicron particles ($< 1 \mu\text{m}$) represented 20% of the particles from fixed-bearing devices and 16% from the mobile-bearing device. Large particles ($> 10 \mu\text{m}$) were rarely observed and represented less than 2% of the particles in both cohorts.

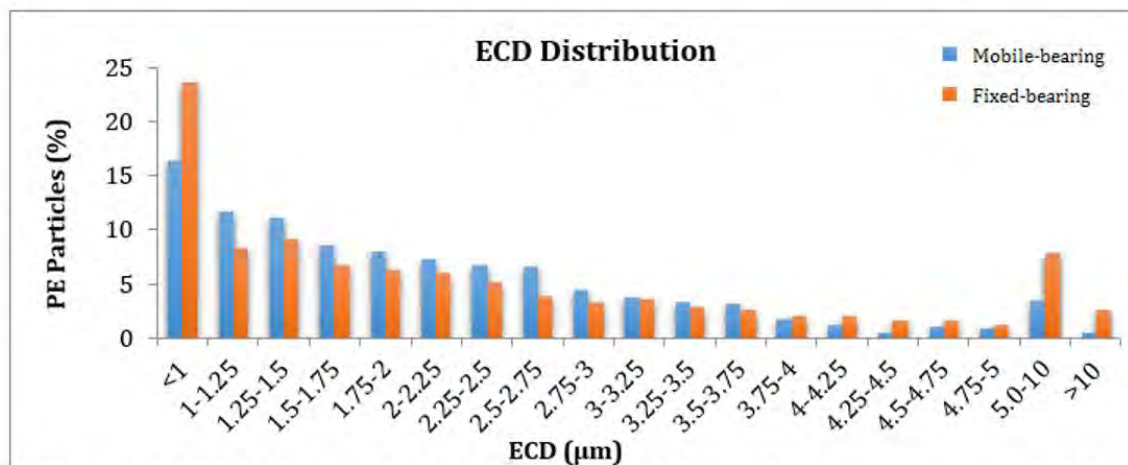


Figure 3-12. Equivalent circular diameter size distribution for wear particles in fixed- and mobile-bearing L-TDR tissues

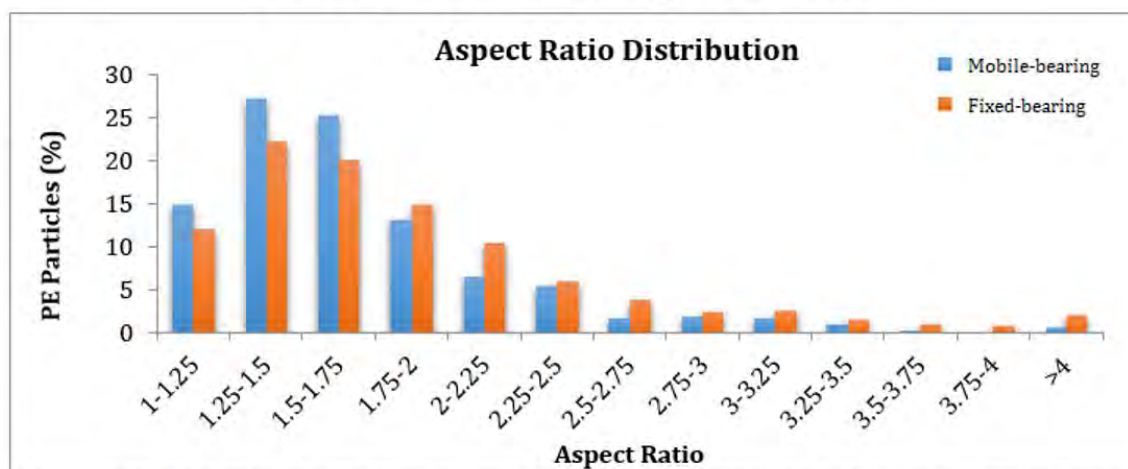


Figure 3-13. Aspect ratio distribution for wear particles in fixed- and mobile-bearing L-TDR tissues

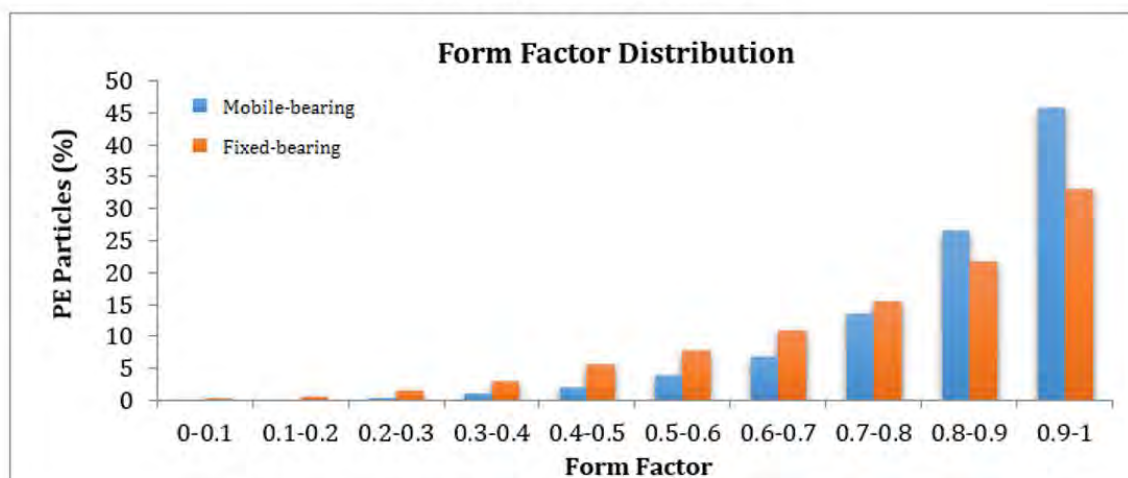


Figure 3-14. Circularity distribution for wear particles in fixed- and mobile-bearing L-TDR tissues

Table 3-5. UHMWPE particle number and characteristics from tissues with wear debris

Patient ID	Implant bearing design	Tissue samples with wear debris	< 0.1-1 μ m (particles/mm ²)	1-10 μ m (particles/mm ²)	> 10 μ m (particles/mm ²)	All sizes (particles/mm ²)	Percent area of particles*	Equivalent circular diameter (μ m)	Perimeter (μ m)	Circularity	Aspect ratio
BHSP 022	Fixed	2/4	0.52	3.14	0.61	4.27	0.12%	6.64 \pm 10.78	28.05 \pm 47.09	0.74 \pm 0.20	1.76 \pm 0.54
BHSP 023	Fixed	6/14	1.15	3.13	0.51	4.78	0.05%	2.68 \pm 5.63	13.43 \pm 39.45	0.67 \pm 0.25	2.02 \pm 0.99
BHSP 025a	Fixed	2/6	4.69	16.70	0.44	21.82	0.03%	2.90 \pm 3.12	11.95 \pm 19.13	0.76 \pm 0.19	1.93 \pm 0.74
BHSP 025b	Fixed	6/12	0.15	1.52	0.06	1.74	0.02%	2.60 \pm 2.71	10.31 \pm 15.69	0.80 \pm 0.18	1.85 \pm 0.67
BHSP 027	Fixed	3/6	6.78	21.79	0.55	29.12	0.07%	2.86 \pm 5.24	11.82 \pm 38.18	0.80 \pm 0.18	1.90 \pm 0.77
BHSP 0032	Fixed	1/1	2.55	10.57	1.28	15.03	0.06%	3.78 \pm 4.65	8.43 \pm 11.45	0.77 \pm 0.20	1.87 \pm 0.82
PDL 004	Fixed	1/3	4.55	15.91	0.45	20.91	0.02%	2.28 \pm 2.40	8.44 \pm 11.43	0.86 \pm 0.17	1.56 \pm 0.44
BRSP 003	Mobile	1/4	17.68	89.12	0.54	107.33	0.11%	2.23 \pm 2.85	8.16 \pm 14.11	0.86 \pm 0.14	1.70 \pm 0.53

*Percent area of particles is the ratio of the total area of all particles to the total area of tissue; † mean \pm SD.

Table 3-6. Comparing UHMWPE particle number and characteristics in patients with wear debris

Comparison	Fixed-Bearing L-TDR	Mobile-Bearing L-TDR	Contemporary L-TDR (Fixed and Mobile)	Historical Mobile-Bearing L-TDR* (Punt et al., 2011) [30]
UHMWPE core	γ -inert-sterilized	γ -inert-sterilized	γ -inert-sterilized	γ -air-sterilized
Patients with wear debris (number)	6 of 7	1 of 4	7 of 11	5 of 5
Particle number** (particles/g x 10 ⁷ ; mean \pm SD)	1.16 \pm 3.09	8.99	2.14 \pm 2.90†	162.10 \pm 27.10
Circularity (mean \pm SD)	0.78 \pm 0.20	0.86 \pm 0.15	0.80 \pm 0.19†	0.40 \pm 0.20
Aspect ratio (mean \pm SD)	1.88 \pm 0.76	1.70 \pm 0.53	1.84 \pm 0.71	2.00 \pm 0.10

*Particle measurements were generated using ESEM and a cutoff of 2 μ m so size characteristics were not comparable; **Measurements from contemporary L-TDR cohorts were converted from particles/mm² for comparison purposes; L-TDR = lumbar total disc replacement; SD = standard deviation; N/A = not available; ESEM = environmental scanning electron microscope. †Significant differences between combined contemporary L-TDRs and historical L-TDRs (p < 0.01)

3.4.4 Comparison of Wear Particle Characteristics to MoP Historical L-TDRs

Compared to five historical L-TDR patients identified in a previous study [32], UHMWPE particle number and circularity in the seven contemporary L-TDR patient tissues were significantly different, but aspect ratio was not (Table 3-6). Specifically, the number of particles per gram of tissue was 99% less ($p = 0.003$) and their shape was 50% rounder ($p = 0.003$) in contemporary L-TDR cohorts, which included both fixed- and mobile-bearing designs. Qualitative observations of particle size revealed that tissues from contemporary L-TDR patients contained more submicron and small ($< 10 \mu\text{m}$) wear debris and less associated inflammation in comparison to the historical L-TDR cohort.

3.5 Discussion

L-TDR was developed as an alternative to spinal fusion for the treatment of degenerative disc disease in the lumbar spine, and is a device that preserves or restores segmental function and motion. However, historical generations of L-TDR devices with γ -air-sterilized UHMWPE cores raised concerns regarding wear debris generation and subsequent immunological responses that may adversely affect clinical outcomes. Today, modern L-TDR designs incorporate purely γ -inert-sterilized UHMWPE cores to improve wear resistance and minimize wear debris generation in an effort to reduce the risk of revision surgery. The aims of this study were to evaluate wear debris and biological responses in tissues from revised contemporary MoP L-TDRs and determine the influence of bearing design on wear particle number, size, and shape. Furthermore, we wanted to know how UHMWPE

wear particle densities and characteristics compared with previous historical MoP L-TDRs. After analyzing retrieved tissues around eight fixed- and four mobile-bearing L-TDRs from 11 patients revised primarily for pain, we found measurable UHMWPE wear debris with corresponding macrophage infiltration in five patients that had fixed-bearing L-TDRs and one patient that had a mobile-bearing L-TDR. The frequency, amount, and shape of wear debris suggested the bearing design of contemporary devices did not influence wear particle characteristics. Furthermore, particle comparisons with a retrieval study of historical devices suggested that γ -inert-sterilized UHMWPE has improved wear resistance and as a result reduced wear-induced periprosthetic tissue reactions.

Not all periprosthetic tissue from the two contemporary MoP L-TDRs examined in this study contained detectable UHMWPE wear debris ($> 0.34 \mu\text{m}$); this was true for tissues from all patients and different tissues from the same patient. However, those tissues that contained UHMWPE wear debris generally had an associated macrophage inflammation. This type of co-localization of wear debris and macrophages is an established phenomenon in total joint arthroplasty and more recently noted in historical L-TDRs [34]. One noteworthy difference observed for the contemporary L-TDRs was a decrease in particles $> 10 \mu\text{m}$ and as a result; unlike historical L-TDRs, giant cells were not observed in these tissues. Periprosthetic UHMWPE particles from both contemporary L-TDR cohorts resulted primarily in a macrophage response, except for three patients with metallic wear debris from fixed-bearing devices where an associated lymphocytic response was observed. These patient tissues also had higher macrophage infiltration scores. The presence

of metallic debris may be attributed to the unintended wear mechanism of impingement between the metallic endplates arising from malpositioning and/or subsidence, which was noted in more than 50% of contemporary fixed-bearing device retrievals in a separate retrieval study [23]. Interestingly, considerable amounts of hemosiderin were present in many of these tissues, indicative of phagocytosis of erythrocytes and degradation of hemoglobin by macrophages [16, 39]. The exact contribution of hemosiderin to revision remains unclear; however, a previous study has associated the deposition with the accumulation of activated macrophages that are positive for osteoclastic cell markers [28]. Although the amount of UHMWPE wear debris in the spine may not be severe enough to directly contribute to osteolysis [21], vertebral osteolysis was noted as a clinical complication in two patients with fixed-bearing L-TDRs, both of whom had tissues containing hemosiderin. The effect of hemosiderin in these tissues on UHMWPE wear-induced inflammation requires further investigation. Other biological tissue responses noted around the fixed-bearing devices included increased vascularization in tissues with wear and necrosis in tissues without wear. In contrast, tissues around mobile-bearing L-TDRs, with and without detectable wear debris, had low to moderate vascularization and necrosis. The presence of these reactions in both cohorts is noteworthy because these reactions have been implicated in the development of pain. Specifically, increased vascularization and sensory nerve growth are closely linked processes [6, 27]; and tissue necrosis or cell death results in the release of proinflammatory cytokines and other factors that initiate persistent pain by directly activating nociceptive sensory neurons [7, 47].

Both reactions can lead to maladaptive plasticity and neural disease states, which raises the question whether these tissue responses contributed to neuropathic pain in both fixed- and mobile-bearing L-TDR patients.

While the observations and data did not explain why wear debris in patients lead to vascularization in some tissues and necrosis in others, we believe the amount of wear debris and the stage of inflammation contributed to pathological modes observed at fixation. It is important to note that nanometre-sized wear debris may still be present in tissues that were indicated for no debris due to our detection limitations ($>0.34 \mu\text{m}$) [36]; and also that particles can be cleared by the lymphatic system when the tissue matrix degenerates [10]. Furthermore, apparition of the inflammatory modes of vascularization and necrosis can depend on the nature and extent of the injury (e.g. wear-debris amount and length of exposure), along with the locale and cell types present in the region [41]. For example, tissue sections that were excised from deeper discal regions with severe wear-induced hypoxic conditions may reflect inflammation that led to ischemic necrosis; contrarily, inflammation and wear-induced hypoxia in outer layers of the disc with access to ingrowing blood vessels may lead to vascularization and more inflammation [14, 38, 41]. Nonetheless, with enough time, it is thought that all wear-induced tissue responses eventually lead to necrosis as inflammatory cells are unable to digest or enzymatically degrade UHMWPE wear particles [40].

UHMWPE wear debris in tissues around fixed-bearing devices qualitatively appeared smaller, less concentrated, and less round than debris in tissues around

the one mobile-bearing retrieval; however, no statistical difference was observed. Austen et al. recently reported a case study of two patients revised for a different set of fixed- and mobile-bearing contemporary L-TDRs, and observed larger UHMWPE particles in tissues from the patient with the mobile-bearing design [2]. Interestingly, retrieval studies of TKA also found comparable findings in which larger UHMWPE particles were found in tissues surrounding failed mobile-bearing TKRs than in tissues around failed fixed-bearing TKRs [11, 29]. Design-dependent differences in loading and wear mechanisms may explain observed qualitative differences of wear particles between designs. All fixed-bearing retrievals in our study showed signs of scratching on UHMWPE dome regions, and the tissues with metal wear corresponded with implant components that had metallic and endplate burnishing as a result of impingement attributable to malposition and/or subsidence. The mobile-bearing patient tissue retrieval with UHMWPE wear corresponded to an implant core that had burnishing, pitting, and unidirectional scratching. The overall density of UHMWPE particles was relatively low in tissues from both cohorts, but the majority were 1 to 10 μm , which falls within a size range that activates macrophages [9]. Lastly, the higher number and rounder particles observed in the mobile-bearing patient tissue may be influenced by the increased mobility of the core. The mobile-bearing implant design has 5 degrees of freedom (DOF) and its instant axes of rotation (IAR) more consistently matches the geometrical center of the UHMWPE core, whereas the fixed-bearing design has only 3 DOF and the IAR is not always as centered [37]. The differing kinematics of bearing design likely contribute to the different wear mechanisms that generate distinct particle amounts and morphology.

However, further research and larger sample sizes are necessary to determine whether design-dependent differences significantly influence particle size and shape differences.

UHMWPE particles from the contemporary L-TDR cohorts were less numerous and rounder in comparison to the historical L-TDR group, suggesting that modern L-TDR designs have improved wear properties. A separate study investigating particles $> 2 \mu\text{m}$ in historical L-TDR cohorts reported a mean of 231 particles/ mm^2 [33], which was roughly 10-fold higher than the amount of similar-sized particles from contemporary TDRs (mean, 22 particles/ mm^2). This comparison paralleled findings from a case report, which noted that the mean number of UHMWPE particles was two orders of magnitude lower in a different set of revised contemporary L-TDRs [2]. Our study also showed that mean particle circularity (roundness) was noticeably higher in the contemporary L-TDR cohort (mean, 0.8 versus mean, 0.4), but aspect ratios were within the same range as those of historical L-TDR particles [32]. Interestingly, UHMWPE particles from conventional THAs fabricated with γ -inert-sterilized UHMWPE acetabular liners have been reported to have shapes similar to the contemporary L-TDR group [4, 12, 13, 15, 26]. Multiple studies have reported that particles with more rounded morphologies trigger less robust macrophage activation compared with fibrillar-shaped particles [13, 35, 46]. Thus, with the samples available in this study, both the decreased number and increased roundness of the particles suggest that wearing of contemporary L-TDRs will result in a reduced inflammatory response.

In summary, the amount of wear debris and subsequent tissue responses were greatly reduced in tissues from contemporary L-TDRs when compared to historical L-TDRs. We showed that periprosthetic tissues from both fixed- and mobile-bearing L-TDR patients contained UHMWPE particles within size ranges known to elicit a macrophage response. Because artificial discs are intended to last the lifetime of the patient, further retrieval studies are still necessary to elucidate the long-term role of UHMWPE wear and its association, if any, to the clinical performance of lumbar disc arthroplasty.

3.6 Study Limitations

As any retrieval study, a few important limitations need to be noted. First, although the primary revision reason for all patients was pain, implant malpositioning and impingement were reported in three of six fixed-bearing and none of the mobile-bearing L-TDR patients. This complication may serve as a confounding variable when comparing the two designs. However, this discrepancy between the two cohorts may be viewed with a little skepticism given that the issue of impingement is not an uncommon finding for L-TDRs; it was previously reported for mobile-bearing L-TDR retrievals as well and contributed to wear debris generation and the immune responses [5]. Second, we were only able to investigate short-term revisions within 5 years of implantation, and of these retrievals, the implantation times varied between the fixed- and mobile-bearing cohorts. The times ranged from 1 to 6 years (mean, 4.1 years) for the fixed-bearing cohort and 2 to 3 years (mean, 2.7 years) for the mobile-bearing cohort, although both cohorts were

short-term revisions. Third, the cohort sizes were small and wear particle characteristics of mobile-bearing devices were extrapolated from particles that were observed in only one of four patients who had wear debris. Nevertheless, to our knowledge, there are no published retrieval studies for contemporary MoP L-TDRs. Lastly, comparisons of particle number and characteristics are provided for historical MoP L-TDRs; however, the previous study used ESEM and excluded wear particles larger than 2 μm , whereas in this study, we used polarized light microscopy and were able to detect particles as small as 0.34 μm . Although polarized light microscopy has been used in other related studies to investigate UHMWPE particles of particular sizes [33, 34], the different approaches make it difficult to make direct comparisons.

3.7 References

1. F 1877-05e Standard Practice for Characterization of Particles. *ASTM International*; 2005.
2. Austen S, Punt IM, Cleutjens JP, Willems PC, Kurtz SM, MacDonald DW, van Rhijn LW, van Ooij A. Clinical, radiological, histological and retrieval findings of Activ-L and Mobidisc total disc replacements: a study of two patients. *European spine journal : official publication of the European Spine Society, the European Spinal Deformity Society, and the European Section of the Cervical Spine Research Society*. 2012;21 Suppl 4:S513-520.
3. Baxter RM, Ianuzzi A, Freeman TA, Kurtz SM, Steinbeck MJ. Distinct immunohistomorphologic changes in periprosthetic hip tissues from historical and highly crosslinked UHMWPE implant retrievals. *Journal of biomedical materials research. Part A*. 2010;95:68-78.
4. Baxter RM, MacDonald DW, Kurtz SM, Steinbeck MJ. Characteristics of highly cross-linked polyethylene wear debris in vivo. *Journal of biomedical materials research. Part B, Applied biomaterials*. 2013;101:467-475.
5. Baxter RM, Macdonald DW, Kurtz SM, Steinbeck MJ. Severe impingement of lumbar disc replacements increases the functional biological activity of polyethylene wear debris. *The Journal of bone and joint surgery. American volume*. 2013;95:e751-759.

6. Brown MF, Hukkanen MV, McCarthy ID, Redfern DR, Batten JJ, Crock HV, Hughes SP, Polak JM. Sensory and sympathetic innervation of the vertebral endplate in patients with degenerative disc disease. *The Journal of bone and joint surgery. British volume.* 1997;79:147-153.
7. Cuellar JM, Scuderi GJ, Cuellar VG, Golish SR, Yeomans DC. Diagnostic utility of cytokine biomarkers in the evaluation of acute knee pain. *The Journal of bone and joint surgery. American volume.* 2009;91:2313-2320.
8. Grammatopoulos G, Pandit H, Kamali A, Maggiani F, Glyn-Jones S, Gill HS, Murray DW, Athanasou N. The correlation of wear with histological features after failed hip resurfacing arthroplasty. *The Journal of bone and joint surgery. American volume.* 2013;95:e81.
9. Green TR, Fisher J, Stone M, Wroblewski BM, Ingham E. Polyethylene particles of a 'critical size' are necessary for the induction of cytokines by macrophages in vitro. *Biomaterials.* 1998;19:2297-2302.
10. Hanson D, Mirkovic S. Lymphatic drainage after lumbar surgery. *Spine (Phila Pa 1976).* 1998;23:956-958.
11. Hirakawa K, Bauer TW, Stulberg BN, Wilde AH, Borden LS. Characterization of debris adjacent to failed knee implants of 3 different designs. *Clinical orthopaedics and related research.* 1996:151-158.
12. Howling GI, Barnett PI, Tipper JL, Stone MH, Fisher J, Ingham E. Quantitative characterization of polyethylene debris isolated from periprosthetic tissue in early failure knee implants and early and late failure Charnley hip implants. *Journal of biomedical materials research.* 2001;58:415-420.
13. Ingham E, Fisher J. The role of macrophages in osteolysis of total joint replacement. *Biomaterials.* 2005;26:1271-1286.
14. Knowles HJ, Athanasou NA. Acute hypoxia and osteoclast activity: a balance between enhanced resorption and increased apoptosis. *The Journal of pathology.* 2009;218:256-264.
15. Kobayashi A, Bonfield W, Kadoya Y, Yamac T, Freeman MA, Scott G, Revell PA. The size and shape of particulate polyethylene wear debris in total joint replacements. *Proceedings of the Institution of Mechanical Engineers. Part H, Journal of engineering in medicine.* 1997;211:11-15.
16. Kockx MM, Cromheeke KM, Knaapen MW, Bosmans JM, De Meyer GR, Herman AG, Bult H. Phagocytosis and macrophage activation associated with hemorrhagic microvessels in human atherosclerosis. *Arteriosclerosis, thrombosis, and vascular biology.* 2003;23:440-446.
17. Kurtz S, Steinbeck M, Ianuzzi A, Van Ooij A, Punt I, Isaza J, Ross ER. Retrieval analysis of motion preserving spinal devices and periprosthetic tissues. *SAS.* 2009;3:161-177.
18. Kurtz SM. *The UHMWPE Biomaterials Handbook.* Burlington, MA: Academic Press; 2009.
19. Kurtz SM, MacDonald D, Ianuzzi A, van Ooij A, Isaza J, Ross ER, Regan J. The natural history of polyethylene oxidation in total disc replacement. *Spine (Phila Pa 1976).* 2009;34:2369-2377.
20. Kurtz SM, Patwardhan A, MacDonald D, Ciccarelli L, van Ooij A, Lorenz M, Zindrick M, O'Leary P, Isaza J, Ross R. What is the correlation of in vivo wear

- and damage patterns with in vitro TDR motion response? *Spine*. 2008;33:481-489.
21. Kurtz SM, Toth JM, Siskey R, Ciccarelli L, Macdonald D, Isaza J, Lanman T, Punt I, Steinbeck M, Goffin J, van Ooij A. The Latest Lessons Learned from Retrieval Analyses of Ultra-High Molecular Weight Polyethylene, Metal-on-Metal, and Alternative Bearing Total Disc Replacements. *Seminars in spine surgery*. 2012;24:57-70.
 22. Kurtz SM, van Ooij A, Ross R, de Waal Malefijt J, Peloza J, Ciccarelli L, Villarraga ML. Polyethylene wear and rim fracture in total disc arthroplasty. *Spine J*. 2007;7:12-21.
 23. Lebl DR, Cammisa FP, Girardi FP, Wright T, Abjornson C. In vivo functional performance of failed Prodisc-L devices: retrieval analysis of lumbar total disc replacements. *Spine (Phila Pa 1976)*. 2012;37:E1209-1217.
 24. Link HD, Keller A. Biomechanics of Total Disc Replacement. In: Buttner-Janzen K, Hochschuler SH, McAfee PC, ed. *The Artificial Disc*. Berlin: Springer Berlin Heidelberg; 2003:33-52.
 25. Link HD, McAfee PC, Pimenta L. Choosing a cervical disc replacement. *Spine J*. 2004;4:294S-302S.
 26. Mabrey JD, Afsar-Keshmiri A, McClung GA, 2nd, Pember MA, 2nd, Wooldridge TM, Mauli Agrawal C. Comparison of UHMWPE particles in synovial fluid and tissues from failed THA. *Journal of biomedical materials research*. 2001;58:196-202.
 27. Mapp PI, Walsh DA. Mechanisms and targets of angiogenesis and nerve growth in osteoarthritis. *Nature reviews. Rheumatology*. 2012;8:390-398.
 28. Margevicius KJ, Bauer TW, McMahon JT, Brown SA, Merritt K. Isolation and characterization of debris in membranes around total joint prostheses. *The Journal of bone and joint surgery. American volume*. 1994;76:1664-1675.
 29. Minoda Y, Kobayashi A, Iwaki H, Miyaguchi M, Kadoya Y, Ohashi H, Takaoka K. Characteristics of polyethylene wear particles isolated from synovial fluid after mobile-bearing and posterior-stabilized total knee arthroplasties. *Journal of biomedical materials research. Part B, Applied biomaterials*. 2004;71:1-6.
 30. Olson E. Particle Shape Factors and Their Use in Image Analysis-Part 1: Theory. *Journal of GxP Compliance*. 2011;15:85-96.
 31. Phillips E, Klein GR, Cates HE, Kurtz SM, Steinbeck MJ. Histological characterization of periprosthetic tissue responses for metal-on-metal hip replacement. *Journal of Long-Term Effects of Medical Implants*. 2014;24.
 32. Punt I, Baxter R, van Ooij A, Willems P, van Rhijn L, Kurtz S, Steinbeck M. Submicron sized ultra-high molecular weight polyethylene wear particle analysis from revised SB Charite III total disc replacements. *Acta biomaterialia*. 2011;7:3404-3411.
 33. Punt IM, Austen S, Cleutjens JP, Kurtz SM, ten Broeke RH, van Rhijn LW, Willems PC, van Ooij A. Are periprosthetic tissue reactions observed after revision of total disc replacement comparable to the reactions observed after total hip or knee revision surgery? *Spine (Phila Pa 1976)*. 2012;37:150-159.

34. Punt IM, Cleutjens JP, de Bruin T, Willems PC, Kurtz SM, van Rhijn LW, Schurink GW, van Ooij A. Periprosthetic tissue reactions observed at revision of total intervertebral disc arthroplasty. *Biomaterials*. 2009;30:2079-2084.
35. Ren W, Yang SY, Fang HW, Hsu S, Wooley PH. Distinct gene expression of receptor activator of nuclear factor-kappaB and rank ligand in the inflammatory response to variant morphologies of UHMWPE particles. *Biomaterials*. 2003;24:4819-4826.
36. Richards L, Brown C, Stone MH, Fisher J, Ingham E, Tipper JL. Identification of nanometre-sized ultra-high molecular weight polyethylene wear particles in samples retrieved in vivo. *The Journal of bone and joint surgery. British volume*. 2008;90:1106-1113.
37. Rousseau MA, Bradford DS, Bertagnoli R, Hu SS, Lotz JC. Disc arthroplasty design influences intervertebral kinematics and facet forces. *Spine J*. 2006;6:258-266.
38. Santavirta S, Takagi M, Gomez-Barrena E, Nevalainen J, Lassus J, Salo J, Konttinen YT. Studies of host response to orthopedic implants and biomaterials. *J Long Term Eff Med Implants*. 1999;9:67-76.
39. Schrijvers DM, De Meyer GR, Herman AG, Martinet W. Phagocytosis in atherosclerosis: Molecular mechanisms and implications for plaque progression and stability. *Cardiovascular research*. 2007;73:470-480.
40. Steinbeck M, Veruva SY. Pathophysiologic Reactions to UHMWPE Wear Particles. In: Kurtz SM, ed. *UHMWPE Biomaterials Handbook: Ultra High Molecular Weight Polyethylene in Total Joint Replacement and Medical Devices*: William Andrew; 2015.
41. Trump BF, Mergner WJ. Cell Injury. In: Zweifach BW, Grant L, McCluskey RT, ed. *The Inflammatory Process*: Academic Press; 1973.
42. van Ooij A, Kurtz SM, Stessels F, Noten H, van Rhijn L. Polyethylene wear debris and long-term clinical failure of the Charite disc prosthesis: a study of 4 patients. *Spine (Phila Pa 1976)*. 2007;32:223-229.
43. van Ooij A, Oner FC, Verbout AJ. Complications of artificial disc replacement: a report of 27 patients with the SB Charite disc. *Journal of spinal disorders & techniques*. 2003;16:369-383.
44. Veruva SY, Lanman TH, Hanzlik JA, Kurtz SM, Steinbeck MJ. Rare complications of osteolysis and periprosthetic tissue reactions after hybrid and non-hybrid total disc replacement. *European spine journal : official publication of the European Spine Society, the European Spinal Deformity Society, and the European Section of the Cervical Spine Research Society*. 2014.
45. Veruva SY, Steinbeck MJ, Toth J, Alexander DD, Kurtz SM. Which Design and Biomaterial Factors Affect Clinical Wear Performance of Total Disc Replacements? A Systematic Review. *Clinical orthopaedics and related research*. 2014.
46. Yang SY, Ren W, Park Y, Sieving A, Hsu S, Nasser S, Wooley PH. Diverse cellular and apoptotic responses to variant shapes of UHMWPE particles in a murine model of inflammation. *Biomaterials*. 2002;23:3535-3543.
47. Zhang JM, An J. Cytokines, inflammation, and pain. *International anesthesiology clinics*. 2007;45:27-37.

CHAPTER 4

Periprosthetic Immune Response to UHMWPE Wear Particles and Inflammatory Factor Production in the Lumbar Spine

4.1 Abstract

The pathophysiology and mechanisms driving the generation of unintended pain after TDR are poorly understood. It has been suggested that pain may be the result of UHMWPE wear debris and the resulting periprosthetic inflammation. We therefore asked whether inflammation could be linked to wear debris generation and the production of inflammatory factors that might contribute to abnormal or enhanced pain sensitization. Tissues were evaluated for three patient groups: periprosthetic tissue samples (n=30) obtained at revision of contemporary metal-on-UHMWPE TDRs from 11 patients (implantation time 1.2-6.0 year, average 3.3 year); painful degenerative disc disease (DDD) tissue samples (n=3) obtained from patients exhibiting pain at the time of initial TDR surgery; and normal disc tissue samples (n=4) obtained at autopsy from patients with no clinical history of back surgery. The wear particle number and size/shape characteristics were determined in tissue sections from TDR patients and immunohistochemistry was performed to identify CD68+ macrophages and the production of tumor necrosis factor- α (TNF α), interleukin-1 β (IL-1 β), vascular endothelial growth factor (VEGF), platelet-derived growth factor-bb (PDGFbb), nerve growth factor (NGF) and substance P, inflammatory factors known to play both a direct and indirect role in inflammatory-

mediated pain sensitization. Clinical and implant factors did not show any correlation with the expression of these factors. However, the amounts of TNF α IL-1 β , VEGF, NGF and substance P strongly correlated with the number of wear particles and also the number of CD68+ macrophages for the TDR patient group. Furthermore, the cytokines, TNF α and IL-1 β , and the vascularization factors, VEGF and PDGFbb, correlated with the presence of the neural innervation and hypersensitization agents, NGF and substance P, suggesting inflammation can contribute to pain sensitization.

4.2 Introduction

The pathophysiology of low back pain remains poorly understood [25], and even less is known about mechanism(s) involved in the generation of unintended pain after metal-on-UHMWPE total disc replacement (TDR). The normal human lumbar disc consists of an avascular/aneural nucleus pulposus, and a surrounding annulus fibrosis that is poorly vascularized and innervated [22]. Painful disc degeneration has been associated with an infiltration of inflammatory cells, as resident macrophages are not present, and responses leading to innervation by sensory nerve fibers, which follow the path of ingrowing blood vessels into disc tissue [6, 11]. This process is mediated by both activated fibroblasts and inflammatory cell infiltrates that release biological factors that may ultimately lead to pain sensitization. In a previous study, we reported an increase in inflammation and vascularization in TDR revision tissues [37]. Thus, it was hypothesized that biological reactions to UHMWPE wear debris in the lumbar spine result in the

production and interplay between key inflammatory mediators that contribute to the abnormal or enhanced pain sensitization in TDR patients.

Studies have suggested that there is a functional link between the immune response and neurological changes that ultimately result in the generation of peripheral pain. Specifically, activated macrophages, derived from circulating monocytes, have been reported to contribute to experimental pain states by releasing pro-inflammatory cytokines such as $\text{TNF}\alpha$ and $\text{IL-1}\beta$ [23, 30, 34]. In addition, these cells can secrete the angiogenic factors, VEGF and PDGFbb, and the neurotrophic factor and neuropeptide, NGF and substance P. Investigations on painful degenerative discs have identified a significant increase in the production of these factors in both the nucleus pulposus and annulus fibrosis [19, 38].

It is important to note that $\text{TNF}\alpha$ and $\text{IL-1}\beta$ are not only potent stimulators of pro-inflammatory reactions in the disc space, but both have the potential to induce neural ingrowths into the disc and mediate hypersensitization by upregulating the expression of factors like NGF and substance P [2]. In addition, $\text{TNF}\alpha$ and $\text{IL-1}\beta$ can directly stimulate pain by acting on nociceptors, sensory neurons that respond by sending signals to the brain that initiate the perception of pain [33, 42]. Furthermore, $\text{TNF}\alpha$ and $\text{IL-1}\beta$ have been shown to induce angiogenesis by stimulating the release of factors like VEGF, PDGFbb and fibroblast growth factor (FGF) [6, 35]. While the underlying mechanisms of vascular ingrowth remain unclear, VEGF can promote blood vessel expansion into the disc space and

subsequently enhance innervation as the growing vessels provide a conduit for ingrowing neurons [26]. Thus, it is feasible that all of these cytokines play a role in the peripheral mediation of the unintended neuropathic pain experienced in some patients after disc replacement. Identifying their presence in the context of wear-debris-induced inflammatory reactions of the lumbar spine could provide valuable insights into the mechanisms that contribute to the unintended pain in some TDR patients.

In this study, we evaluated periprosthetic tissues collected at the time of TDR revision surgery using immunohistochemistry (IHC) to quantify the levels of select inflammatory factors that are known to play a major role in inflammation, vascularization and inflammatory-mediated pain/innervation, and investigate their associations with wear debris and macrophages. The inclusion criteria for the factors focused on identifying secretory proteins that are known to be involved in both direct and indirect mediation of pain, and included $\text{TNF}\alpha$, $\text{IL-1}\beta$, VEGF, PDGF-bb, NGF and substance P. Understanding the inflammatory responses and factors present in TDR periprosthetic tissues with and without detectable UHMWPE wear debris will enable us to discover mechanistic pathways that may link wear particles to pain sensitization. It will also provide information needed to identify therapeutic targets and treatment strategies to mitigate chronic pain after TDR.

4.3 Materials & Methods

4.3.1 Tissue Collection & Patient Information

Tissues were evaluated from three patient groups: periprosthetic tissue samples (n = 30) from TDR patients (*see Chapter 3.3.1 and Table 3-1*), tissues samples obtained from patients with disc degenerative disease (n = 3) exhibiting pain at the time of initial TDR surgery, and intervertebral disc (IVD) tissue samples (n = 2) obtained at autopsy from normal patients with no clinical history of back surgery or lower back pain. Periprosthetic revision and initial TDR surgical tissues were collected as part of a public, multi-center retrieval research program initiated in 2004 [16, 17]. Normal IVD tissues samples were obtained from the Cooperative Human Tissue Network (CHTN) of the National Cancer Institute (NCI), the National Institutes of Health, Bethesda, MD (<http://faculty.virginia.edu/chn-tma/home.html>). Additional IVD tissue samples were obtained from the Life Legacy Foundation (Tucson, AZ). Visual analog scale (VAS) pain scores and other demographic data was collected when available (Table 4-1).

4.3.2 Tissue Preparation

Tissues collected from revision surgeries, primary surgeries for treatment of DDD and autopsy were fixed in either formalin or Universal Molecular Fixative (UMFIX; Sakura Finetek USA, Inc, Torrance, CA, USA). One to two 4-mm punches from each tissue, considering variations in color, texture, and size of specimen, were embedded in paraffin blocks, and 6- μ m serial sections were mounted onto ProbeOnPlus (Fischer Scientific Co, Pittsburgh, PA, USA) slides.

Table 4-1. Clinical Information of Patient Cohorts

Patient ID	Tissue Type	Device	Bearing design	Sex	Age	Implantation Time (years)	VAS Score
BHSP 022	Periprosthetic	ProDisc-L	Fixed	Male	36	5.0	N/A
BHSP 023	Periprosthetic	ProDisc-L	Fixed	Male	53	3.0	N/A
BHSP 025a BHSP 025b	Periprosthetic	ProDisc-L ProDisc-L	Fixed Fixed	Male	45	4.0	N/A
BHSP 026	Periprosthetic	ProDisc-L	Fixed	Female	N/A	N/A	N/A
BHSP 027	Periprosthetic	ProDisc-L	Fixed	Female	28	5.0	N/A
BHSP 0032	Periprosthetic	ProDisc-L	Fixed	Male	40	6.0	N/A
PDL 004	Periprosthetic	ProDisc-L	Fixed	Female	25	1.3	N/A
BRSP 003	Periprosthetic	CHARITÉ	Mobile	Male	26	1.5	8
BRSP 004	Periprosthetic	CHARITÉ	Mobile	Female	18	3.3	7
BRSP 006	Periprosthetic	CHARITÉ	Mobile	N/A	N/A	2.7	5
BRSP 007	Periprosthetic	CHARITÉ	Mobile	N/A	N/A	3.3	10
BRSP Pri 002	DDD			N/A	N/A		9
BRSP Pri 003	DDD			F	34		8
BRSP Pri 004	DDD			F	31		7
CHTN 38422T	IVD			F	55		0
CHTN 55035T	IVD			M	42		0
LLF I	IVD			N/A	N/A		0
LLF II	IVD			N/A	N/A		0

4.3.3 Wear Particle Analysis

For UHMWPE particle analysis, hematoxylin and eosin (H&E) (ThermoFisher Scientific, Waltham, MA) stained tissue sections were evaluated for wear debris (*see Chapter 3.3.4*). In brief, a 36-image (200X magnification) composite was created from each tissue section under polarized light that corresponded to the transmitted light tissue composites. In each individual image, UHMWPE wear particle number, size, and shape were determined by first using a customized image threshold operation programmed in MATLAB® (MathWorks Inc, Natick, MA, USA) followed by counting/measuring particles using NIH ImageJ (National Institutes of Health, Bethesda, MD, USA). Equivalent circular diameter (ECD), aspect ratio and circularity measurements were calculated to determine particle size and shape (as described in *Chapter 3.3.4*).

4.3.4 Immunohistochemistry

Immunohistochemistry was performed on prepared slides to evaluate the expression of six secretory factors and a pan-macrophage marker: pro-inflammatory cytokines, TNF α (Rabbit IgG, Novus Biologicals, NBP1-19532) and IL-1 β (Rabbit IgG, Abcam, AB2105); vascularization factors, VEGF (Rabbit IgG, SantaCruz, sc-507) and PDGFbb (Rabbit IgG, Abcam,); pain-related factors, NGF (Rabbit IgG, Abcam, AB6199) substance P (Rabbit IgG, EMD Millipore, AB1566); and macrophage marker, CD68 (Rabbit IgG, Abcam, AB125157). Optimal conditions for the inflammatory and pain-related antibodies were determined using periprosthetic tissues of total hip replacement patients that had severe pain and wear debris;

mouse kidney tissues for the vascularization factors; and human tonsil tissue for the macrophage marker. The antibody concentrations were: TNF α 1:100, IL-1 β 1:400, VEGF 1:100, PDGFbb 1:100, NGF 1:500, substance P 1:500 and CD68 1:100. Slides with tissues originally fixated in formalin, as opposed to UMFIX (Sakura Finetek, Torrance, CA), were first treated with an antigen retrieval solution (Vector Labs). All slides were incubated in 0.5% Triton in PBS to enhance permeability, 3% H₂O₂ in methanol to block endogenous peroxidases, and to block non-specific background in 4% BSA, 0.1% Tween 20 in PBS. Lastly, slides were incubated at 4 °C overnight with the primary antibodies. For antibody visualization, samples were incubated with pan-specific secondary antibody, followed by horseradish peroxidase (Santa Cruz Biotech) and DAB solution (Vector Labs), and then counterstained with 50% hematoxylin.

In an attempt to identify macrophage phenotype subsets, M1, M2a and M2c cells, the monoclonal antibodies CCR7 (Rat IgG, Origene, TA320232), CD206 (Mouse IgG, Abcam, AB8919) and CD163 (Rabbit IgG, Labome, MBS302586) were employed. However, these antibodies failed to recognize their intended targets in the TDR revision tissues despite multiple trials with both immunofluorescent and chromogen-based staining techniques. We believe the detection was not possible because these proteins are minimally expressed or not present in TDR tissues.

4.3.5 Imaging & Analysis

Each stained tissue section was imaged (200X objective) using an Olympus BX50 microscope (Olympus, Melville, NY, USA) equipped with a stepper motor-controlled stage. DAB expression was determined by first employing a customized

image threshold operation programmed in MATLAB® (MathWorks Inc, Natick, MA), followed by measuring area via NIH ImageJ (National Institutes of Health, Bethesda, MD). In brief, the red, green and blue channels for the 24-bit bright field DAB-labelled images were normalized by the sum of the three channels. Pixel values for 8-bit images were calculated using a published formula that allows for maximal separation of DAB-stained pixels from the background tissue: $255 \cdot \text{blue} / (\text{red} + \text{green} + \text{blue})$ (Figure 5-1) [8]. See *Appendix 1B* for MATLAB script.

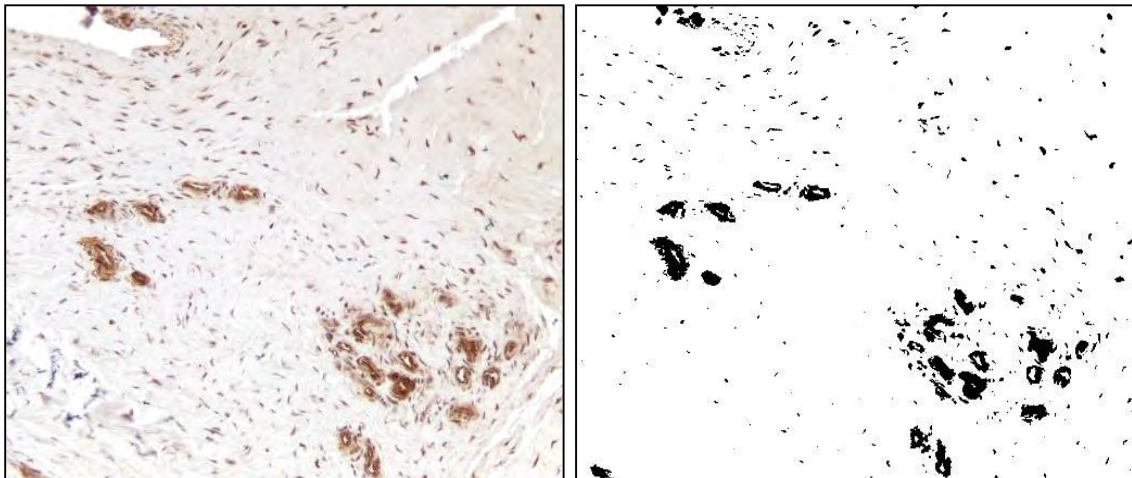


Figure 4-1. Representative image of a tissue with DAB deposition after immunohistochemistry (left) followed by thresholding for DAB-stained pixels in MATLAB (right).

CD68+ macrophages were quantified in each image (200x) of the stained tissue sections with the aid of Image-Pro Plus 6.0 (Media Cybernetics, Silver Spring, MD, USA). A customized macro was generated to count DAB-stained cells. A quantitative value of the inflammatory response was then presented as the number of positive cells (DAB) was normalized to total area. In brief, images were split into three eight-bit channels (red, green, and blue). Signal from blue channels were converted into masks based on a threshold value relative to the average signal

intensity of each image. Next, count/size operations were employed along with water-shed split commands in order to maximize accuracy of counts. See *Appendix 3-1* for macro.

4.3.6 Statistical Analysis

The normality of the data was determined using Shapiro-Wilk test (IBM SPSS Statistics V22 software package, IBM Corporation, Armonk, NY, USA). To statistically compare immunohistochemical levels between different patient groups, the Mann-Whitney U-test was employed. Significance was based on $P < 0.05$. Correlations for wear debris, inflammatory cells and the six immunohistological markers were determined using Spearman Rho correlation test for non-parametric data. Significance was based on $P < 0.05$.

4.4 Results

4.4.1 Mean Inflammatory Factor Expression in Patient Tissues

The levels of six inflammatory-associated secretory factors, TNF α , IL-1 β , VEGF, PDGF-bb, NGF and substance P, were evaluated in TDR revision tissues and compared to levels in DDD patient tissue samples retrieved at the time of initial TDR surgery, as well as IVD tissue samples from autopsy patients with no history of back surgery or lower back pain (Figure 4-2). Percent area of expression for each factor was determined based on the amount of DAB (pixels per total tissue area (mm²) in each section.

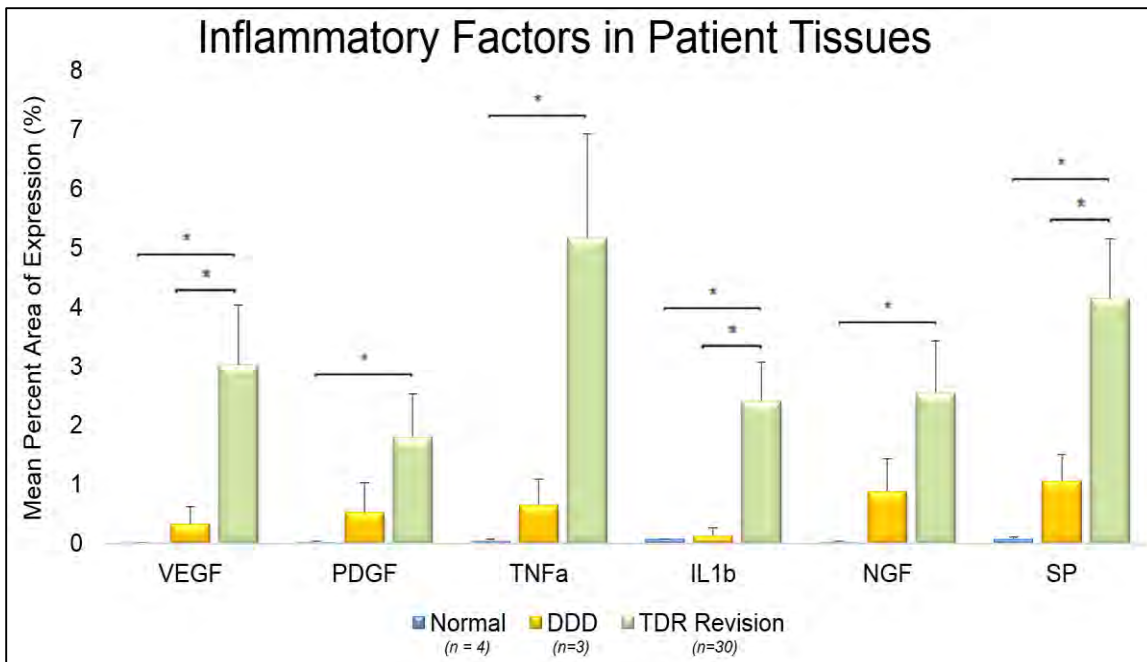


Figure 4-2. Mean expression of inflammatory factors in tissues for TDR, DDD and normal IVD patients. * $p < 0.05$

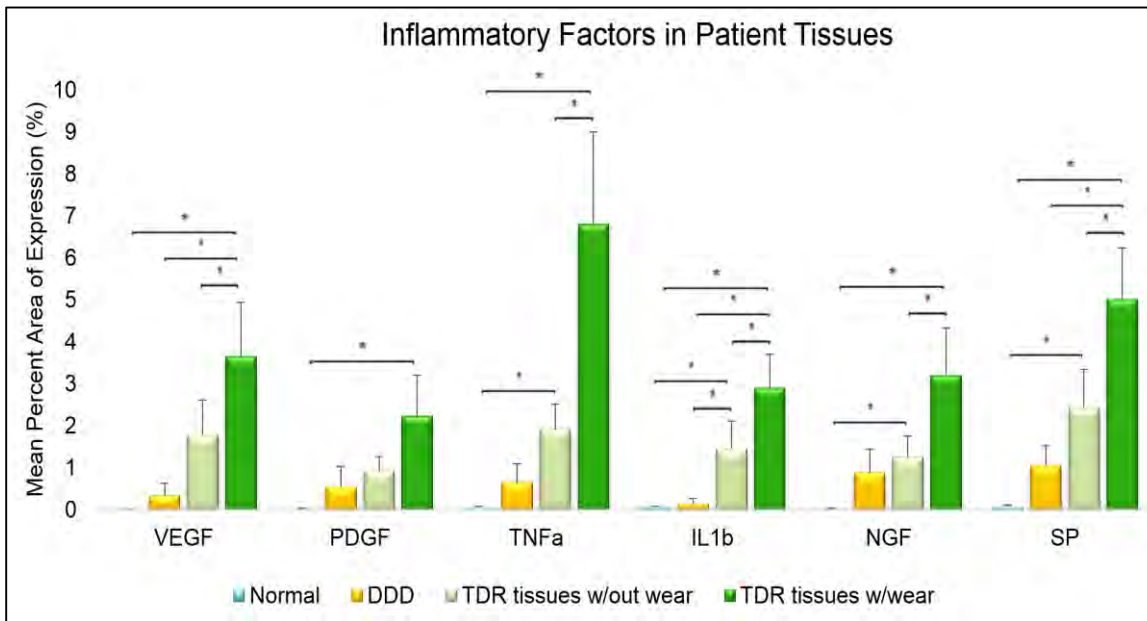


Figure 4-3. Mean expression of inflammatory factors in TDR tissues with (n=14) and without (n=16) wear debris, DDD and normal patient tissues. * $p < 0.05$

We found that the mean percent area of expression for IL-1 β ($p = 0.01$), VEGF ($p = 0.04$), and substance P ($p=0.01$) were significantly higher in TDR tissues when compared to tissues obtained from DDD patients. TNF α ($p = 0.06$) and NGF ($p = 0.19$) were also increased in the TDR patient tissues. When compared to normal, IVD, tissues, the mean percent area for all six factors, TNF α , IL-1 β , VEGF, PDGFbb, NGF and substance P, were statistically increased in TDR tissues ($p < 0.05$). Interestingly, no statistical differences were observed between DDD and normal IVD tissues.

To further evaluate differences in the tissue cohorts, TDR tissues were separated into sections that had detectable ($> 0.34 \mu\text{m}$) UHMWPE wear particles ($n = 14$) and sections that did not ($n = 16$). The expression of all of the factors, except PDGFbb, was significantly higher ($p < 0.05$) in TDR tissues with UHMWPE wear particles (Figure 4-3). Overall, TDR patient tissues with detectable wear debris had the highest expression of each factor compared to the DDD and IVD patient cohort tissues.

4.4.2 Mean Inflammatory Factor Expression in Tissues from TDR Patients and Associations with Patient Clinical and Implant Factors

As patient, clinical and implant factors may contribute to the overall biological response, associations with the inflammatory secreted factors were investigated. Five male revision patients did not express any significant differences in mean percent area of expression for the six inflammatory factors when compared to the four female patients (Figure 4-4A). Next, implant complications of malpositioning, subsidence, dissociation and/or migration were noted in five revision patients, but there was no relationship with the factors when compared to the seven other TDR patients with no reported complications (Figure 4-4B). Based on short-term

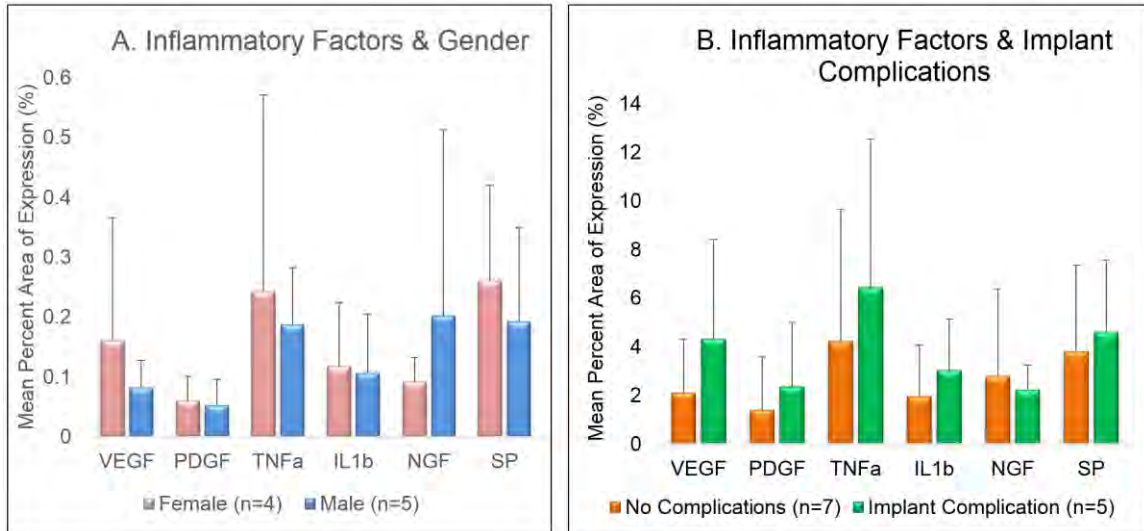


Figure 4-4. Gender (A) and implant complications (B) showed no significant association with inflammatory factors.

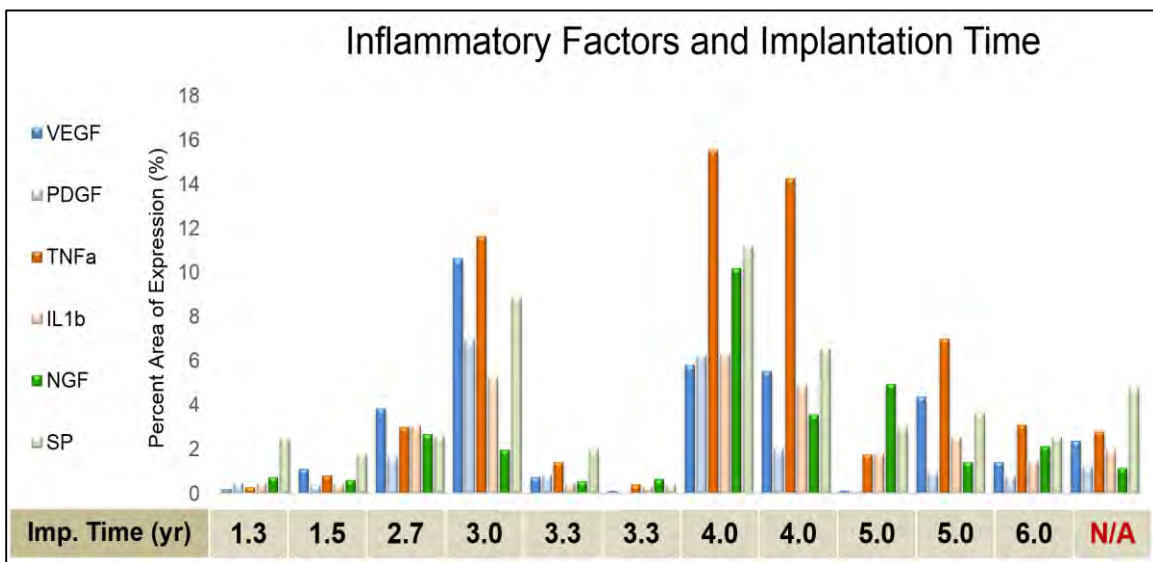


Figure 4-5. Implantation time showed no significant association with inflammatory factors.

to mid-term TDR revision patients, ranging from 1.3 years to 6.0 years of implantation, increasing implantation times also failed to correlate with the percent area expression of these factors (Figure 4-5). Similarly, other available clinical and implant information on patient demographics such as age and implant design (fixed-

versus mobile-bearing cores) did not show any association with the expression of these factors (not shown).

4.4.3 Correlations between the Amount of Wear Debris and Inflammatory Factors in TDR Tissues

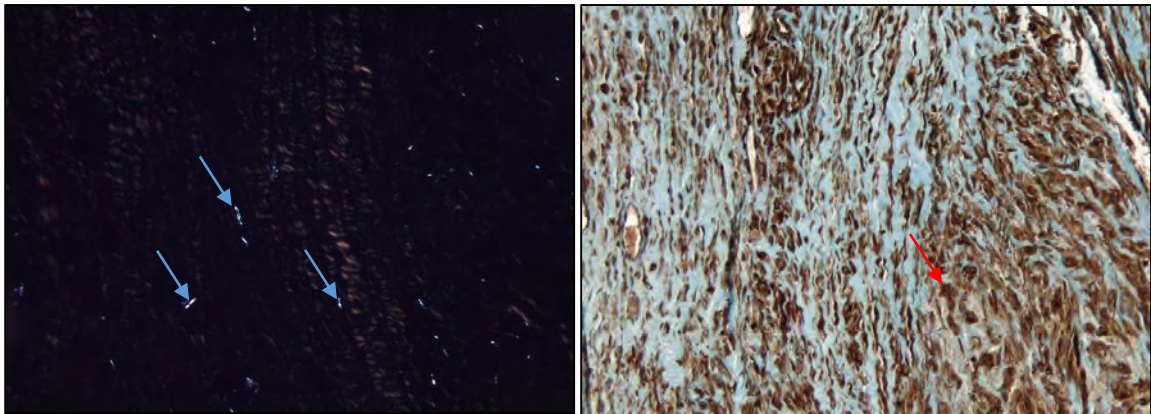


Figure 4-6. Representative tissue sections with wear debris (left, polarized light) and TNF α immunostaining (right). The blue arrows indicate wear particles and the red arrow a macrophage surrounded by TNF α expressing fibroblasts.

To determine whether UHMWPE wear particle accumulation affected the six inflammatory factors, particle number per tissue section was compared to the amount of each factor. In general, tissues that contained wear debris also showed substantially increased amounts of the inflammatory factors (Figure 4-6). The quantity of wear debris showed a significant and moderately positive correlation to the percent area of both TNF α and IL-1 β ($p < 0.001$, $\rho = 0.63$; $P = 0.015$, $\rho = 0.50$; Figure 4-7). Both factors were expressed at substantially lower levels when no particles were present, with the exception of highly necrotic tissues (statistical outliers). Comparisons to VEGF and PDGFbb expression revealed the amount of wear debris showed a significant and moderately positive correlation with VEGF ($p = 0.003$, $\rho = 0.56$), but not PDGFbb

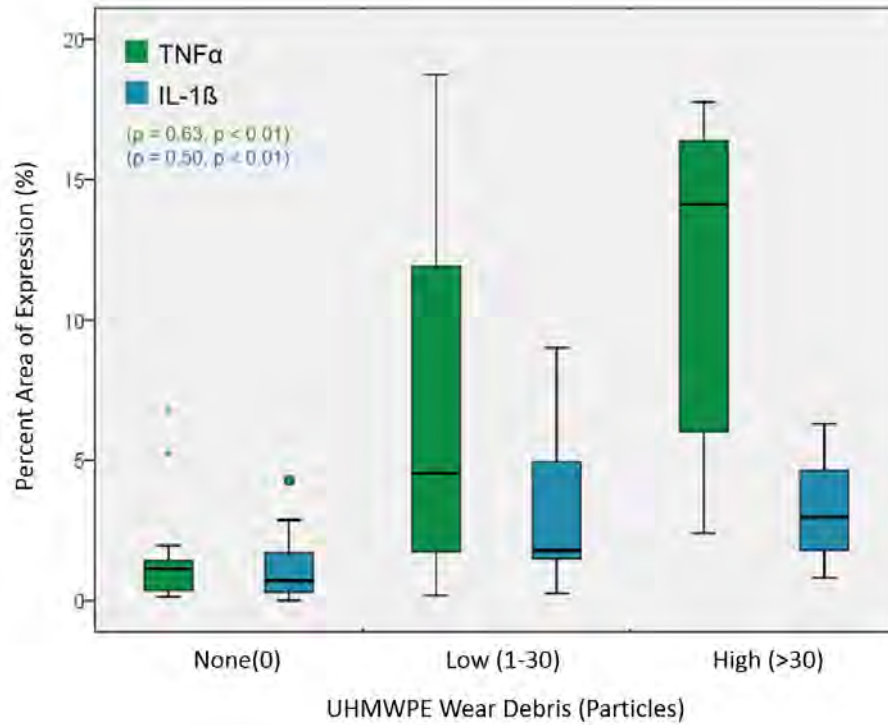


Figure 4-7. UHMWPE wear debris correlated with TNF α & IL-1 β

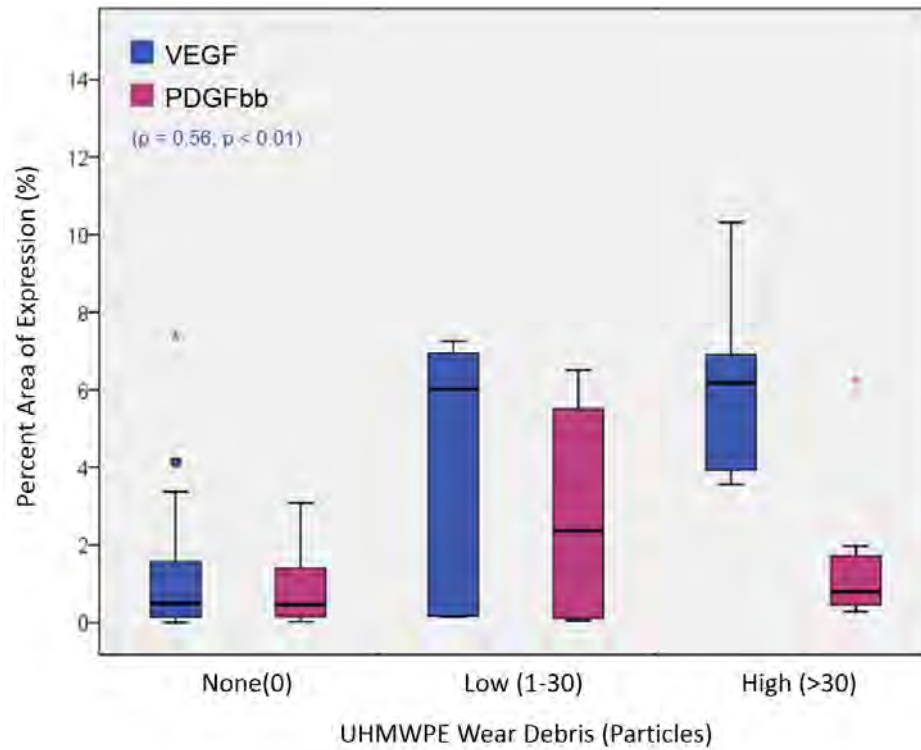


Figure 4-8. UHMWPE wear debris correlated with VEGF.

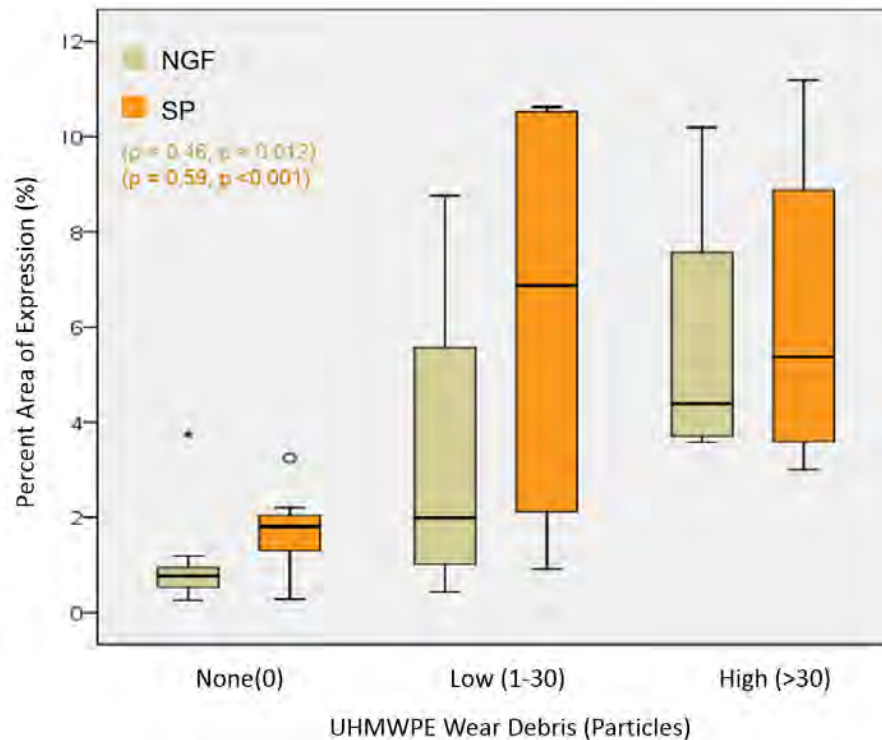


Figure 4-9. UHMWPE wear debris correlated with NGF and SP.

(Figure 4-8). Nonetheless, both factors were expressed at lower levels when no particles were present in the tissues. Lastly, comparisons to NGF and substance P expression showed the amount of wear debris had a significant and positive correlation with both factors, respectively ($p = 0.012$, $\rho = 0.46$; $p < 0.001$, $\rho = 0.59$; Figure 4-9).

4.4.4 Correlations between Wear Debris Characteristics and Inflammatory Factors in TDR Tissues

To determine whether UHMWPE wear particle size and shape affected the six inflammatory factors, mean measurements for particle ECD, aspect ratio and circularity, in each tissue section with detectable wear debris, were compared to inflammatory factor expression. Mean values for the wear particle size and shape showed no significant correlation with any of the factors, with the exception of mean particle aspect ratio to the percent area of TNF α ($p < 0.001$, $\rho = 0.71$, Figures 4-10 A-C).

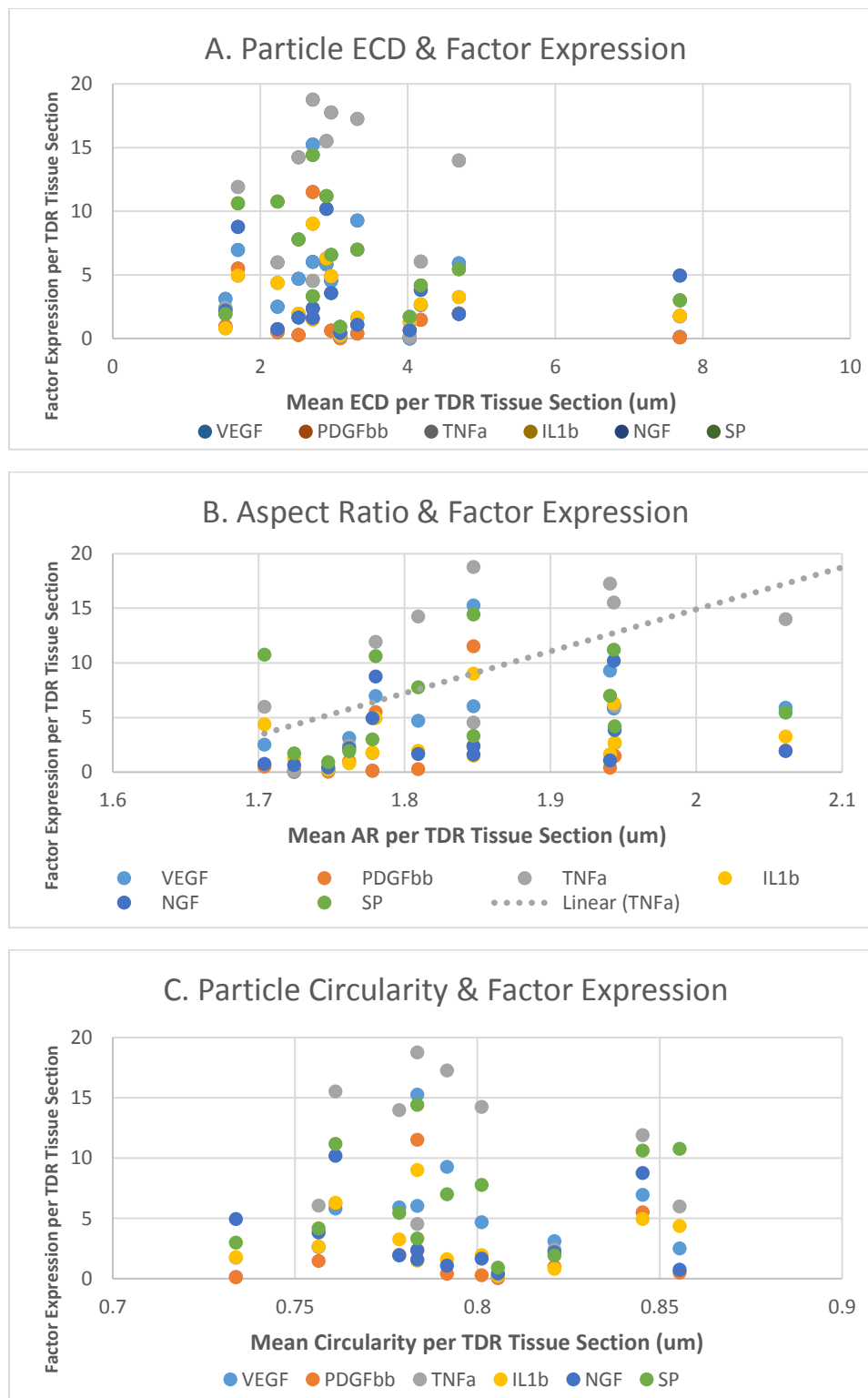


Figure 4-10. Particle ECD means did not correlate with any factor expression (A). Particle aspect ratio means correlated with TNF α (B). Particle circularity means did not correlate with any factor expression (C).

4.4.5 Correlations between Wear Debris, Inflammatory Factors and the Number of Macrophages

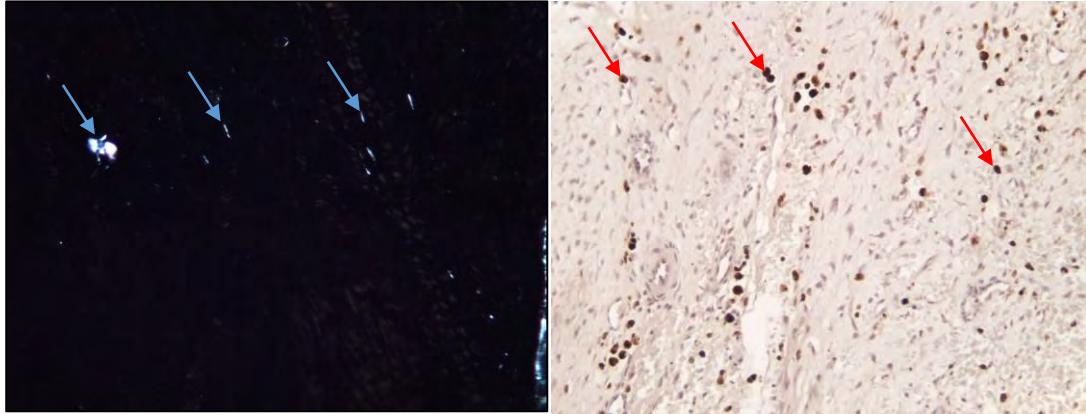


Figure 4-11. Representative tissue sections with wear debris (left) and CD68+ macrophages (right). The blue arrows indicate wear particles and the red arrows macrophage.

To investigate the presence and influence of macrophages during the immune response to wear particles in TDR tissues, the number of CD68+ cells in each tissue section was compared to particle accumulation and inflammatory factor amounts in serial sections. The majority of sections that contained wear particles also showed localized macrophage infiltration (Figure 4-11). The number of CD68+ cells showed an expected significant and strong positive correlation to the number of detectable wear particles (Figure 4-12). In addition, the number of CD68+ cells had a significant and strong positive correlation to the amount of TNF α and IL-1 β in these tissues ($p < 0.001$, $\rho = 0.85$; $p = 0.001$, $\rho = 0.69$; Figure 4-13). The number of CD68+ cells also showed a significant and strong positive correlation to VEGF ($p = 0.001$, $\rho = 0.71$), however there was a poor relationship with PDGFbb ($p = 0.090$, $\rho = 0.40$) (Figure 4-14). Lastly, the number of CD68+ cells showed a significant and positive correlation to NGF and substance P ($p = 0.003$, $\rho = 0.63$; $p = 0.002$, $\rho = 0.65$; Figure 4-15).

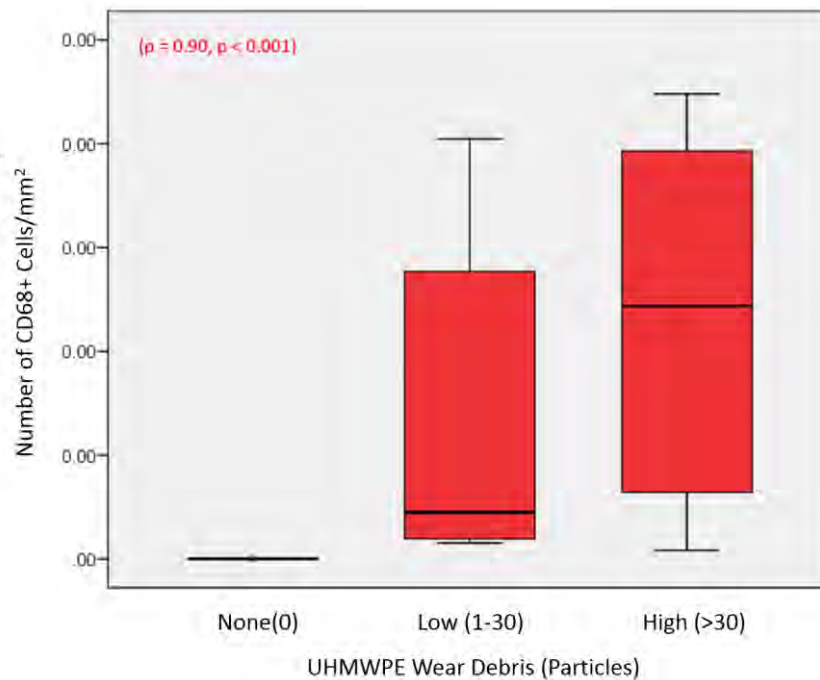


Figure 4-12. UHMWPE wear debris strongly correlated with CD68+ macrophages.

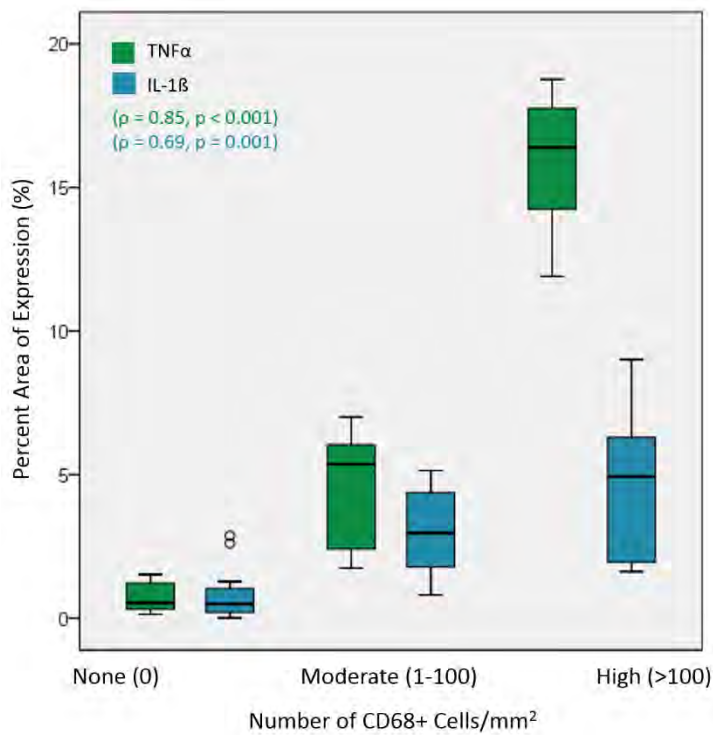


Figure 4-13. CD68+ cells correlated with TNF α and IL-1 β .

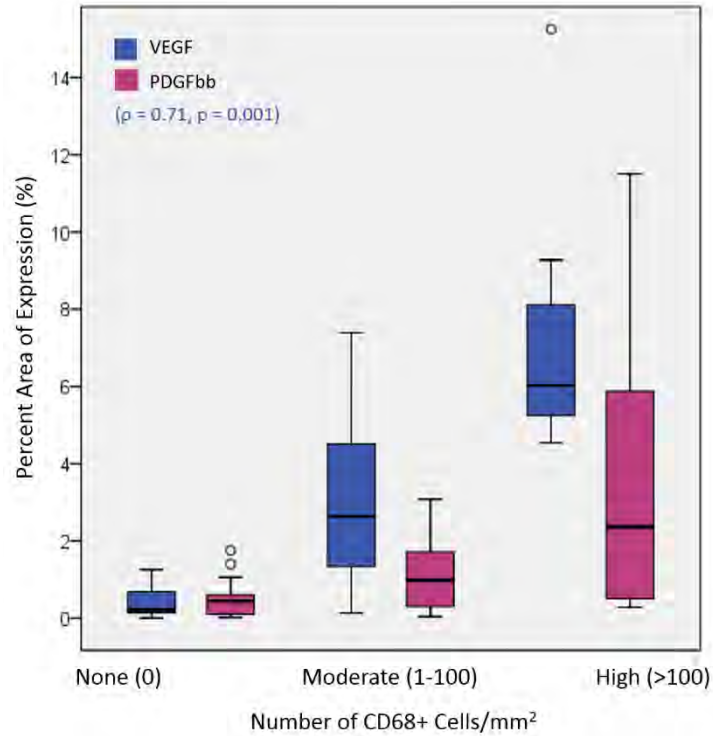


Figure 4-14. CD68+ cells correlated with VEGF, but not PDGFbb.

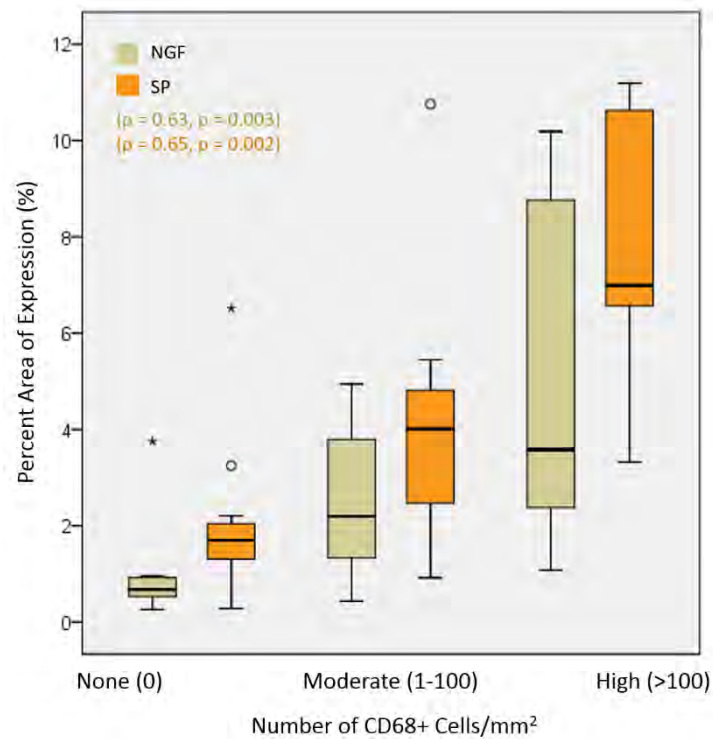


Figure 4-15. CD68+ cells correlated with NGF and substance P.

4.4.6 Correlations of NGF and Substance P with Other Factors

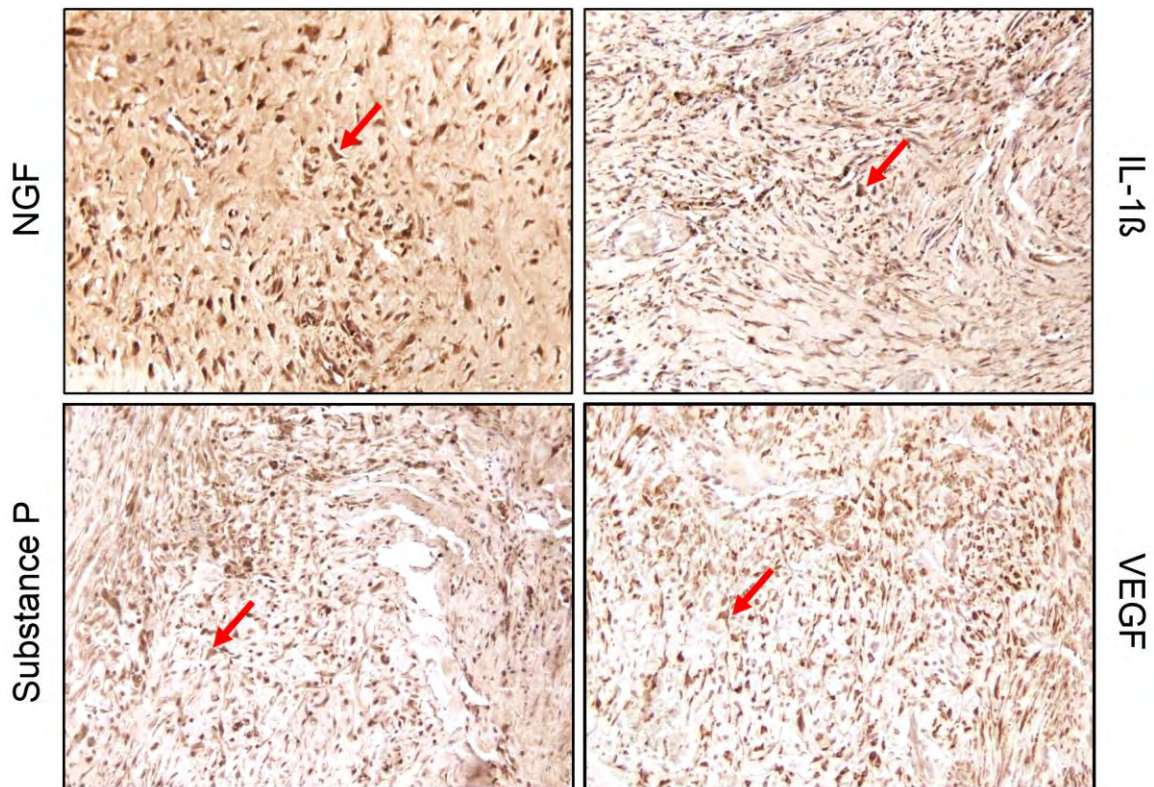


Figure 4-16. Representative inflamed tissue samples from serial sections immunostained for NGF and substance P (left) that matched proportionally with inflammatory and vascularization factors (right). The red arrows indicate a macrophage positive for the respective immunostain.

The amounts of the inflammatory, neural innervation agents and pain mediators, NGF and substance P, were identified in TDR tissues and their associations with pro-inflammatory and vascularization factors were determined (Figure 4-16). Both NGF and substance P showed statistically significant correlations with the amounts of $\text{TNF}\alpha$, $\text{IL-1}\beta$, VEGF and PDGFbb ($p < 0.01$ for all; Figure 4-17). NGF had a strongly positive relationship with the $\text{TNF}\alpha$ and $\text{IL-1}\beta$ ($\rho = 0.77$; $\rho = 0.79$), while substance P had a strongly positive relationship with the vascularization factor, VEGF ($\rho = 0.77$).

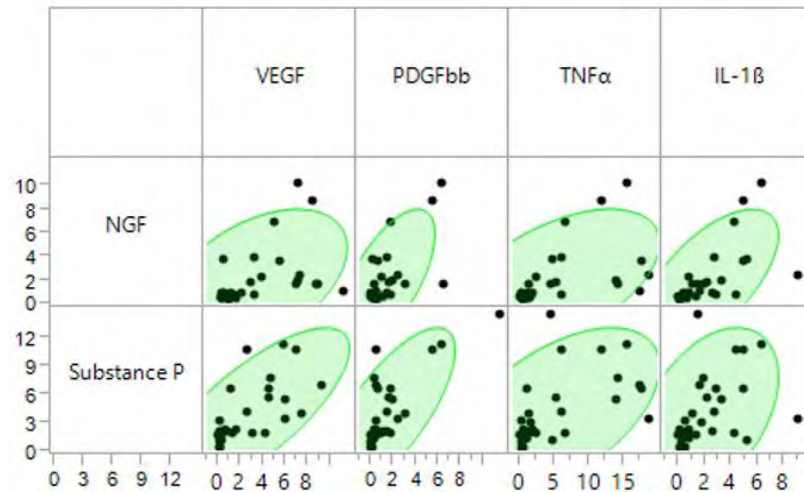


Figure 4-17. Spearman Rho correlations for NGF & SP.

4.5 Discussion

To better understand the pathophysiology and mechanisms of unintended pain after TDR, we investigated whether inflammation could be linked to wear debris generation and the production of inflammatory factors that could contribute to abnormal or enhanced pain sensitization. Inflammatory factors that promote inflammation, vascularization, pain and innervation were all elevated in TDR periprosthetic tissues when compared to tissues from DDD patients and IVD tissues from normal autopsy patients with no history of lower back pain. While no association was found between these factors and patient clinical/implant factors, TNF α IL-1 β , VEGF, NGF and substance P correlated with the number of wear particles and also the number of CD68+ macrophages in the TDR tissue sections. Furthermore, the pro-inflammatory cytokines, TNF α and IL-1 β , and the vascularization factors, VEGF and PDGFbb, correlated with the neural innervation and hypersensitization agents, NGF and substance P suggesting not only the

presence of inflammatory reactions but also the presence of factors that can directly and indirectly contribute to pain at periprosthetic sites.

Although the inflammatory pain factors showed no associations with any patient demographic information, clinical indications or implant factors, these findings may be an artifact of low sample size and power of study. Both gender and implant complications were expected to show at least some association with the inflammatory pain factors. In regards to gender differences in pain perception, recent studies clearly suggest men and women differ in both pain perception and how they respond [1, 13]. In the context of low back pain, women present with symptoms more frequently, undergo spine surgery more commonly [1], and report higher levels of back pain than men [7, 18]. However, this was not evident in our study cohort, which was again limited by sample size and also the availability of VAS scores. Limited sample size may have also contributed to the non-associations with implant factors such as malpositioning that can not only lead to severe wear debris generation [5], but can also physically impinge upon neighboring nerve roots [41]. Both of these outcomes can lead to the development of pain. Unfortunately, malpositioning is often unreported by the surgeon [12], which may explain why patients with implant complications had similar inflammatory pain factor production compared to patients not indicated for any complication. Nonetheless, it is also possible the non-associations of the inflammatory factors with patient and clinical factors simply adds weight to the associations we observed for TDR tissue biological responses and wear debris.

While TDR tissues do not contain resident macrophages and are initially poorly vascularized, the generation of wear debris increased the infiltration of CD68+ macrophages. Past studies on hips and knees have suggested these changes are initiated by wear debris activation of fibroblasts. Tunyogi-Csapo and colleagues (2007) found that fibroblasts in periprosthetic tissues from joint replacements secrete pro-inflammatory cytokines in response to particulate wear as well as the angiogenic factors, VEGF and fibroblast growth factor [35]. Moreover, the production of pro-inflammatory factor-recruitment of peripheral blood monocytes and the production of angiogenic factors lead to extensive vascularization of periprosthetic hip tissue [14, 35]. While we hypothesized a similar upregulation of angiogenic factors, only VEGF was significantly increased and associated with the number of wear particles. Although increases in PDGFbb were observed when particle number was high. Based on the high ratio of VEGF to PDGFbb we believe the pro-inflammatory M1 macrophage responses predominate rather than M2 macrophage response [29, 32].

It is well accepted from joint arthroplasty studies that UHMWPE particles can activate cells, including fibroblasts, to secrete $\text{TNF}\alpha$, which can induce subsequent $\text{IL-1}\beta$ secretion, and together these factors can synergistically contribute to the recruitment and polarization of macrophages towards the M1 phenotype [21, 29]. Accordingly, our previous work showed an increased infiltration of macrophages in TDR tissues containing wear particles [37]. In support of these findings, the current study showed increased expression of both $\text{TNF}\alpha$ and $\text{IL-1}\beta$, which correlated with the number of wear particles and inflammatory cells. Particle size and shape have

been previously reported to influence biological reactions as well [37], however only the aspect ratio of the particles in our study showed a significant relationship with TNF α . This may however be due to our limited range ($> 0.34 \mu\text{m}$) of particle size detection capabilities.

While the current study is the first to identify vascularization and neurological factors in TDR periprosthetic tissues, a number of DDD studies have reported the presence of pro-inflammatory factors, blood vessel ingrowth and nerve ingrowth into layers of the disc, which are thought to result in chronic lower back pain [6, 11, 24, 27]. Specifically, NGF-expressing blood vessels have been detected and co-localized to sensory nerve fibers in the annulus fibrosis and even deeper into the nucleus pulposus of the spinal disc [11]. These nerve fibers are known to produce neurotransmitters, including substance P, involved in pain transmission [4]. Activated macrophages can further exacerbate the condition by signaling the release of more neurotrophins and neuropeptides by neighboring macrophages and neurons [2]. Purmessur et al. (2008) have shown *in vitro* that TNF α stimulation of normal cells from the IVD increases the production of substance P, whereas IL-1 β stimulation increases NGF [28]. Altogether, the current findings, combined with previous research, suggest a possible signaling cascade starting with fibroblast activation, macrophage infiltration, increased vascularization and innervation/nociception (pain response to inflammation and tissue damage).

The importance of NGF and substance P production in periprosthetic tissues is 2-fold. First, NGF is a known mediator of sensory and nociceptive nerve function and substance P is a sensory pain-associated neuropeptide released at synapses;

thus, both contribute to hyperalgesia (increased sensitivity to pain) [3, 20, 40]. Second, NGF can contribute to nerve ingrowth [2, 9, 15], and without it, all sensory neurons will undergo apoptosis [10]; substance P is also involved in nerve ingrowth and is predominantly secreted at sensory nerve endings during innervation [39]. Both factors work in synergy and may be directly involved in mediating innervation and pain in the lower back [31, 36]. Taken together, the association with wear-debris induced inflammation elucidates key mechanisms that may be involved in the development of pain in TDR patients.

4.6 References

1. United States Bone and Joint Initiative. *The Burden of Musculoskeletal Diseases in the United States, 2nd ed.* American Association of Orthopaedic Surgeons. Rosemont, IL 2011.
2. Abe Y, Akeda K, An HS, Aoki Y, Pichika R, Muehleman C, Kimura T, Masuda K. Proinflammatory cytokines stimulate the expression of nerve growth factor by human intervertebral disc cells. *Spine (Phila Pa 1976)*. 2007;32:635-642.
3. Ahmed M, Bjurholm A, Kreicbergs A, Schultzberg M. Sensory and autonomic innervation of the facet joint in the rat lumbar spine. *Spine (Phila Pa 1976)*. 1993;18:2121-2126.
4. Ashton IK, Roberts S, Jaffray DC, Polak JM, Eisenstein SM. Neuropeptides in the human intervertebral disc. *Journal of orthopaedic research : official publication of the Orthopaedic Research Society*. 1994;12:186-192.
5. Baxter RM, Macdonald DW, Kurtz SM, Steinbeck MJ. Severe impingement of lumbar disc replacements increases the functional biological activity of polyethylene wear debris. *The Journal of bone and joint surgery. American volume*. 2013;95:e751-759.
6. Binch AL, Cole AA, Breakwell LM, Michael AL, Chiverton N, Cross AK, Le Maitre CL. Expression and regulation of neurotrophic and angiogenic factors during human intervertebral disc degeneration. *Arthritis research & therapy*. 2014;16:416.
7. Brattberg G, Parker MG, Thorslund M. A longitudinal study of pain: reported pain from middle age to old age. *The Clinical journal of pain*. 1997;13:144-149.
8. Brey EM, Lalani Z, Johnston C, Wong M, McIntire LV, Duke PJ, Patrick CW, Jr. Automated selection of DAB-labeled tissue for immunohistochemical

- quantification. *The journal of histochemistry and cytochemistry : official journal of the Histochemistry Society*. 2003;51:575-584.
9. Edwards RH, Rutter WJ, Hanahan D. Directed expression of NGF to pancreatic beta cells in transgenic mice leads to selective hyperinnervation of the islets. *Cell*. 1989;58:161-170.
 10. Freeman RS, Burch RL, Crowder RJ, Lomb DJ, Schoell MC, Straub JA, Xie L. NGF deprivation-induced gene expression: after ten years, where do we stand? *Progress in brain research*. 2004;146:111-126.
 11. Freemont AJ, Watkins A, Le Maitre C, Baird P, Jeziorska M, Knight MT, Ross ER, O'Brien JP, Hoyland JA. Nerve growth factor expression and innervation of the painful intervertebral disc. *The Journal of pathology*. 2002;197:286-292.
 12. Kim DH. *Dynamic Reconstruction of the Spine*: Thieme; Ed.1: 2006.
 13. Kim HJ, Suh BG, Lee DB, Park JY, Kang KT, Chang BS, Lee CK, Yeom JS. Gender difference of symptom severity in lumbar spinal stenosis: role of pain sensitivity. *Pain physician*. 2013;16:E715-723.
 14. Koreny T, Tunyogi-Csapo M, Gal I, Vermes C, Jacobs JJ, Glant TT. The role of fibroblasts and fibroblast-derived factors in periprosthetic osteolysis. *Arthritis and rheumatism*. 2006;54:3221-3232.
 15. Korsching S, Thoenen H. Nerve growth factor in sympathetic ganglia and corresponding target organs of the rat: correlation with density of sympathetic innervation. *Proceedings of the National Academy of Sciences of the United States of America*. 1983;80:3513-3516.
 16. Kurtz S, Steinbeck M, Ianuzzi A, Van Ooij A, Punt I, Isaza J, Ross ER. Retrieval analysis of motion preserving spinal devices and periprosthetic tissues. *SAS*. 2009;3:161-177.
 17. Kurtz SM, van Ooij A, Ross R, de Waal Malefijt J, Pelozza J, Ciccarelli L, Villarraga ML. Polyethylene wear and rim fracture in total disc arthroplasty. *Spine J*. 2007;7:12-21.
 18. Lavsky-Shulan M, Wallace RB, Kohout FJ, Lemke JH, Morris MC, Smith IM. Prevalence and functional correlates of low back pain in the elderly: the Iowa 65+ Rural Health Study. *Journal of the American Geriatrics Society*. 1985;33:23-28.
 19. Le Maitre CL, Freemont AJ, Hoyland JA. The role of interleukin-1 in the pathogenesis of human intervertebral disc degeneration. *Arthritis research & therapy*. 2005;7:R732-745.
 20. Lewin GR, Ritter AM, Mendell LM. Nerve growth factor-induced hyperalgesia in the neonatal and adult rat. *The Journal of neuroscience : the official journal of the Society for Neuroscience*. 1993;13:2136-2148.
 21. Lin TH, Kao S, Sato T, Pajarinen J, Zhang R, Loi F, Goodman SB, Yao Z. Exposure of polyethylene particles induces interferon-gamma expression in a natural killer T lymphocyte and dendritic cell coculture system in vitro: a preliminary study. *Journal of biomedical materials research. Part A*. 2015;103:71-75.

22. Malinsky J. The ontogenetic development of nerve terminations in the intervertebral discs of man. (Histology of intervertebral discs, 11th communication). *Acta anatomica*. 1959;38:96-113.
23. Marchand F, Perretti M, McMahon SB. Role of the immune system in chronic pain. *Nature reviews. Neuroscience*. 2005;6:521-532.
24. Melrose J, Roberts S, Smith S, Menage J, Ghosh P. Increased nerve and blood vessel ingrowth associated with proteoglycan depletion in an ovine annular lesion model of experimental disc degeneration. *Spine (Phila Pa 1976)*. 2002;27:1278-1285.
25. Mooney V. Where is the lumbar pain coming from? *Annals of medicine*. 1989;21:373-379.
26. Nerlich AG, Schaaf R, Walchli B, Boos N. Temporo-spatial distribution of blood vessels in human lumbar intervertebral discs. *European spine journal : official publication of the European Spine Society, the European Spinal Deformity Society, and the European Section of the Cervical Spine Research Society*. 2007;16:547-555.
27. Peng B, Wu W, Hou S, Li P, Zhang C, Yang Y. The pathogenesis of discogenic low back pain. *The Journal of bone and joint surgery. British volume*. 2005;87:62-67.
28. Purmessur D, Freemont AJ, Hoyland JA. Expression and regulation of neurotrophins in the nondegenerate and degenerate human intervertebral disc. *Arthritis research & therapy*. 2008;10:R99.
29. Rao AJ, Gibon E, Ma T, Yao Z, Smith RL, Goodman SB. Revision joint replacement, wear particles, and macrophage polarization. *Acta biomaterialia*. 2012;8:2815-2823.
30. Ribeiro RA, Vale ML, Thomazzi SM, Paschoalato AB, Poole S, Ferreira SH, Cunha FQ. Involvement of resident macrophages and mast cells in the writhing nociceptive response induced by zymosan and acetic acid in mice. *European journal of pharmacology*. 2000;387:111-118.
31. Richardson SM, Doyle P, Minogue BM, Gnanalingham K, Hoyland JA. Increased expression of matrix metalloproteinase-10, nerve growth factor and substance P in the painful degenerate intervertebral disc. *Arthritis research & therapy*. 2009;11:R126.
32. Spiller KL, Anfang RR, Spiller KJ, Ng J, Nakazawa KR, Daulton JW, Vunjak-Novakovic G. The role of macrophage phenotype in vascularization of tissue engineering scaffolds. *Biomaterials*. 2014;35:4477-4488.
33. Thacker MA, Clark AK, Marchand F, McMahon SB. Pathophysiology of peripheral neuropathic pain: immune cells and molecules. *Anesthesia and analgesia*. 2007;105:838-847.
34. Thomazzi SM, Ribeiro RA, Campos DI, Cunha FQ, Ferreira SH. Tumor necrosis factor, interleukin-1 and interleukin-8 mediate the nociceptive activity of the supernatant of LPS-stimulated macrophages. *Mediators of inflammation*. 1997;6:195-200.
35. Tunyogi-Csapo M, Koreny T, Vermes C, Galante JO, Jacobs JJ, Glant TT. Role of fibroblasts and fibroblast-derived growth factors in periprosthetic

- angiogenesis. *Journal of orthopaedic research : official publication of the Orthopaedic Research Society*. 2007;25:1378-1388.
36. Verge VM, Tetzlaff W, Richardson PM, Bisby MA. Correlation between GAP43 and nerve growth factor receptors in rat sensory neurons. *The Journal of neuroscience : the official journal of the Society for Neuroscience*. 1990;10:926-934.
 37. Veruva SY, Lanman TH, Isaza JE, MacDonald DW, Kurtz SM, Steinbeck MJ. UHMWPE Wear Debris and Tissue Reactions Are Reduced for Contemporary Designs of Lumbar Total Disc Replacements. *Clinical orthopaedics and related research*. 2015;473:987-998.
 38. Weiler C, Nerlich AG, Bachmeier BE, Boos N. Expression and distribution of tumor necrosis factor alpha in human lumbar intervertebral discs: a study in surgical specimen and autopsy controls. *Spine (Phila Pa 1976)*. 2005;30:44-53; discussion 54.
 39. Wojtys EM, Beaman DN, Glover RA, Janda D. Innervation of the human knee joint by substance-P fibers. *Arthroscopy : the journal of arthroscopic & related surgery : official publication of the Arthroscopy Association of North America and the International Arthroscopy Association*. 1990;6:254-263.
 40. Woolf CJ, Ma QP, Allchorne A, Poole S. Peripheral cell types contributing to the hyperalgesic action of nerve growth factor in inflammation. *The Journal of neuroscience : the official journal of the Society for Neuroscience*. 1996;16:2716-2723.
 41. Yue JJ, Bertagnoli R, McAfee PC, Howard S. *Motion Preservation Surgery of the Spine: Advanced Techniques and Controversies*: Saunders; 2008.
 42. Zhang JM, An J. Cytokines, inflammation, and pain. *International anesthesiology clinics*. 2007;45:27-37.

CHAPTER 5

Investigations into the Pathogenesis of Inflammatory Particle Disease in the Lumbar Spine based on Localized Changes in Vascularization & Innervation

5.1 Abstract

The mechanisms involved in the generation of unintended pain after metal-on-UHMWPE total disc replacement (TDR) remain poorly understood. While wear-debris and subsequent inflammation have been established in this dissertation as the biological response to UHMWPE wear particles, increased vascularization is another key histomorphological change that may provide the link to pathological innervation and ultimately pain sensitization. Our hypothesis was that ingrowth of blood vessels may provide a conduit for nociceptive innervation. Thus, the aim of this study was to explore the contributions of a neurovascular component in wear-debris-triggered tissue responses. We evaluated the expression of six inflammatory factors in tissue sections from eleven TDR patients and their association with tissue vascularity using immunohistochemistry. To assess the production of these factors by cells other than macrophages or fibroblasts, we masked blood vessels/nerves in individual images of tissue sections with wear-debris and varying degrees of vascularity for five TDR patients. Macrophages were also quantified to assess their relationship with angiogenesis. Our results showed the total number of blood vessels strongly correlated with the levels of TNF α , IL-1 β , VEGF, PDGFbb, NGF and substance P,

confirming that vascular changes and inflammatory-mediated responses are interrelated. Furthermore, the innervation/pain factors, NGF and substance P, were predominantly localized to vascular channels, strongly suggesting increased innervation of these tissues. Lastly, comparing blood vessel number with factor production and macrophage number in images from tissue sections with low and high vascularity suggested that a temporal link exists between increased inflammatory factors, macrophages and angiogenesis.

5.2 Introduction

Angiogenesis is the growth of new blood vessels from existing vasculature that can play a critical role in development [6], but may also be involved in pathological conditions of wear-debris-induced inflammation (i.e. particle disease) after total disc replacement (TDR) [28]. While the term “particle disease” was originally coined to describe the failure of local tissue homeostatic mechanisms for total hip replacements (THRs), wear particles in both the hip and spine may also indirectly lead to the induction of angiogenesis and other tissue functional changes [9, 28]. These changes are a consequence of wear particle-induced release of inflammatory factors by resident fibroblasts and recruited macrophages. In addition, these “activated” cells also proliferate and the increased cellular activity/metabolism results in higher oxygen consumption in the local tissue. In turn, this process induces hypoxic or oxygen-deficient microenvironments [26]. Subsequently, fibroblasts, macrophages and other hypoxic cells (even neurons) in the tissues secrete factors such as vascular endothelial growth factor (VEGF) to promote an increase in vascularization in an

attempt to alleviate hypoxia [13, 18]. Although the annulus fibrosis of the spinal disc regions is poorly vascularized [19], activated fibroblasts and macrophages in close proximity to existing blood vessels can coordinate signals with endothelial cells (ECs) and other stromal cells to stimulate angiogenesis [6, 12]. Specifically, activated macrophages, given their ability to play a trophic role in pathological angiogenesis and anastomosis [20, 23], can induce blood vessel ingrowth, which can consequently result in the infiltration of more monocytes. Thus, increased vascularization can ultimately lead to enhanced inflammation and more VEGF production, thereby creating a viscous cycle.

In addition to increasing oxygenation, angiogenesis can lead to increased innervation of the tissue by nociceptive nerve fibers. It is well established and has been published in anatomy textbooks for decades that peripheral nerves track alongside blood vessels. During development of the sympathetic nervous system, neural crest stem cells migrate to positions adjacent to the aorta and extend axons in close proximity to the peripheral vasculature [5]. Similarly, degenerative disc disease stimulates sympathetic nerve fibers to follow the trajectories of ingrowing blood vessels into the relatively avascular and aneural disc [5, 8]. Studies have shown that ECs from infiltrating vessels can secrete neurotrophins such as nerve growth factor (NGF), whereas peripheral sensory nerves can secrete VEGF, creating a complex, but coordinated pattern of growth between large blood vessels (typically arteries and veins that connect the vascular network and provide a capillary source for nutrient and oxygen exchange) and nerve fibers [8, 18]. In degenerative disc studies involving painful discogenic pain, these infiltrating nerve fibers are positive for proteins like

substance P, indicative of nerves originating from the dorsal root ganglion; and thus, these fibers are nociceptive [2, 4, 10, 21].

While there is already a dearth of knowledge on the mechanisms underlying vascular and nerve ingrowth into painful intervertebral discs, there are no reports regarding the contributions of a neurovascular component in the pathogenesis of inflammatory particle disease after TDR. We hypothesized that wear-debris-induced inflammatory mediators and cells noted in our previous retrieval studies of TDR tissues (*see Chapter 4*), may be intimately linked to vascularization and innervation. To investigate this link, we focused on localized relationships between inflammatory factors, CD68+ macrophages, vascularization and innervation factors in these periprosthetic spine tissues. We evaluated whether: (1) the total number of large blood vessels present in tissue sections from revised TDRs were associated with the inflammatory factors, TNF α , IL-1 β , VEGF, PDGFbb, NGF and substance P in the respective sections; (2) the innervation and pain factors, NGF and substance P, were localized to large blood vessels and surrounding nerve fibers; (3) the localization of large blood vessels, inflammatory factors and macrophages suggested temporal differences in tissue sections with varying levels of vascularity.

5.3 Materials & Methods

5.3.1 Tissue Selection & Patient Information

All periprosthetic revision and initial TDR surgical tissues were collected as part of a public, multi-center retrieval research program initiated in 2004 [15, 16]. For the initial analysis studying associations between the vasculature and

inflammatory factors in the periprosthetic spine, 30 periprosthetic tissue samples were evaluated from 11 TDR patients (*see Chapter 3.3.1 and Table 3-1*). For the investigations focused on the localization of blood vessels, inflammatory factors and macrophages, five representative tissue sections were chosen from five TDR patients (Table 5-1). The inclusion criteria for this selection process were: (1) the presence of wear debris to specifically study wear-induced tissue responses; (2) the presence of at least 10 blood vessels per section to match baseline levels of vascularization noted in intervertebral disc tissue controls; and (3) a range of low to high vascularity based on the Oxford scoring system (*see Chapter 3.3.2 and Table 3-3*) to study temporal differences.

Table 5-1. Tissue Selection and Clinical Information for TDR Patients

Patient ID	Section ID	Age at TDR Implantation (years)	Implantation Time (years)	UHMWPE Wear Debris	Vascularization Score (0-3)*
BHSP 023	Right Intradiscal	56	5.0	Yes	3
BHSP 025	Left Posterior L5-S1	49	4.0	Yes	3
BHSP 027	Left Discal	33	5.0	Yes	1
BHSP 0032	L5-S1	46	6.0	Yes	3
BRSP 003	Inferior L4-L5	28	1.5	Yes	1

**Values based on modified Oxford scoring system developed in Chapter 4.*

5.3.2 Tissue Preparation & Immunohistochemistry

Tissues collected from revision surgeries were fixed in either formalin or Universal Molecular Fixative (UMFIX; Sakura Finetek USA, Inc, Torrance, CA, USA). One to two 4-mm punches from each tissue, considering variations in color, texture, and size of

specimen, were embedded in paraffin blocks, and 6- μ m serial sections were mounted onto ProbeOnPlus (Fischer Scientific Co, Pittsburgh, PA, USA) slides. Immunohistochemistry was performed on prepared slides to evaluate the expression of six secretory factors and a pan-macrophage marker: pro-inflammatory cytokines, TNF α (Rabbit IgG, Novus Biologicals, NBP1-19532) and IL-1 β (Rabbit IgG, Abcam, AB2105); vascularization factors, VEGF (Rabbit IgG, SantaCruz, sc-507) and PDGFbb (Rabbit IgG, Abcam,); pain-related factors, NGF (Rabbit IgG, Abcam, AB6199) substance P (Rabbit IgG, EMD Millipore, AB1566); and macrophage marker, CD68 (Rabbit IgG, Abcam, AB125157). Optimal conditions for the inflammatory and pain-related antibodies were determined using periprosthetic tissues of total hip replacement patients that had severe pain and wear debris; mouse kidney tissues for the vascularization factors; and human tonsil tissue for the macrophage marker. The antibody concentrations were: TNF α 1:100, IL-1 β 1:400, VEGF 1:100, PDGFbb 1:100, NGF 1:500, substance P 1:500 and CD68 1:100. Slides with tissues originally fixated in formalin, as opposed to UMFIX (Sakura Finetek, Torrance, CA), were first treated with an antigen retrieval solution (Vector Labs). All slides were incubated in 0.5% Triton in PBS to enhance permeability, 3% H₂O₂ in methanol to block endogenous peroxidases, and to block non-specific background in 4% BSA, 0.1% Tween 20 in PBS. Lastly, slides were incubated at 4 °C overnight with the primary antibodies. For antibody visualization, samples were incubated with pan-specific secondary antibody, followed by horseradish peroxidase (Santa Cruz Biotech) and DAB solution (Vector Labs), and then counterstained with 50% hematoxylin.

5.3.3 Imaging & Analysis

Each stained tissue section was imaged (200X objective) using an Olympus BX50 microscope (Olympus, Melville, NY, USA) equipped with a stepper motor-controlled stage. DAB expression was determined by first employing a customized image threshold operation programmed in MATLAB® (MathWorks Inc, Natick, MA), followed by measuring area via NIH ImageJ (National Institutes of Health, Bethesda, MD). In brief, the red, green and blue channels for the 24-bit bright field DAB-labelled images were normalized by the sum of the three channels. Pixel values for 8-bit images were calculated using a published formula that allows for maximal separation of DAB-stained pixels from the background tissue: $255 * \text{blue} / (\text{red} + \text{green} + \text{blue})$ [3].

CD68+ macrophages were quantified in each image (200x) of the stained tissue sections with the aid of Image-Pro Plus 6.0 (Media Cybernetics, Silver Spring, MD, USA). A customized macro was generated to threshold and count DAB-stained cells, in which the algorithm allowed the non-stop analysis of up to 50 consecutive images. In brief, images were split into three eight-bit channels (red, green, and blue). Signal from blue channels were converted into masks based on a threshold value relative to the average signal intensity of each image. Next, count/size operations were employed along with water-shed split commands in order to maximize accuracy of counts. See *Appendix 1-3* for macro.

Lastly, automation for the quantification of blood vessels was not possible through conventional thresholding and edge-detection. Large blood vessels were quantified through manual counts conducted by at least two individuals. For localization analysis, the tunics of blood vessels were manually traced in each image,

creating regions of interest that could be masked. Note that the tunics are not visible at 200X magnification for smaller vessels such as capillaries, postcapillary venules or arterioles. However, the focus of the analysis was to determine the number of large vessels (i.e. arteries and veins) that theoretically provide a conduit for in-growing nerve fibers [8, 18]. All analysis was performed in a blinded fashion.

5.3.4 Statistical Analysis

The normality of the data was determined using Shapiro-Wilk test (IBM SPSS Statistics V22 software package, IBM Corporation, Armonk, NY, USA). To statistically compare immunohistochemical levels between different patient groups, the Mann-Whitney U-test was employed. Significance was based on $p < 0.05$. Correlations for blood vessels, inflammatory factors and inflammatory cells were determined using Spearman Rho correlation test for non-parametric data. Significance was based on $p < 0.05$.

5.4 Results

5.4.1 Correlations between the Total Number of Blood Vessels and Inflammatory-mediated Pain Factors in TDR Tissues

To determine whether inflammatory-mediated pain factors correlated with tissue vascularity, the number of blood vessels in each tissue section was compared to factor expression for eleven TDR patients. The number of blood vessels, showed an expectedly significant and strongly positive correlation to the percent area of VEGF ($p < 0.001$, $\rho = 0.70$), but only a significant and weakly positive correlation to PDGFbb ($p = 0.022$, $\rho = 0.46$) (Figure 5-1). In the majority of cases, PDGFbb was only expressed

in high amounts when the tissue sections were highly vascularized (>45 blood vessels). For the pro-inflammatory cytokines, the number of blood vessels also showed a significant and strongly positive correlation to the percent area of TNF α ($p = 0.001$, $\rho = 0.70$), and a significant and moderately positive correlation to IL-1 β ($p = 0.002$, $\rho = 0.57$) (Figure 5-2). However, high TNF α levels were predominantly observed only when the tissue sections were highly vascularized (>45 blood vessels). Lastly, comparisons to the innervating/pain factors revealed the number of blood vessels also showed a significant and strongly positive correlation to the percent area of NGF ($p < 0.001$, $\rho = 0.70$), and a significant and moderately positive correlation to substance P ($p = 0.003$, $\rho = 0.57$)

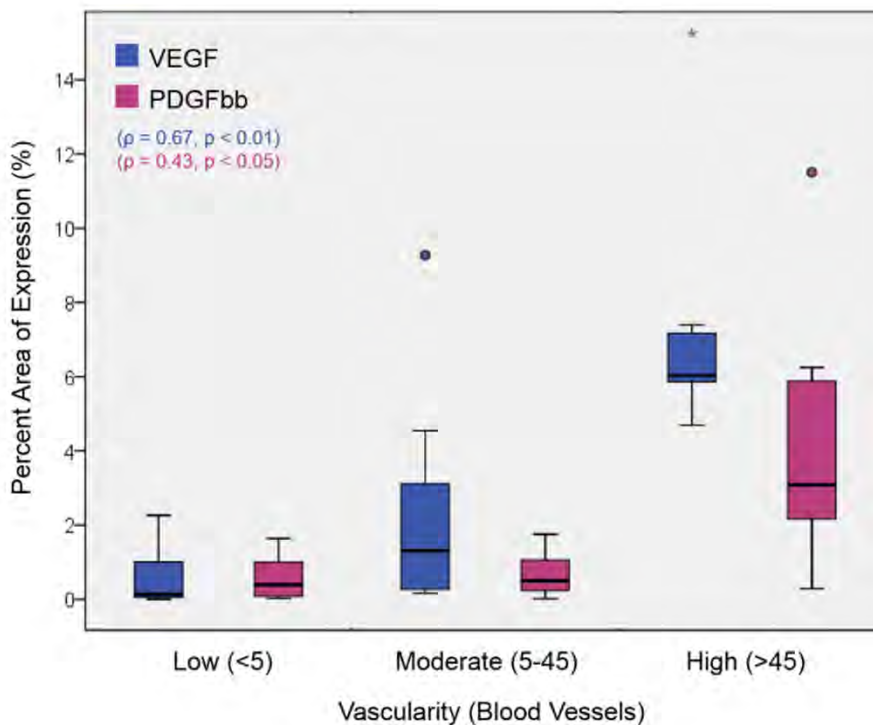


Figure 5-1. Blood vessel number correlated with VEGF and PDGFbb.

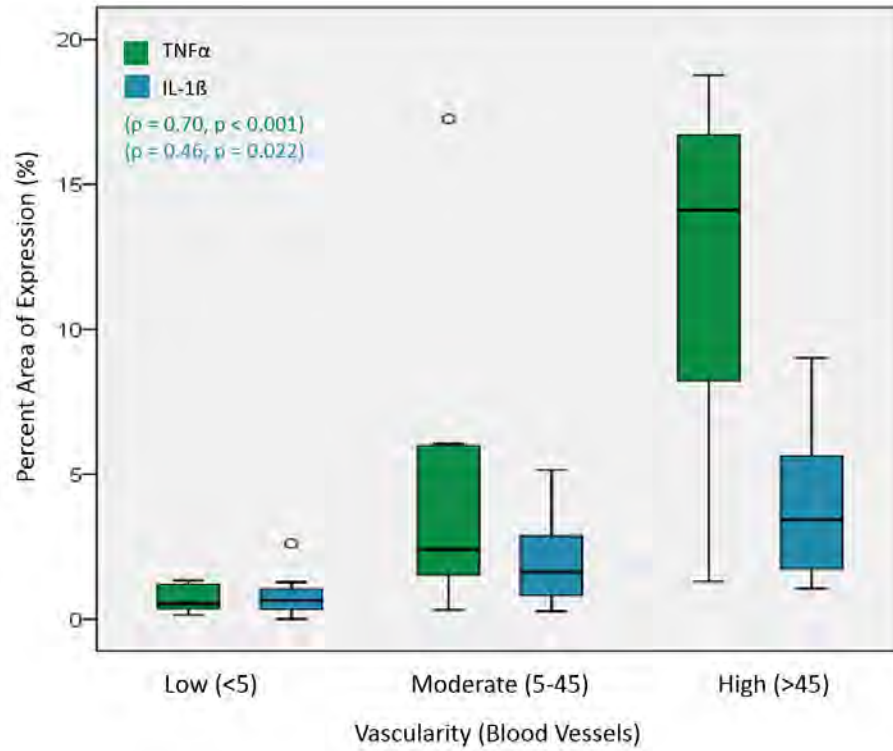


Figure 5-2. Blood vessel number correlated with TNF α and IL-1 β .

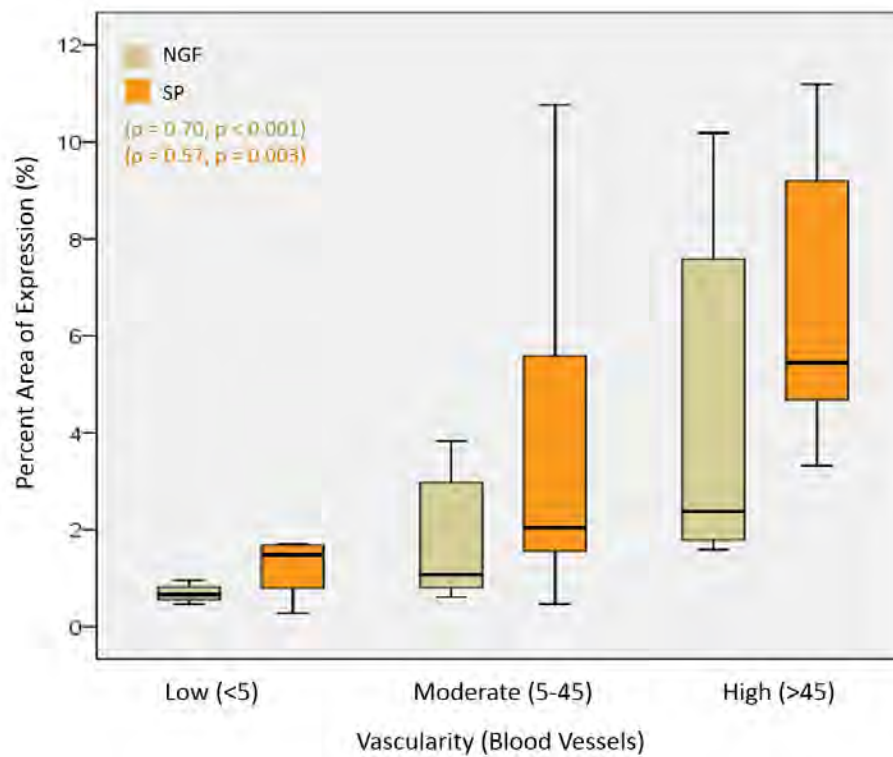


Figure 5-3. Blood vessel number correlated with NGF and substance P.

(Figure 5-3). While both factors showed a correlative relationship with blood vessel number, variations in expression levels were noted in both tissues sections with moderate and high vascularity.

5.4.2 Co-localization of Factors with Blood Vessels

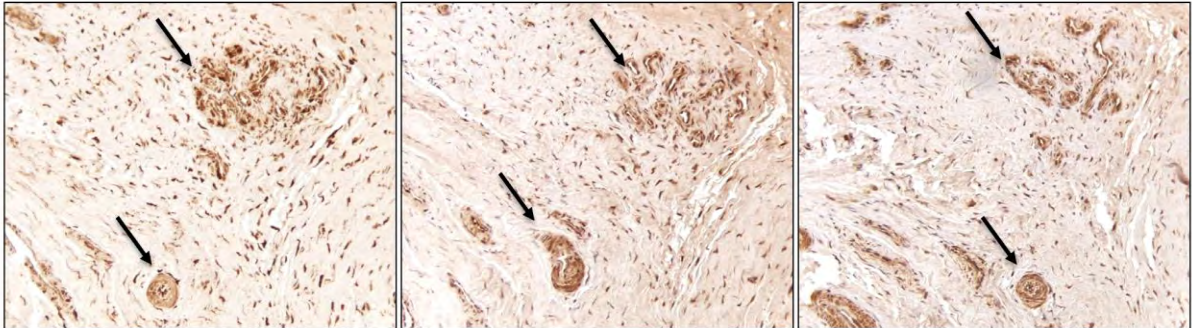


Figure 5-4. Representative images of TDR tissues immunostained for PDGFbb (left), NGF (middle) and substance P (right) illustrating co-localization of all three factors to blood vessels (black arrows).

Five vascularized tissue sections with wear debris from five TDR patients were selected to determine whether the inflammatory factors and particularly, innervation factors were co-localized to ingrown blood vessels in the periprosthetic spine tissues; each DAB-stained image was individually analyzed at 200X magnification and factor expression was averaged for each of the selected tissues. All six factors, VEGF, PDGFbb, TNF α , IL-1 β , NGF and substance P, were expressed in some blood vessels to a certain degree (Figure 5-4), however only three factors appeared to be specifically localized to blood vessels.

Masking blood vessels in images from the five tissue sections showed a decrease in amounts for all six factors at varying levels. Quantifying the percentage decrease of the factors when blood vessels were masked showed that PDGFbb and the innervation/pain factors NGF and substance P were reduced by more than 25%,

inferring that they were largely localized to blood vessels, and being produced by ECs, vascular smooth muscle cells and/or peripheral nerves (Figure 5-5). Furthermore, NGF was significantly higher in blood vessels compared to $\text{TNF}\alpha$ ($p = 0.016$), and PDGFbb was significantly higher in blood vessels compared to VEGF, $\text{TNF}\alpha$, IL-1 β and substance P, respectively ($p = 0.008$; $P = 0.008$; $p = 0.016$; $p = 0.016$).

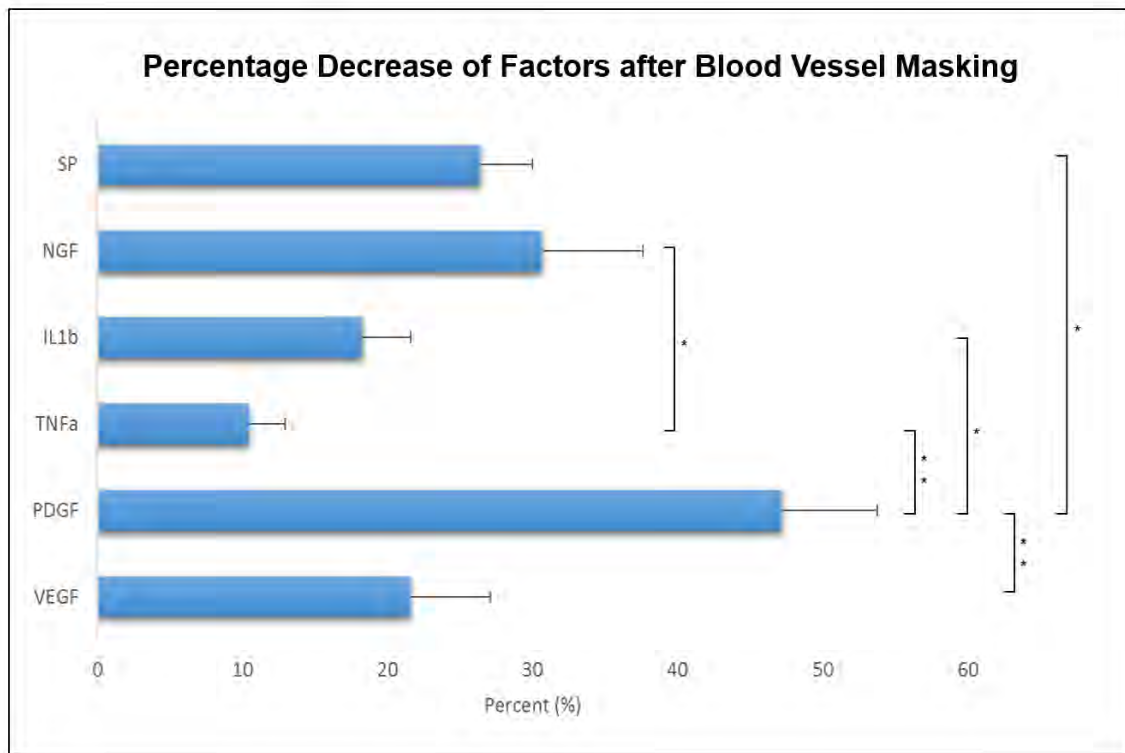


Figure 5-5. Percentage decrease of all six factors in periprosthetic tissues when blood vessels were masked.

5.4.3 Correlations for Blood Vessel Number with Inflammatory-mediated Pain Factor Expression and Macrophages in Tissues with Varying Levels of Vascularity

To assess how vasculature is related to local production of these factors, representative tissue sections (selected for wear debris and varying levels of vascu-

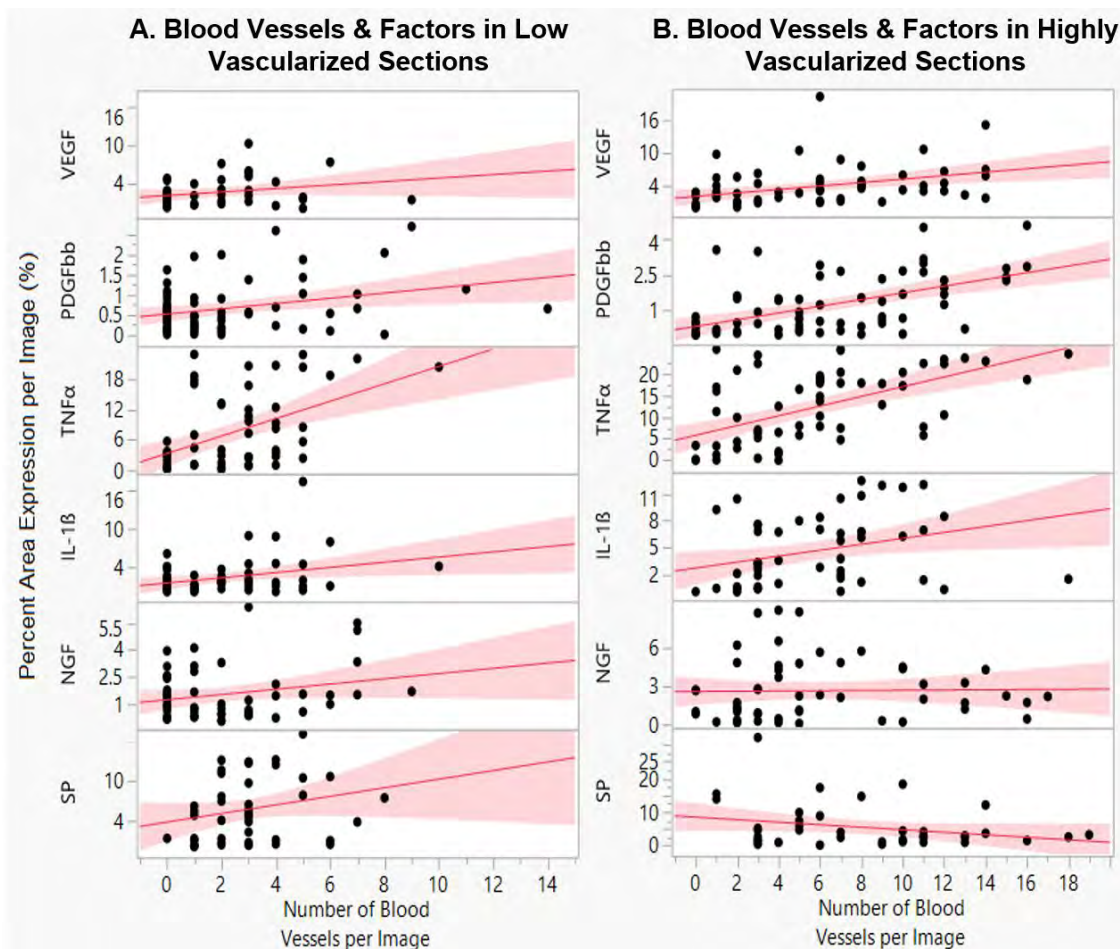


Figure 5-6. Blood vessel number and factor amounts per image in (A) low and (B) highly vascularized patient tissues.

larity) from five TDR patients were chosen in which blood vessels and inflammatory-mediated pain factors were quantified in individual images (at 200X magnification). These results were then separated based on low and highly vascularized tissue sections (Figure 5-6A & B). In less vascularized tissue sections, the number of blood vessels weakly correlated with only TNF α ($p = 0.007$; $\rho = 0.33$) and substance P ($p = 0.039$, $\rho = 0.27$). In highly vascularized tissue sections, the number of blood vessels correlated significantly with decreasing strength to TNF α ($p < 0.001$, $\rho = 0.58$), PDGFbb ($p < 0.001$, $\rho = 0.55$) and VEGF ($p = 0.004$, $\rho = 0.35$). Contrary to results from less vascularized tissue sections, substance P, although not statistically significant,

showed a negative association ($p = 0.115$, $\rho = -0.24$). NGF and IL-1 β showed no significant correlation in either case, but maintained a weakly positive association in both low and highly vascular tissues. A larger sample size may be necessary to identify the production of NGF and IL-1 β by ECs, vascular smooth muscle cells and/or peripheral nerves. Nonetheless, taken together, this data suggests a differential expression of factors depending on vascularity.

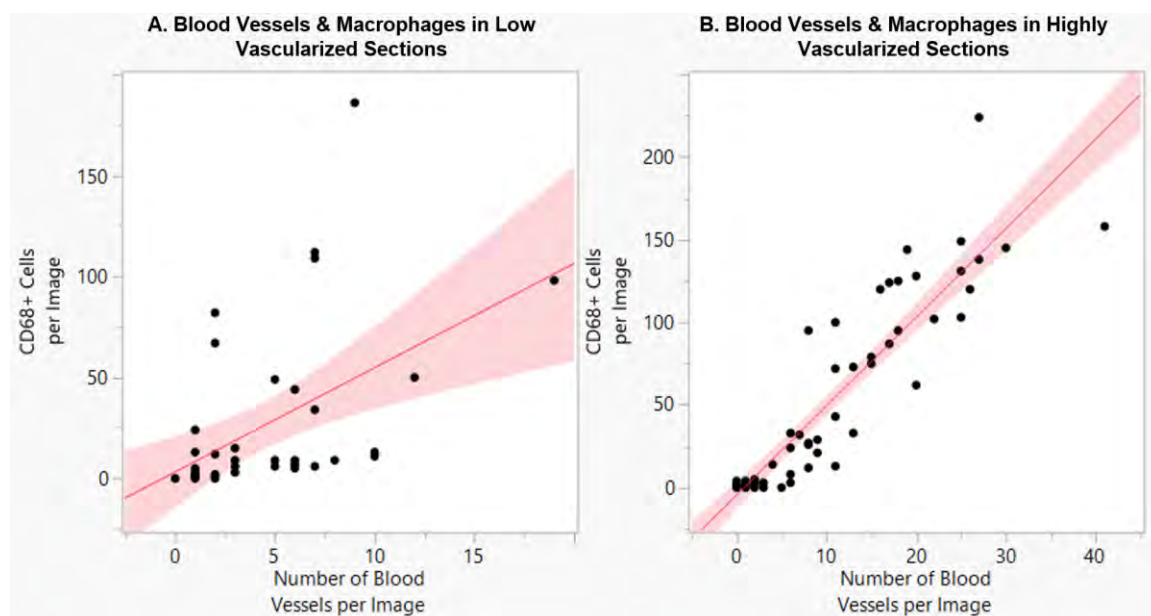


Figure 5-7. Blood vessel number and macrophage number per image in low (A) and highly vascularized (B) patient tissues.

To determine how vessel number is related to the local presence of macrophages, blood vessel and CD68+ macrophage number were quantified in individual images (at 200X magnification) and then collectively compared for low and highly vascularized tissue sections (Figure 5-7A & B). In less vascularized tissue sections, the number of blood vessels correlated significantly, but very weakly, to the number of CD68+ macrophages ($p = 0.001$, $\rho = 0.55$). In contrast, in highly

vascularized tissue sections, the number of blood vessels correlated significantly and very strongly to the number of CD68+ macrophages ($p < 0.001$, $\rho = 0.92$).

Although no significant correlations were originally found for implantation time (see Chapter 4), the mean implantation time for the low and high vascularity groups was 3.25 years and 4.3 years, respectively.

5.5 Discussion

Wear-debris and subsequent inflammation have been established in TDR revision tissues (see Chapters 4 & 5). In this study, increased vascularization has been identified as a consistent histomorphological change in response to wear debris. As such, the ingrowth of blood vessels may be providing a conduit for nociceptive innervation. Thus the aim of this study was to explore the contributions of a neurovascular component in wear-debris-mediated tissue responses. By determining the production of six inflammatory-mediated pain factors in tissue sections for all eleven patients making up the original TDR cohort, we found the total number of blood vessels was significantly associated with $\text{TNF}\alpha$, $\text{IL-1}\beta$, VEGF, PDGFbb, NGF and substance P, confirming that vascular changes and inflammatory-mediated responses are interrelated. Based on individual images of tissue sections with wear-debris from five TDR patients (*a new approach*), we found that in addition to PDGFbb, the innervation/pain factors, NGF and substance P, were predominantly localized to vascular channels. Lastly, correlations for blood vessel number with factor expression and macrophage number in images from tissue sections with low and high vascularity revealed a temporal link between $\text{TNF}\alpha$, macrophages and angiogenesis.

The significant localization of NGF and substance P with vascular channels supported our hypothesis that innervation is intertwined with the trajectories of in-growing blood vessels. Although this study does not provide evidence for the presence of actual nerves or pain, it is well established that these factors are involved in nerve ingrowth and predominantly secreted at sensory nerve endings resulting in nonciception or pain [1, 7, 14, 29]. Furthermore, both factors work in synergy and may be directly involved in mediating innervation and pain of the lower back [24, 27]. Taken together, the association of NGF and substance P with wear-debris induced inflammation and vascularization elucidates key mechanisms that may be involved in the development of pain in TDR patients.

Tissue sections with low and high vascularity (and noted for the presence of wear debris) were selected with the idea that the latter group contains more in-grown blood vessels and thus, systematic analysis of individual images in the two sets may provide insight into the temporal component of particle-induced pathogenesis. Substance P was the only factor that showed a strong association to low, but not highly vascular tissues, suggesting that it may be one of the initiating factors for the coordinated in-growth of blood vessels and nerves. Whereas, $\text{TNF}\alpha$, VEGF and PDGFbb showed stronger associations with blood vessel number in highly vascular tissue sections, suggesting they may be playing a more prominent role during relatively late stages of particle-induced tissue response.

Interestingly, $\text{TNF}\alpha$ showed a progressive correlation to low and high vascularity, suggesting that even though this factor is not co-localized to blood

vessels, it may be playing an essential role in regulating angiogenic progression. Although the role of TNF α in angiogenesis is the subject of some controversy, the duration of TNF α signaling can differentially regulate EC cell responses [25]. For example, *in vitro* studies have shown the initial secretion of TNF α can block signaling of VEGF receptor-2 and delay the VEGF-driven angiogenic response by inhibiting EC cell proliferation and migration [11, 22]. On the other hand, depending on the duration of TNF α signaling, it can also prime EC cells for sprouting by inducing tip cell phenotype via macrophage nuclear factor- κ B (NF- κ B) activation [25]. Since macrophages are a major source of TNF α , and their numbers also increased in highly vascularized tissues this strengthens a synergistic association of inflammation and TNF α with angiogenesis. Supporting this synergistic hypothesis, animal studies in mice and chicks indicate inflammatory factors like TNF α are essential for macrophage-induced angiogenesis [17]. Furthermore, a reduced number of macrophages can result in a significant delay in the onset of the angiogenic switch, suggesting inflammatory factors, which includes all six factors in this study, may be required for increased vascularization of periprosthetic TDR tissues. In conclusion, while the current results reveal some temporal differences and potential stages in wear-debris-induced vascularization, more research with a larger sample size is necessary to better understand the systematic progression of particle disease.

5.6 References

1. Abe Y, Akeda K, An HS, Aoki Y, Pichika R, Muehleman C, Kimura T, Masuda K. Proinflammatory cytokines stimulate the expression of nerve growth factor by human intervertebral disc cells. *Spine (Phila Pa 1976)*. 2007;32:635-642.

2. Ashton IK, Roberts S, Jaffray DC, Polak JM, Eisenstein SM. Neuropeptides in the human intervertebral disc. *Journal of orthopaedic research : official publication of the Orthopaedic Research Society*. 1994;12:186-192.
3. Brey EM, Lalani Z, Johnston C, Wong M, McIntire LV, Duke PJ, Patrick CW, Jr. Automated selection of DAB-labeled tissue for immunohistochemical quantification. *The journal of histochemistry and cytochemistry : official journal of the Histochemistry Society*. 2003;51:575-584.
4. Brown MF, Hukkanen MV, McCarthy ID, Redfern DR, Batten JJ, Crock HV, Hughes SP, Polak JM. Sensory and sympathetic innervation of the vertebral endplate in patients with degenerative disc disease. *The Journal of bone and joint surgery. British volume*. 1997;79:147-153.
5. Carmeliet P. Blood vessels and nerves: common signals, pathways and diseases. *Nature reviews. Genetics*. 2003;4:710-720.
6. Carmeliet P, Jain RK. Molecular mechanisms and clinical applications of angiogenesis. *Nature*. 2011;473:298-307.
7. Edwards RH, Rutter WJ, Hanahan D. Directed expression of NGF to pancreatic beta cells in transgenic mice leads to selective hyperinnervation of the islets. *Cell*. 1989;58:161-170.
8. Freemont AJ, Watkins A, Le Maitre C, Baird P, Jeziorska M, Knight MT, Ross ER, O'Brien JP, Hoyland JA. Nerve growth factor expression and innervation of the painful intervertebral disc. *The Journal of pathology*. 2002;197:286-292.
9. Gallo J, Goodman SB, Konttinen YT, Raska M. Particle disease: biologic mechanisms of periprosthetic osteolysis in total hip arthroplasty. *Innate immunity*. 2013;19:213-224.
10. Garcia-Cosamalon J, del Valle ME, Calavia MG, Garcia-Suarez O, Lopez-Muniz A, Otero J, Vega JA. Intervertebral disc, sensory nerves and neurotrophins: who is who in discogenic pain? *Journal of anatomy*. 2010;217:1-15.
11. Guo DQ, Wu LW, Dunbar JD, Ozes ON, Mayo LD, Kessler KM, Gustin JA, Baerwald MR, Jaffe EA, Warren RS, Donner DB. Tumor necrosis factor employs a protein-tyrosine phosphatase to inhibit activation of KDR and vascular endothelial cell growth factor-induced endothelial cell proliferation. *The Journal of biological chemistry*. 2000;275:11216-11221.
12. Hughes CC. Endothelial-stromal interactions in angiogenesis. *Current opinion in hematology*. 2008;15:204-209.
13. Knowles HJ, Athanasou NA. Acute hypoxia and osteoclast activity: a balance between enhanced resorption and increased apoptosis. *The Journal of pathology*. 2009;218:256-264.
14. Korsching S, Thoenen H. Nerve growth factor in sympathetic ganglia and corresponding target organs of the rat: correlation with density of sympathetic innervation. *Proceedings of the National Academy of Sciences of the United States of America*. 1983;80:3513-3516.
15. Kurtz S, Steinbeck M, Ianuzzi A, Van Ooij A, Punt I, Isaza J, Ross ER. Retrieval analysis of motion preserving spinal devices and periprosthetic tissues. *SAS*. 2009;3:161-177.

16. Kurtz SM, van Ooij A, Ross R, de Waal Malefijt J, Pelozo J, Ciccarelli L, Villarraga ML. Polyethylene wear and rim fracture in total disc arthroplasty. *Spine J*. 2007;7:12-21.
17. Leibovich SJ, Polverini PJ, Shepard HM, Wiseman DM, Shively V, Nuseir N. Macrophage-induced angiogenesis is mediated by tumour necrosis factor-alpha. *Nature*. 1987;329:630-632.
18. Mukouyama YS, Shin D, Britsch S, Taniguchi M, Anderson DJ. Sensory nerves determine the pattern of arterial differentiation and blood vessel branching in the skin. *Cell*. 2002;109:693-705.
19. Nerlich AG, Schaaf R, Walchli B, Boos N. Temporo-spatial distribution of blood vessels in human lumbar intervertebral discs. *European spine journal : official publication of the European Spine Society, the European Spinal Deformity Society, and the European Section of the Cervical Spine Research Society*. 2007;16:547-555.
20. Newman AC, Hughes CC. Macrophages and angiogenesis: a role for Wnt signaling. *Vascular cell*. 2012;4:13.
21. Ohtori S, Takahashi K, Chiba T, Yamagata M, Sameda H, Moriya H. Substance P and calcitonin gene-related peptide immunoreactive sensory DRG neurons innervating the lumbar intervertebral discs in rats. *Annals of anatomy = Anatomischer Anzeiger : official organ of the Anatomische Gesellschaft*. 2002;184:235-240.
22. Patterson C, Perrella MA, Endege WO, Yoshizumi M, Lee ME, Haber E. Downregulation of vascular endothelial growth factor receptors by tumor necrosis factor-alpha in cultured human vascular endothelial cells. *The Journal of clinical investigation*. 1996;98:490-496.
23. Pollard JW. Trophic macrophages in development and disease. *Nature reviews. Immunology*. 2009;9:259-270.
24. Richardson SM, Doyle P, Minogue BM, Gnanalingham K, Hoyland JA. Increased expression of matrix metalloproteinase-10, nerve growth factor and substance P in the painful degenerate intervertebral disc. *Arthritis research & therapy*. 2009;11:R126.
25. Sainson RC, Johnston DA, Chu HC, Holderfield MT, Nakatsu MN, Crampton SP, Davis J, Conn E, Hughes CC. TNF primes endothelial cells for angiogenic sprouting by inducing a tip cell phenotype. *Blood*. 2008;111:4997-5007.
26. Santavirta S, Takagi M, Gomez-Barrena E, Nevalainen J, Lassus J, Salo J, Konttinen YT. Studies of host response to orthopedic implants and biomaterials. *J Long Term Eff Med Implants*. 1999;9:67-76.
27. Verge VM, Tetzlaff W, Richardson PM, Bisby MA. Correlation between GAP43 and nerve growth factor receptors in rat sensory neurons. *The Journal of neuroscience : the official journal of the Society for Neuroscience*. 1990;10:926-934.
28. Veruva SY, Lanman TH, Isaza JE, MacDonald DW, Kurtz SM, Steinbeck MJ. UHMWPE Wear Debris and Tissue Reactions Are Reduced for Contemporary Designs of Lumbar Total Disc Replacements. *Clinical orthopaedics and related research*. 2015;473:987-998.

29. Wojtys EM, Beaman DN, Glover RA, Janda D. Innervation of the human knee joint by substance-P fibers. *Arthroscopy : the journal of arthroscopic & related surgery : official publication of the Arthroscopy Association of North America and the International Arthroscopy Association*. 1990;6:254-263.

CHAPTER 6

Rare and Abnormal Biological Complications of Osteolysis after Total Disc Replacement: A Case Series[†]

6.1 Abstract

While this dissertation has focused on elucidating the clinical relevance of wear debris in the spine with an emphasis on pain, which is the primary reason for revision, osteolysis is a rare complication that should not be entirely discounted. Although few such complications have been reported for lumbar total disc replacement (TDR) and hybrid TDR fixations, our retrieval center identified and evaluated retrieved implants and periprosthetic tissue reactions for two cases of osteolysis following disc arthroplasty with ProDisc-L prostheses. Implants were examined for wear and surface damage, and tissues for inflammation, polyethylene wear debris by polarized light microscopy and metal debris by energy-dispersive X-ray spectroscopy. Despite initial good surgical outcomes, osteolytic cysts were noted in both patients at vertebrae adjacent to the implants. For the hybrid TDR case, heterotopic ossification and tissue necrosis due to wear-induced inflammation were observed. In contrast, the non-hybrid implant showed signs of abrasion and impingement, and inflammation was observed in tissue regions with metal and polyethylene wear debris. In both cases, wear debris and inflammation may have contributed to osteolysis. Surgeons using ProDisc prostheses should be aware of these rare complications.

[†]The content of this chapter was published in the journal of Clinical Orthopaedics and Related Research: Veruva SY, Lanman TH, Hanzlik JA, Kurtz SM and Steinbeck MJ. Rare complications of osteolysis and periprosthetic tissue reactions after hybrid and non-hybrid total disc replacement. *Eur Spine J.* 2015 May;24 Suppl 4:S494-501.

6.2 Introduction

Total disc replacement (TDR) is an established alternative to lumbar fusion for the treatment of back and leg pain that is associated with degenerative disc disease (DDD). In cases of 2-level DDD, hybrid fixation is a new approach that involves combining the advantages of TDR with spinal fusion at the adjacent (typically inferior) level. This approach preserves motion at one level and maintains stiffness in the lower segment to prevent adjacent segment degeneration. Aunoble and colleagues have shown that the clinical outcomes for patients that received hybrid surgery may be superior to 2-level TDRs or fusion in certain cases as there was a mean reduction of 24.9 in the Oswestry disability index (ODI) and a 64.6% improvement in the visual analog scale (VAS)[2]. Nevertheless, this does not mean every patient will benefit from hybrid fixation; for instance, the condition of the facet joints also serves as a central factor when determining the type of construct that is appropriate for a particular patient.

Although the majority of patients attain clinically significant pain reduction after 1-level TDR or hybrid fixation, foreign-body response to wear debris and rare instances of osteolysis have been noted for other devices. Historical generations of polyethylene-core devices such as the Charité Disc [originally Waldemar Link, Hamburg, Germany, later fabricated by DePuy Spine, Raynham, MA and currently discontinued] prostheses have shown evidence of polyethylene wear debris in periprosthetic tissues, accompanied by histological changes, the presence of histiocytes and multinuclear giant cells [9, 18]. Polyethylene wear particles are released from the implant as a consequence of abrasive and adhesive wear

mechanisms and are then ingested by resident macrophages initiating a chronic immune response that can lead to osteolysis[4]. Evidence of lumbar periprosthetic osteolysis appeared in 1 of 21 implant revisions from 18 patients who received a Charité Disc in our previously reported study, but little is known about osteolysis around ProDisc-L implants [9].

Interestingly, the one osteolysis case reported in our previous study occurred in a patient that underwent hybrid fixation. This raises the question of whether the combination of TDR and fusion may create a loading and kinematic environment conducive to potential osteolysis. Another potential factor that may contribute to osteolysis in the spine is the use of bone morphogenic protein (BMP) during fusion. McKay et al. noted that resorption rates around the implant increase with the use of BMP-2, presumably due to BMP-induced enhancement of osteoclast activity, which results in vertebral osteolysis [6, 14].

The purpose of this study was to report two unusual cases of osteolysis with a ProDisc-L lumbar disc replacement—one in which the patient underwent TDR at the level superior to BMP-induced interbody fusion at L5-L6 and another who had similar osteolytic lesions after 1-level TDR without any exposure to BMP-2. Both patients underwent TDR with ProDisc-L [Synthes, West Chester, PA] prosthesis, which consists of an ultra-high molecular weight polyethylene (UHMWPE) core and two metallic endplates made of a cobalt-chromium (CoCr) alloy and plasma-coated on the outside with titanium, similar to the Charité [10]. However, unlike the Charité, the UHMWPE core of ProDisc-L is locked into the inferior endplate, thus allowing relative motion only between the UHMWPE core and the superior endplate. To our

knowledge, there have been no previous reports on complications associated with osteolysis with the use of ProDisc-L.

6.3 Materials & Methods

6.3.1 Patients and Clinical Information

Two patients who suffered from lumbar disc herniation and radiculopathy underwent surgery. One patient required multi-level treatment and opted for hybrid fixation with ProDisc-L TDR and fusion, while the other received 1-level ProDisc-L TDR. Both TDRs were extracted during revision surgery and periprosthetic tissue specimens selected from regions adjacent to the implant were obtained. Retrievals, operative notes and radiographs were de-identified and collected in accordance with an IRB-approved protocol.

6.3.2 Implant Retrieval Analysis

The two sets of retrieved components were cleaned in 10 % bleach and examined under a stereomicroscope equipped with a digital camera (Leica DFC490) to assess for surface damage and gross fracture. All components were inspected to identify surface damage mechanisms (plastic deformation, scratching, burnishing, pitting, and embedded debris). Damaged regions of the implants were analyzed using scanning electron microscopy (SEM; Supra 50 VP, Zeiss Peabody, MA, USA), energy-dispersive X-ray spectroscopy (EDS) and x-ray fluorescence (XRF).

6.3.3 Tissue Preparation and Histological Analysis

Tissues collected from revision surgeries were fixed in Universal Tissue Fixative (Sakura Finetek USA, Inc., Torrance, CA, USA), and decalcified based on the presence of heterotopic ossification determined by microCT (μ CT 80, Scanco Medical, Bru'ttisellen, Switzerland). One to two 4-mm punches from each tissue, considering variations in color, texture, and size of specimen, were embedded in paraffin blocks for 6- μ m serial sectioning and staining with Alcian blue (Electron Microscopy Sciences, Hatfield, PA, USA), hematoxylin, and eosin (H&E) (ThermoFisher Scientific, Waltham, MA, USA). Entire tissue sections were imaged under transmitted light microscopy using a Motic BA300POL microscope (Motic, Richmond, British Columbia, Canada), equipped with an elliptically polarized light imaging system and ProgRes SpeedXT core 5 (Jenoptik, Jena, Germany) microscope camera. Inflammatory cells were confirmed using the Wright-Giemsa stain (Electron Microscopy Sciences, Hatfield, PA, USA). Tissues with notable chronic inflammation were examined using environmental scanning electron microscopy (ESEM; XL-30 ESEM-FEG, FEI Company, Hillsboro, OR, USA) with backscatter and were analyzed with EDS.

6.4 Case 1

A 40-year-old male suffering from discogenic collapse with lower back pain and radiculopathy at L5-S1 underwent anterior discectomy at L5-S1 and interbody arthrodesis with 17x24mm titanium-threaded fusion cages filled with BMP-2. The cages were inserted on each side of the vertebrae. A few months later, a posteriorly displaced cage, along with osteophyte formation and foraminal stenosis, required the

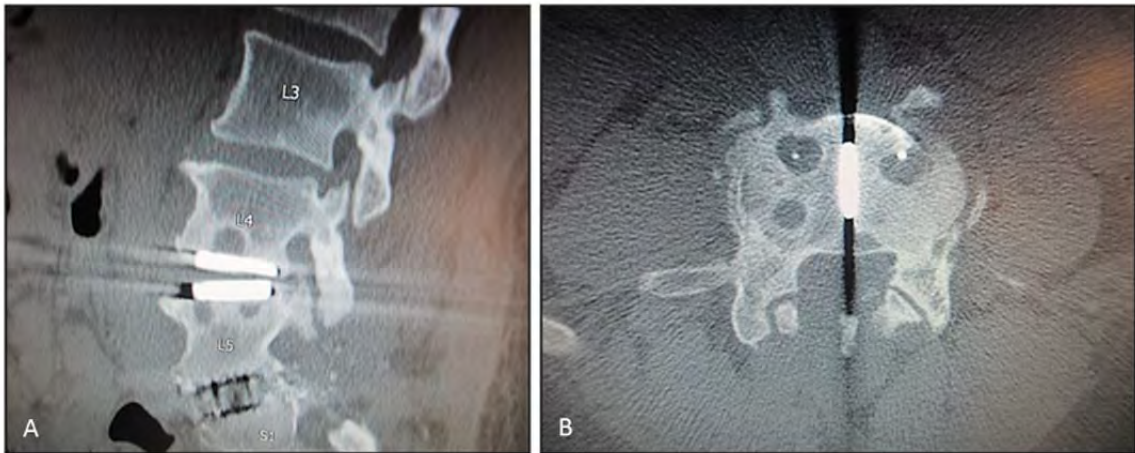


Figure 6-1. Sagittal (A) and axial (B) CT scans from case 1 illustrating discogenic herniation and osteolytic cysts at inferior L4 and superior L5. The axial scan also shows that there may be facet osteophytes and nerve root compression at the foramen

patient to undergo revision of the cage. Segmental pedicle screws were used to stabilize the cage on the right side; 6.5mm Xia (Stryker Spine, Allendale, NJ) pedicle screws were inserted at L5 and S1. Once the cages were locked, posterior interbody arthrodesis was then implemented at L5-S1 with the use of BMP-2 in two small sponges placed between each cage. One year later, with continued back pain and disc herniation at L4-L5, the patient opted for hybrid fixation and underwent anterior interbody placement of 12mm-large and 6-degree ProDisc-L (Synthes, West Chester, PA) prosthesis at L4-L5. The following year, the patient had removal of pedicle screw instrumentation at L5-S1 and there was solid fusion at the level. It may be important to note that the patient also required mass resection of osteophytes, other bony spurs and scar tissue.

Three years after fusion, persistent pain was experienced by the patient and severe arthropathy and degeneration was noted at right L4-L5. As the patient refused

to undergo disc removal and anterior fusion, posterior fusion was undertaken; 6.5mm screws were inserted and a PEEK rod was implemented at L4-L5, followed by posterolateral arthrodesis using local bone autograft, BMP-2, and DBX Demineralized Bone Matrix Allograft (Musculoskeletal Transplant Foundation, Edison, NJ). However, computed tomographic (CT) scans in the following year revealed osteolytic cysts at L4-L5 (Figure 6-1). The patient now consented to artificial disc removal. The PEEK rod stabilization system (2 PEEK rods and 4 pedicle screws) was removed and sent for retrieval analysis, along with the explanted artificial disc. Preoperative work up and intraoperative cultures ruled out infection. Tissue samples adjacent to the disc were also removed for histological analysis. After explantation of disc, the patient underwent spinal fusion with vertebral corpectomy. The area was filled and sealed with allograft bone and BMP-2. In the same year, pedicle screws were placed with rods for stabilization and posterior lateral arthrodesis was conducted with more local bone autograft and BMP-2. An overview of clinical information is provided in Table 6-1.

Table 6-1. Clinical information for the hybrid case 1 & non-hybrid case 2.

Implant	Level	Sex	Age at Implantation	Age at Revision	Primary Diagnosis	Revision Reason	Previous Surgeries	Implantation Time
Case 1	L4-L5	M	41	46	Lumbar disc herniation, radiculopathy	Pain, osteolysis	11	5 years
Case 2	L4-L5	M	56	59	Lumbar disc herniation, radiculopathy	Pain, subsidence, osteolysis	4	3 years

6.4.1 Device Retrieval Analysis

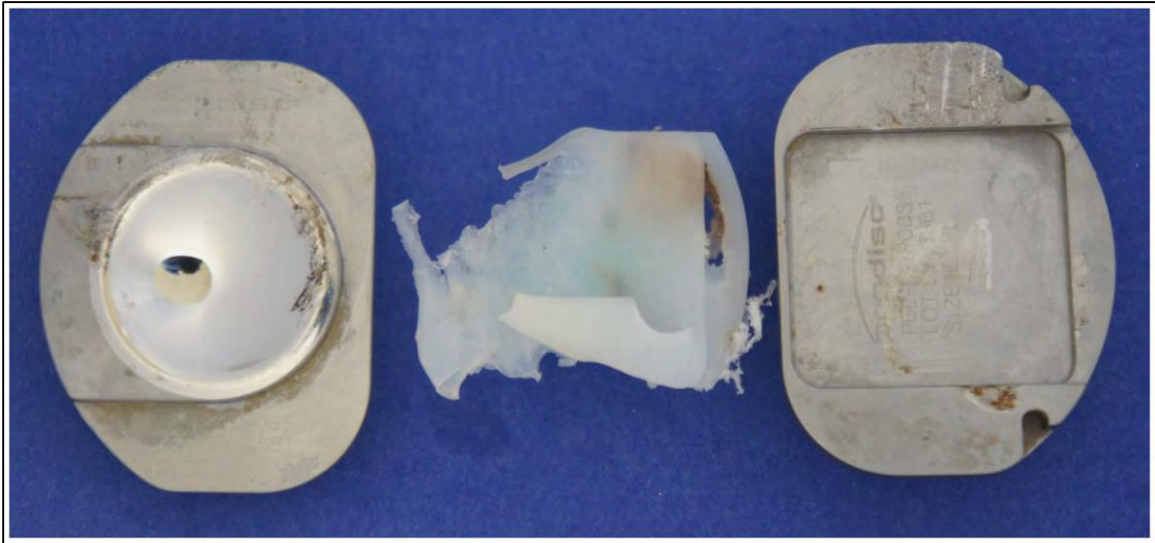


Figure 6-2. Retrieved ProDisc-L TDR, 5 years after insertion. The device was damaged during explantation. While it is unclear as to whether the polyethylene core was damaged in-vivo, there is no evidence of wear mechanisms on the end-plates.

The ProDisc-L prosthesis was retrieved five years after implantation. The polyethylene core was damaged during explantation, particularly the dome of the core (Figure 6-2). Due to iatrogenic damage, we could not determine if the rims of the polyethylene core experienced impingement with the superior endplate. While the backside surface also experienced iatrogenic damage, there was evidence of burnishing and scratching that occurred *in vivo*. There were no obvious signs of impingement on the metallic endplates, and the abrasive scratches were not patterned in any physiological manner, suggesting they were formed by surgical tools during device removal. Analysis using environmental scanning electron microscopy (ESEM) (XL-30 ESEM-FEG, FEI Company, Hillsboro, Oregon) and energy X-ray dispersive spectroscopy (EDS) revealed no abnormal surface deposits on the metallic endplates. As expected, x-ray fluorescence (XRF) scans consistently detected cobalt-

chromium ratios matching ASTM F-75 cobalt alloy weight-standards in the interior of the endplates, and the exterior plasma-coated elements consisted of alloy compositions seen in commercially pure titanium.

6.4.2 Tissue Analysis

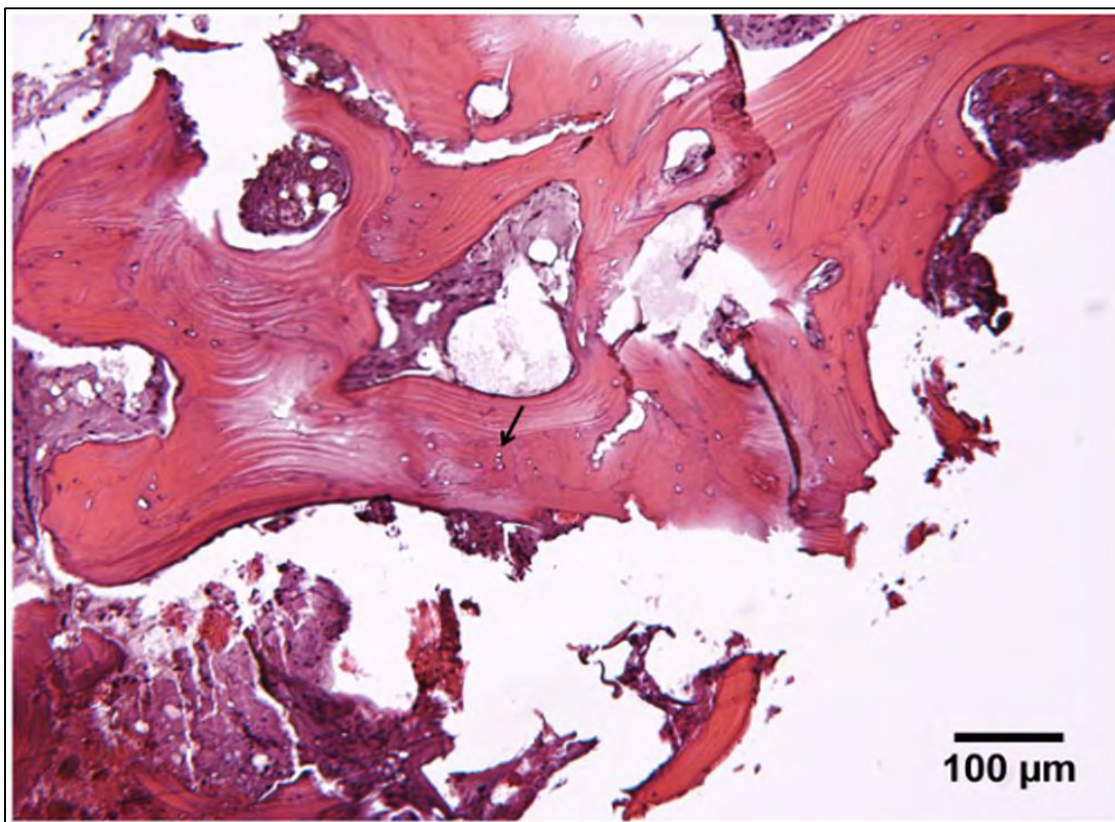


Figure 6-3. Bony tissue from case 1 stained with H&E (100X) showed necrotic bone with empty osteocyte lacunae (arrow) and necrotic marrow.

Periprosthetic tissues from this patient were obtained from two unclassified regions around the implant. Two tissue samples from one region were identified to be fibrocartilage, the other two samples from the second region were mature trabecular bone. One isolated region in the fibrocartilage tissue contained hemosiderin deposits and macrophages; consistent with an innate response to hemorrhage prior to explantation. There was no evidence of metal wear debris in any

tissues and only minor polyethylene debris was detected in isolated regions of the trabecular bone at a mean density of 1.13 particles/mm². In bony tissue samples, the fatty marrow in the intertrabecular spaces contained only a small number of viable cells; isolated regions of these samples consisted of necrotic bone marrow along with necrotic bone with empty osteocyte lacunae (Figure 6-3). An overview of tissue morphology is provided in Table 6-2.

6.5 Case 2



Figure 6-4. Sagittal (A) and axial (B) CT scans from case 2 showing L4 subsidence on the right side of the vertebra and one large osteolytic cyst in L5. Smaller osteolytic formations are also evident at superior L5.

A 56-year old male with a herniated disc and radiculopathy at L4-L5 underwent anterior TDR with a 10mm-large and 6-degree ProDisc-L. Three years after, subsidence of disc was noted at L4 on the right side, along with the formation of osteolytic cysts in CT scans at L5 that appear similar to the lesions seen in case 1 (Figure 6-4). Progressive back pain led to removal of ProDisc-L, followed by placement of 22mm PEEK interbody graft filled with BMP-2 for interbody fusion at

Table 6-2. An overview of tissue morphology for the two cases.

Implant	Tissue Location	Degeneration	Bone/Cartilage	Hemosiderin	Innate/ Adaptive Inflammation	PE Wear Debris (particles /mm²)	Metal Wear Debris
Case 1	*Region 1	No	No/Yes	Minor	Minor/No	None	No
	*Region 2	Yes	Yes/None	None	No/No	1.13	No
Case 2	Lateral Annulus I	No	No/Isolated	None	No/No	None	No
	Lateral Annulus II	Yes	Isolated/Yes	None	No/No	None	No
	Left Lateral	Yes	No/Yes	Moderate; Isolated	Moderate/No	None	No
	Lateral Spur I	Yes	Yes/Isolated	None	No/No	None	No
	Lateral Spur II	Yes	Yes/No	None	No/No	None	No
	Posterior Lateral	Yes	Yes/No	Mild	Moderate/Yes	2.74	No
	Superior End Plate	No	Yes/No	None	No/No	None	No
	Left Cyst	No	Isolated/No	Mild	Severe/Yes	2.96	Yes
	Right Cyst	Isolated	Isolated/No	Moderate	Severe/Yes	2.88	Yes
	Inner Cyst	Yes	No/No	Moderate	Severe/Yes	2.90	Yes
	Intradiscal	Isolated	Isolated/ Isolated	Moderate; Isolated	Severe/Yes	None	Yes
	Right Intradiscal	No	No/No	Severe	Moderate/Yes	None	Yes
	Posterior Intradiscal	Yes	No/No	Mild; Isolated	Moderate/Yes	1.01	Yes
	Anterior Intradiscal	Yes	Yes/Yes	None	No/No	1.25	No

*Exact tissue region of extraction is unknown.

L4-L5. Preoperative workup and intraoperative cultures were negative for infection.

6.5.1 Device Retrieval Analysis

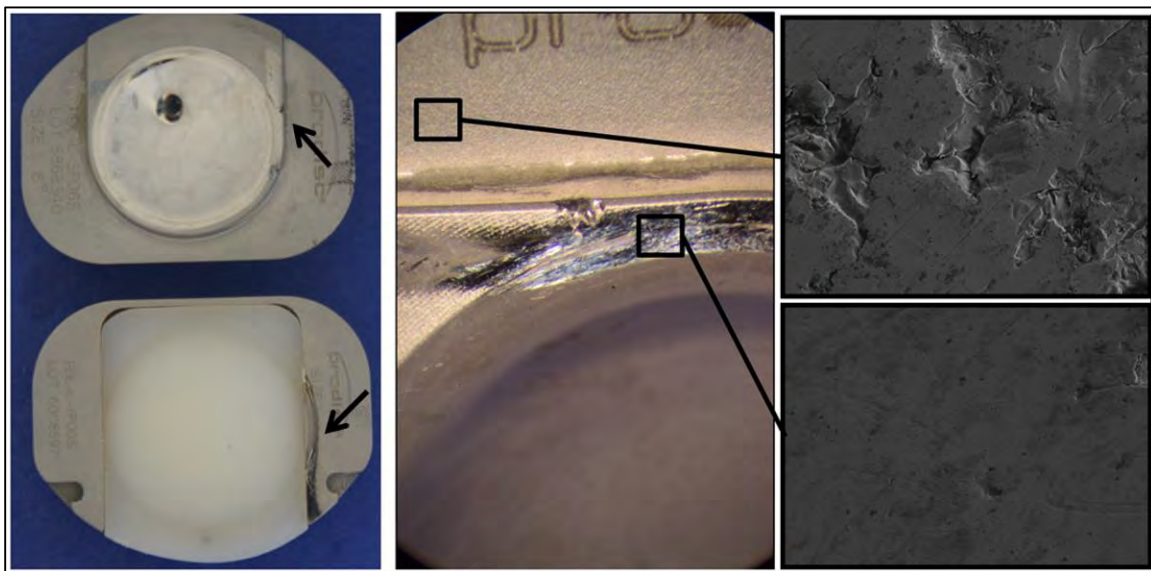


Figure 6-5. Retrieved ProDisc-L TDR, 3 years after insertion. Note the signs of impingement on both endplates (arrows). The impinged region on the metallic plate (lower right) has a smooth surface compared to the unimpinged region (upper right).

The ProDisc-L prosthesis was retrieved three years after implantation. There was clear evidence of chronic impingement between the endplates and burnishing at the core's edge; microscopic scratches of fan-shaped pattern were found on the interior of the metallic plates and a glossy appearance on the polyethylene core, respectively (Figure 6-5). SEM images of the impinged regions showed a polished appearance in comparison to the as-manufactured texture seen in non-impinged regions of the metallic plate. The unidirectional and circumferential wear patterns seen on the endplates suggest the wear may have occurred during axial rotation and/or lateral bending of the articulating surfaces. The impingement was most likely due to implant subsidence which was observed by the surgeon during surgery. The

dome of the core also had evidence of multi-directional scratches and burnishing. There were no indications of fatigue wear or fracture of the polyethylene core. No abnormal surface deposits were observed by SEM/EDS analysis. XRF scans showed the metallic surface-constituents on the interior of the endplates consistently matched CoCr ratios seen in ASTM F-75 cobalt alloy standards, and the exterior of plates consisted of weight compositions seen in commercially pure titanium.

6.5.2 Tissue Analysis

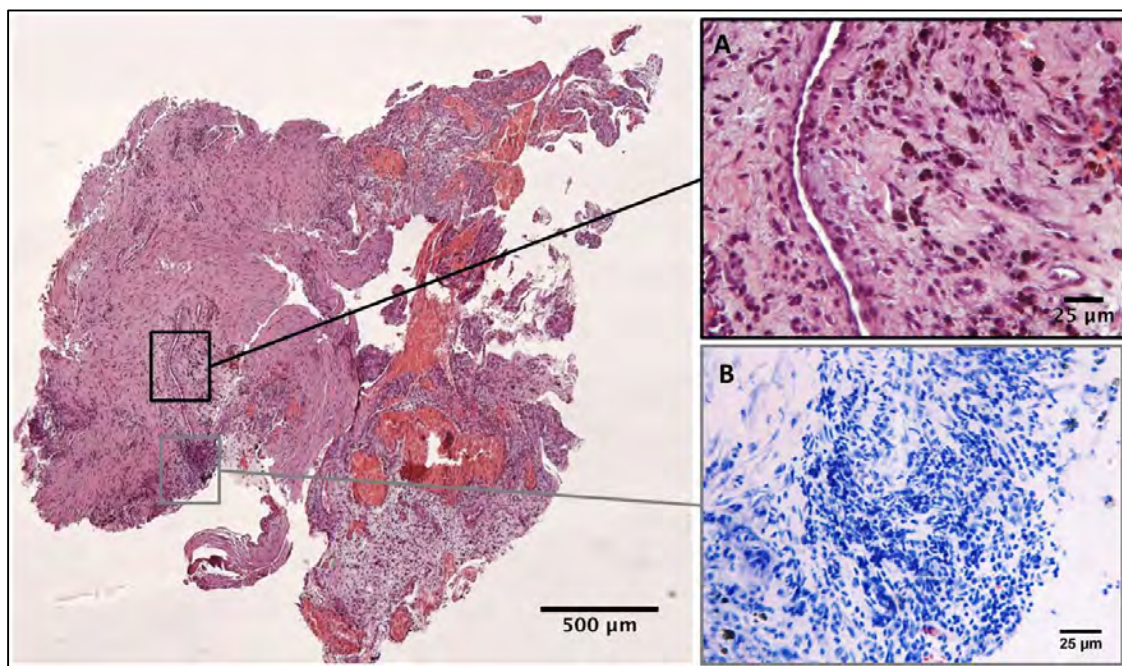


Figure 6-6. Histology of inner-cyst tissue with H/E stain showing mixed inflammation throughout. Inset A shows presence of macrophage-ingested metallic debris (H/E, 400X). Inset B shows presence of lymphocytes in the tissue (Wright-Giemsa, 400X).

The periprosthetic tissues in this patient showed several abnormalities such as progressive degeneration, varied inflammation levels, and metal and polyethylene wear debris (Table 6-2). While degeneration was observed in tissues from various regions, inflammation was predominantly in the intradiscal and cyst tissue; there

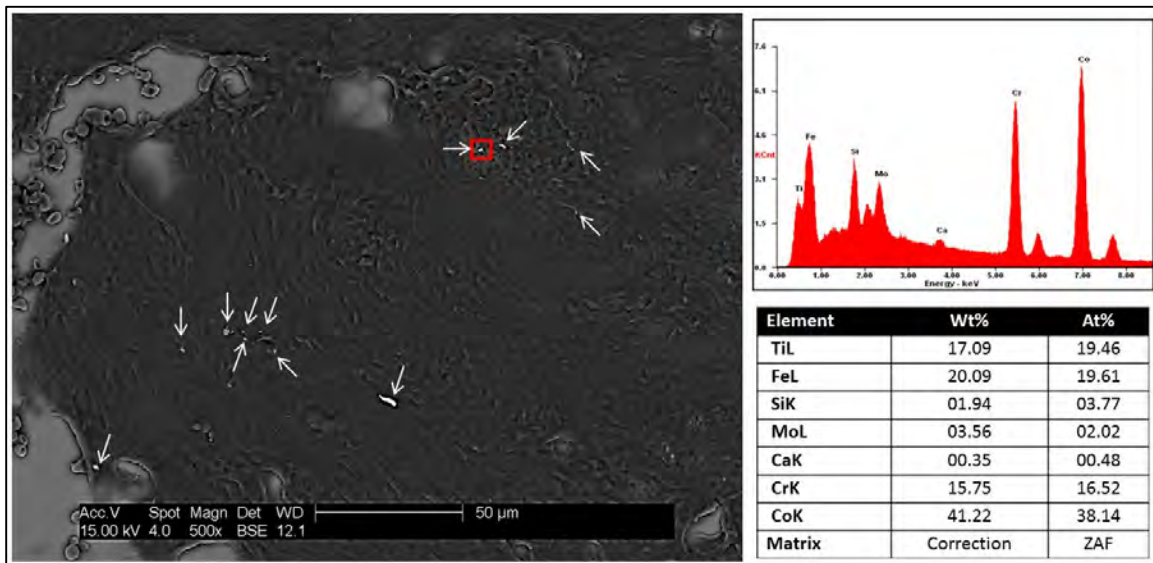


Figure 6-7. Titanium alloy and cobalt-chrome particles (arrows) were confirmed by use of backscatter scanning electron microscopy with elemental dispersive spectroscopy. Analysis of a region of interest (square) evidenced cobalt as the most abundant metal visualized by scanning electron microscopy. Wt = weight; At = atomic weight

were no signs of inflammation in tissues from the lateral annulus, left lateral, lateral spur, superior end plate and anterior intradiscal regions. Cyst tissue from L5 regions showed signs of both innate and adaptive immune response; macrophage ingested metal-wear-debris was present throughout the tissue and isolated areas of lymphocytes were also present (Figure 6-6). Cyst and intradiscal tissues also contained hemosiderin deposits (not shown), suggesting a prior hemorrhage that may have contributed to or exacerbated the chronic inflammation. To confirm metallic wear debris, tissues with notable inflammation were examined by ESEM using backscatter and were analyzed with EDS. The particles from cyst and intradiscal tissues were predominantly cobalt and chromium, however titanium was also detected (Figure 6-7). Polyethylene wear debris was present in relatively low numbers in all cyst, posterior-intradiscal, anterior-intradiscal and posterior-lateral

tissues. The mean polyethylene particles in these tissues was 2.08 particles/mm². These particles varied from oval to amorphous in shape and were localized to regions of chronic inflammation (Figure 6-8).

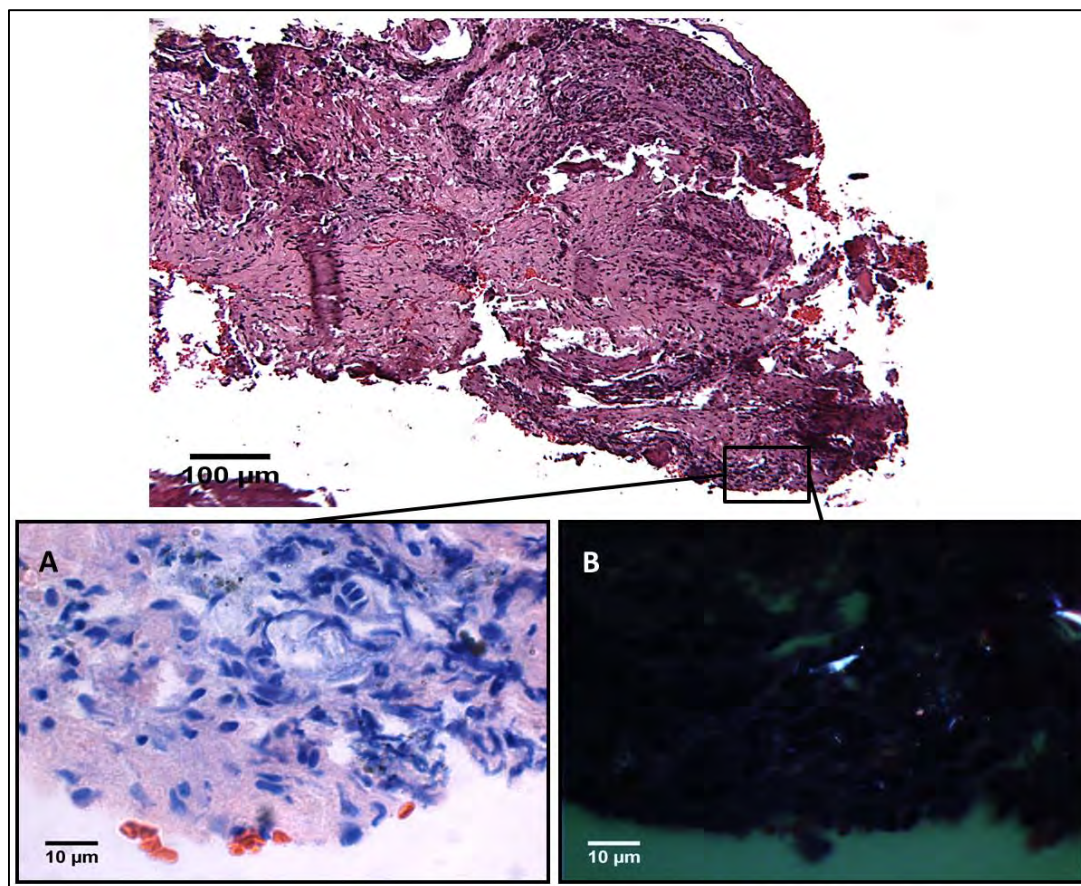


Figure 6-8. An H/E stained region of left-cyst tissue was stained with Wright-Giemsa (A, 1000X) and observed under polarized light (B, 1000X), showing evidence of mixed inflammation and polyethylene particles, respectively.

6.6 Discussion

This study reported two unusual cases of osteolysis in TDR patients with a ProDisc-L. The first patient suffered from multi-level DDD and opted for hybrid fixation, while the second had a 1-level TDR. Both patients developed osteolytic lesions in vertebrae adjacent to the prostheses. Infection was ruled out in both cases.

Retrieval and histological analysis of the hybrid case showed minor amounts of wear, however tissue responses included fibrocartilage generation, heterotopic ossification, and necrosis due to inflammation. The second case showed signs of endplate impingement and adverse local tissue reactions (ALTRs) in intradiscal and cystic tissues. In this second, impingement case, the amount of polyethylene wear debris was relatively low, but there was CoCr wear debris and associated inflammation. In both cases, inflammatory tissue responses may have contributed to the osteolytic lesions.

One difference between the hybrid and non-hybrid case was the use of BMP-2. The hybrid patient was exposed to BMP-2 on five occasions, in comparison to the patient that had a 1-level TDR who received none. Although osteolysis was a late observation after BMP-2 application, the hybrid patient only sought medical attention due to pain. A number of tissue responses to BMP-2 have been noted after spine surgery including heterotopic ossification observed in the hybrid patient's retrieved tissue [1, 7, 12]. Although previously believed to be asymptomatic, heterotopic ossification can lead to delayed neural compression and pain [7]. Furthermore, recent studies reported increased resorption rates with the use of BMP-2 around implants, raising the question whether BMP-2 contributes to osteolysis in regions adjacent to the fused segment [6, 14]. Authors have reported asymptomatic osteolysis after interbody fusion and attributed bone loss to endplate violation during disc space preparation and/or to overdosing of BMP-2 [11, 13, 17]. Whether BMP-2 has a dose-

responsive effect on the activation of osteolytic pathways remains unclear, since an optimal BMP-2 dose for fusions is still not agreed upon.

Osteolysis, along with tissue reactions involving mixed immune responses have been previously reported in a CHARITÉ by Kurtz et al. [9], but these devices consisted of polyethylene cores that were gamma-air-sterilized. ProDisc devices utilize conventional gamma-inert-sterilized polyethylene that has been previously reported in total joint replacements to significantly lower oxidation, wear debris generation and inflammation [5, 8]. ProDisc TDRs have been approved by the Food and Drug Administration, and only a limited number of complications have been documented with the use of either ProDisc-L or ProDisc-C. While hybrid fixation with ProDisc-L and fusion remains under clinical evaluation, there have been no previous reports of osteolysis with the use of ProDisc-L. However, with use of ProDisc-C for cervical TDR, one exceptional case of progressive osteolysis was reported and attributed to a possible immune-mediated metal sensitivity reaction [16].

In contrast to the minimal immune reaction in the hybrid case, there were substantial ALTRs in the intradiscal and cyst tissue of the non-hybrid case. Wear debris-induced inflammation is known to mediate osteolysis; thus, impingement and subsequent pro-inflammatory processes may explain the clinical symptoms and radiographic progression seen in the non-hybrid case [15]. All samples of cyst tissue showed signs of chronic inflammation and lymphocytic infiltration which were similar to ALTRs to metal ions from implant corrosion of metal-on-metal total hip

replacements (THRs) [3]. These findings suggest that ALTRs from THRs share some characteristics with the cyst tissue from the non-hybrid case.

The present study reported two rare osteolysis cases following implantation of the ProDisc-L. In one case, wear-debris induced inflammation; in the second case, inflammation induced heterotopic ossification. As surgeons incorporate ProDisc technology into their clinical practice, the rare complication of osteolysis and its occurrence should be taken into account when defining contraindications for spinal arthroplasty.

6.7 References

1. Anderson CL, Whitaker MC. Heterotopic Ossification Associated With Recombinant Human Bone Morphogenetic Protein-2 (Infuse) in Posterolateral Lumbar Spine Fusion. *Spine*. 2012;37:E502-E506.
2. Aunoble S, Meyrat R, Al Sawad Y, Tournier C, Leijssen P, Le Huec JC. Hybrid construct for two levels disc disease in lumbar spine. *European spine journal : official publication of the European Spine Society, the European Spinal Deformity Society, and the European Section of the Cervical Spine Research Society*. 2010;19:290-296.
3. Campbell P, Ebramzadeh E, Nelson S, Takamura K, De Smet K, Amstutz HC. Histological Features of Pseudotumor-like Tissues From Metal-on-Metal Hips. *Clinical orthopaedics and related research*. 2010;468:2321-2327.
4. Campbell P, Ma S, Yeom B, McKellop H, Schmalzried TP, Amstutz HC. Isolation of predominantly submicron-sized UHMWPE wear particles from periprosthetic tissues. *Journal of biomedical materials research*. 1995;29:127-131.
5. Choma TJ, Miranda J, Siskey R, Baxter R, Steinbeck MJ, Kurtz SM. Retrieval Analysis of a ProDisc-L Total Disc Replacement. *Journal of spinal disorders & techniques*. 2009;22:290-296.
6. Choudhry OJ, Christiano LD, Singh R, Golden BM, Liu JK. Bone morphogenetic protein-induced inflammatory cyst formation after lumbar fusion causing nerve root compression Case report. *J Neurosurg-Spine*. 2012;16:296-301.
7. Chrastil J, Patel AA. Complications Associated With Posterior and Transforaminal Lumbar Interbody Fusion. *J Am Acad Orthop Surg*. 2012;20:283-291.

8. Kurtz SM, MacDonald D, Ianuzzi A, van Ooij A, Isaza J, Ross ER, Regan J. The Natural History of Polyethylene Oxidation in Total Disc Replacement. *Spine*. 2009;34:2369-2377.
9. Kurtz SM, van Ooij A, Ross R, de Waal Malefijt J, Pelozo J, Ciccarelli L, Villarraga ML. Polyethylene wear and rim fracture in total disc arthroplasty. *Spine J*. 2007;7:12-21.
10. Kurtz SMV, M.L.; Ianuzzi, A. The clinical performance of UHMWPE in the spine. *UHMWPE Biomaterials Handbook*. Burlington, MA: Academic Press; 2009:180.
11. Lewandrowski KU, Nanson C, Calderon R. Vertebral osteolysis after posterior interbody lumbar fusion with recombinant human bone morphogenetic protein 2: a report of five cases. *The spine journal : official journal of the North American Spine Society*. 2007;7:609-614.
12. Mannion RJ, Nowitzke AM, Wood MJ. Promoting fusion in minimally invasive lumbar interbody stabilization with low-dose bone morphogenetic protein-2--but what is the cost? *The spine journal : official journal of the North American Spine Society*. 2011;11:527-533.
13. McClellan JW, Mulconrey DS, Forbes RJ, Fullmer N. Vertebral bone resorption after transforaminal lumbar interbody fusion with bone morphogenetic protein (rhBMP-2). *Journal of spinal disorders & techniques*. 2006;19:483-486.
14. McKay B, Sandhu HS. Use of recombinant human bone morphogenetic protein-2 in spinal fusion applications. *Spine*. 2002;27:S66-S85.
15. Purdue PE, Koulouvaris P, Nestor BJ, Sculco TP. The central role of wear debris in periprosthetic osteolysis. *HSS journal : the musculoskeletal journal of Hospital for Special Surgery*. 2006;2:102-113.
16. Tumialan LM, Gluf WM. Progressive Vertebral Body Osteolysis After Cervical Disc Arthroplasty. *Spine*. 2011;36:E973-E978.
17. Vaidya R, Sethi A, Bartol S, Jacobson M, Coe C, Craig JG. Complications in the Use of rhBMP-2 in PEEK Cages for Interbody Spinal Fusions. *Journal of spinal disorders & techniques*. 2008;21:557-562.
18. van Ooij A, Kurtz SM, Stessels F, Noten H, van Rhijn L. Polyethylene wear debris and long-term clinical failure of the Charite disc prosthesis: a study of 4 patients. *Spine (Phila Pa 1976)*. 2007;32:223-229.

CHAPTER 7

Conclusions & Future Directions

7.1 Conclusions

This research was conducted to evaluate the present efficacy of TDR technology by performing retrieval analyses of revised implants and periprosthetic tissues. Much of what is known about conventional or gamma-inert-sterilized metal-on-UHMWPE TDRs was originally derived from *in vitro* simulations. However, given the extensive complexity of the musculoskeletal system, there is no *in vitro* testing, simulation or analytical modeling that can truly and fully predict the performance of these implants. Furthermore, *in vivo* testing of spinal implants in animal models to assess the interactions of the living tissue environment provide limited and subjective information on implant performance, tissue-implant interface and biocompatibility due to varied anatomy, healing rates and biomechanical environments. For this reason, it is hard to overstate the importance of implant retrieval analyses of implants and tissues, as they provide unique and crucial insights of *in situ* performance, along with vital information on mechanisms of both failure and success.

Implants and their corresponding tissue retrievals from eleven patients revised for TDRs were extensively studied and documented in this body of work. Despite the small sample size, this is presently the only research (to the author's knowledge) on contemporary TDR implant and corresponding tissue retrievals. This

study has uncovered several unknown issues related to UHMWPE wear generation and subsequent biological responses in the lumbar spine. Specifically, this dissertation addressed the following broad questions: (1) Are wear particles and associated biological reactions present in tissues from patients revised for painful gamma-inert sterilized TDRs and how do design and/or biomaterials of these newer TDRs compare to each other and previous devices? (2) Are UHMWPE wear debris and particle-induced inflammation linked to implant and/or clinical factors and are both associated with the production of inflammatory factors that can potentially contribute to the development of pain in TDR patients? (3) Is there a relationship between inflammation, vascularization and innervation in the periprosthetic lumbar spine and how do these wear-debris-induced morphological changes contribute to the pathogenesis of particle disease?

To answer the first question, fixed- and mobile-bearing implant retrievals and their corresponding tissues were evaluated. Not only was this investigation itself novel, but this was the first study to identify and quantify wear debris and corresponding biological reactions in periprosthetic tissues from contemporary gamma-inert-sterilized TDRs. UHMWPE wear particles were characterized and the number, size and shape were found to affect tissue inflammatory responses. Interestingly, no association was shown between wear debris generation and the TDR designs when comparing fixed- versus mobile-bearing devices. Overall, the current generation of contemporary TDRs were found to result in reduced wear debris generation and inflammatory reactions compared to historical or gamma-air-sterilized TDRs.

Investigating the immune response to UHMWPE wear particles by evaluating immunohistochemical markers of inflammatory pain resulted in some intriguing and unexpected results. First, given that malpositioning was a concern in a couple of revision patients, implant complications such as impingement and clinical factors such as implantation time were expected to affect the extent of biological responses; however, there was no indication of this based on correlation studies with the inflammatory pain factors. Interestingly, all six inflammatory factors were expressed to a greater extent in TDR patient tissues compared to IVD tissues from patients with no history of back pain. Factors were also more highly expressed in TDR patient tissues compared to DDD patients (with non-implant related pain). Further investigation revealed the interesting finding that separating TDR tissues with and without wear debris provided distinct differences in inflammatory factor expressions. Based on this finding, TDR patient tissues were pooled and wear particle number was found to be correlated with $\text{TNF}\alpha$, $\text{IL-1}\beta$, VEGF, NGF and Substance P, but not PDGFbb. Given that macrophages have the potential to secrete all of the above factors, their numbers were quantified and also found to be correlated with the expression of these five factors. Taken together, this report was the first to show that UHMWPE wear debris and subsequent inflammation in the periprosthetic spine may lead to the production of factors that are directly associated with inflammatory pain and nociception.

These results led us to identify the potential missing links that can connect wear-debris induced inflammation to pain: vascularization and innervation. Building on the hypothesis that in-growing blood vessels are providing a conduit for

nerve fibers, it was found that all of the aforementioned inflammatory pain factors correlated with increasing numbers of blood vessels. Additionally, the innervating factors NGF and SP (which are primarily secreted by neurons) were localized to the vascular channels. Lastly, comparing blood vessel number with factor expression and macrophage number in images from tissue sections with low and high vascularity suggested the possibility of a temporal link between increased inflammatory factors, macrophages and angiogenesis. Even though this study does not provide evidence for the presence of actual nerves or pain in the discal regions, unveiling and linking wear-induced inflammation and innervation factors with associated morphological changes of increased vascularization provides an important insight in the pathology that may directly contribute to pain sensitization.

The data generated from this study provide crucial insight into the spectrum of neuroimmunological responses to UHMWPE wear debris, and help to identify biological pathways associated with pain that can be targeted to potentially prevent the need for TDR revision surgery. It is worth noting that the TDR hardware from all of the patients in this study were relatively uncompromised from a mechanical standpoint, and thus, finding ways to either minimize wear-debris generation even further and/or inhibiting wear-induced inflammatory cascades will be invaluable to the field of total disc arthroplasty to improve clinical outcomes.

7.2 Implications & Future Directions

7.2.1 Therapeutic Strategies for Treatment

A better understanding of the pathogenesis of inflammatory particle disease in the spine, provided the TDR hardware remains mechanically uncompromised, allows the potential to develop novel therapeutic strategies to inhibit and/or mitigate pain sensitization. The importance of alleviating wear-debris associated pain in TDR patients is to improve the overall longevity of TDR implants and avoid complex and high-risk revision surgical procedures. Based on the findings embodied in this dissertation, these strategies include: (1) modulation of macrophage phenotype; (2) local inhibition of TNF α ; and (3) local inhibition of VEGF.

Macrophages, like other immune cells, have various phenotypes or polarization states. As such, macrophages are involved in not only innate inflammation and adaptive immunity, but also tissue repair/regeneration. Thus, modulation of the macrophage polarization state could provide a target for therapeutic intervention of particle-disease-induced pain. In our study, the significant amounts of TNF α and IL-1 β , in conjunction with a high ratio of VEGF to PDGFBbb in TDR periprosthetic tissues, suggested that M1 macrophage pro-inflammatory responses predominated over anti-inflammatory/healing responses driven by M2 macrophages (*see Chapter 4*). A number of joint replacement studies have also reported similar findings suggesting an M1 rather than an M2 response in periprosthetic tissues [1, 3, 5-7, 14, 16, 20, 21]. Furthermore, preliminary *in vitro* and *in vivo* prospective investigations on the modulation of macrophage polarization from an M1 to an M2 response have reported favorable outcomes. Specifically, the addition of interleukin-4 (IL-4) to cultured human peripheral blood monocytes, which had been activated by wear particles, promoted macrophage

polarization from M1 to M2 and reduced the production of pro-inflammatory factors TNF α , IL-1 β and interleukin-6 (IL-6) [4, 15]. In a separate *in vitro* study, the addition of IL-4 to cultured monocytes reduced TNF- α production as the macrophage phenotype was sequentially converted from a neutral M0 phenotype to M1 and then to an M2 phenotype [10], suggesting IL-4 treatment is effective on infiltrating or activated macrophages rather than modulating resident macrophages that are neutral [13]. Consistent with *in vitro* findings, recent *in vivo* studies using rodent models to investigate particle-induced inflammation and osteolysis also showed IL-4 treatment suppressed TNF α production and attenuated bone resorption [11, 17]. While more research is certainly necessary (especially in the spine) to clearly understand macrophage polarization in regards to implant wear debris, early IL-4 studies provide evidence that it may be possible to suppress or attenuate wear-debris-induced inflammation and thus down-stream responses that lead to pain.

While the above studies showed that modulating macrophage polarization also suppresses TNF α production, this potent pro-inflammatory cytokine can serve as an attractive therapeutic target by itself in the spine. In our study, TNF α production in TDR periprosthetic tissues was integrally associated with wear-induced inflammatory pain, as it was strongly correlated with the number of wear particles, CD68+ macrophages, blood vessels and the presence of the neural innervation and hypersensitization agents, NGF and substance P (*see Chapter 4 & 5*). Furthermore, TNF α showed a progressive correlation with low and high vascularity, suggesting that it may be playing an essential role in regulating the angiogenic progression/innervation that can contribute to pain sensitization. Hence, TNF α

inhibitors or blockers may be effective in inhibiting or suppressing wear-induced inflammatory reactions that lead to pain. A number of TNF α blockers have already been cleared by the FDA and deemed effective for the treatment of rheumatoid arthritis (RA), a disease characterized by inflammation and pain. Some of the commonly used drugs that block TNF α binding to its receptor include infliximab, etanercept and adalimumab, all of which have been shown to successfully reduce inflammation in randomized double-blind placebo-controlled studies [2, 8, 18, 19]. More recently, these inhibitors have been used to decrease inflammation in a number of autoimmune diseases besides RA [12]. Given the relatively low and infrequent side effects of these drugs (compared to other immunosuppressive and cytotoxic agents) [12], future research investigating their therapeutic potential in the periprosthetic spine may be warranted.

Although inflammation is the driving force of wear-induced adverse reactions, this body of work showed vascularization is arguably the most important link that is specific to the pain-associated pathogenesis of particle disease in the lumbar spine; and thus can serve as a relatively new avenue of research for therapeutic intervention. In this regard, the angiogenic factor VEGF, like TNF α , was strongly correlated with the number of wear particles, CD68+ macrophages, blood vessels and with the presence of the neural innervation and hypersensitization agents, NGF and substance P (*see Chapter 4 & 5*). Furthermore, VEGF was not only produced by inflammatory cells including fibroblasts and macrophages, but it was also produced by endothelial cells. Hence, it can be hypothesized that VEGF inhibitors would reduce blood vessel ingrowth and presumably innervation in

periprosthetic spine tissues. Although FDA-approved VEGF inhibitors like bevacizumab have been well-established to inhibit angiogenesis in ovarian cancer [9], there is a dearth of knowledge on their use in the context of inflammatory-mediated pain, and therefore warrants future attention.

7.2.2 Cervical Total Disc Replacement

The systematic review presented in *Chapter 2* showcased current cervical retrieval studies of metal-on-polymer TDRs with fixed-bearing designs reporting similar outcomes of wear debris generation and tissue responses to lumbar TDRs. However, this was only based on five studies with very limited sample sizes and study designs; there still exists a scarcity of data to clearly understand implant wear debris generation and biological responses that are specific to the cervical spine. Interestingly, as of the time of this writing, only one lumbar, but five cervical disc artificial disc designs have been approved by the Food and Drug Administration (FDA). This raises the question of whether artificial disc replacements fare better in cervical regions. Cervical segments and discs are anatomically smaller and biomechanically experience less stresses and movements than lumbar regions [22]. Whereas, the vertebral bodies of the lumbar spine are much larger and transversely wider in order to withstand and transmit discal loads that are substantially greater than the cervical regions. For this reason, it can be hypothesized that the clinical wear performance of cervical TDRs may possibly be superior to lumbar devices. Considering that chronic neck pain can be just as debilitating as lower back pain,

extrapolating both the pitfalls and successes of lumbar TDR technology to the cervical regions could prove very valuable.

7.3 References

1. Chiba J, Rubash HE, Kim KJ, Iwaki Y. The characterization of cytokines in the interface tissue obtained from failed cementless total hip arthroplasty with and without femoral osteolysis. *Clinical orthopaedics and related research*. 1994;304-312.
2. Genta MS, Kardes H, Gabay C. Clinical evaluation of a cohort of patients with rheumatoid arthritis treated with anti-TNF-alpha in the community. *Joint, bone, spine : revue du rhumatisme*. 2006;73:51-56.
3. Hukkanen M, Corbett SA, Batten J, Konttinen YT, McCarthy ID, Maclouf J, Santavirta S, Hughes SP, Polak JM. Aseptic loosening of total hip replacement. Macrophage expression of inducible nitric oxide synthase and cyclooxygenase-2, together with peroxynitrite formation, as a possible mechanism for early prosthesis failure. *The Journal of bone and joint surgery. British volume*. 1997;79:467-474.
4. Im GI, Han JD. Suppressive effects of interleukin-4 and interleukin-10 on the production of proinflammatory cytokines induced by titanium-alloy particles. *Journal of biomedical materials research*. 2001;58:531-536.
5. Ishiguro N, Kojima T, Ito T, Saga S, Anma H, Kurokouchi K, Iwahori Y, Iwase T, Iwata H. Macrophage activation and migration in interface tissue around loosening total hip arthroplasty components. *Journal of biomedical materials research*. 1997;35:399-406.
6. Kim KJ, Rubash HE, Wilson SC, D'Antonio JA, McClain EJ. A histologic and biochemical comparison of the interface tissues in cementless and cemented hip prostheses. *Clinical orthopaedics and related research*. 1993:142-152.
7. Konttinen YT, Xu JW, Waris E, Li TF, Gomez-Barrena E, Nordsletten L, Santavirta S. Interleukin-6 in aseptic loosening of total hip replacement prostheses. *Clinical and experimental rheumatology*. 2002;20:485-490.
8. Lipsky PE, van der Heijde DM, St Clair EW, Furst DE, Breedveld FC, Kalden JR, Smolen JS, Weisman M, Emery P, Feldmann M, Harriman GR, Maini RN. Infliximab and methotrexate in the treatment of rheumatoid arthritis. Anti-Tumor Necrosis Factor Trial in Rheumatoid Arthritis with Concomitant Therapy Study Group. *The New England journal of medicine*. 2000;343:1594-1602.
9. Perren TJ, Swart AM, Pfisterer J, Ledermann JA, Pujade-Lauraine E, Kristensen G, Carey MS, Beale P, Cervantes A, Kurzeder C, du Bois A, Sehouli J, Kimmig R, Stahle A, Collinson F, Essapen S, Gourley C, Lortholary A, Selle F, Mirza MR, Leminen A, Plante M, Stark D, Qian W, Parmar MK, Oza AM. A phase 3 trial of bevacizumab in ovarian cancer. *The New England journal of medicine*. 2011;365:2484-2496.

10. Rao AJ, Gibon E, Ma T, Yao Z, Smith RL, Goodman SB. Revision joint replacement, wear particles, and macrophage polarization. *Acta biomaterialia*. 2012;8:2815-2823.
11. Rao AJ, Nich C, Dhulipala LS, Gibon E, Valladares R, Zwingenberger S, Smith RL, Goodman SB. Local effect of IL-4 delivery on polyethylene particle induced osteolysis in the murine calvarium. *Journal of biomedical materials research. Part A*. 2013;101:1926-1934.
12. Reimold AM. New indications for treatment of chronic inflammation by TNF-alpha blockade. *The American journal of the medical sciences*. 2003;325:75-92.
13. Spiller KL, Nassiri S, Witherel CE, Anfang RR, Ng J, Nakazawa KR, Yu T, Vunjak-Novakovic G. Sequential delivery of immunomodulatory cytokines to facilitate the M1-to-M2 transition of macrophages and enhance vascularization of bone scaffolds. *Biomaterials*. 2015;37:194-207.
14. Stea S, Visentin M, Granchi D, Ciapetti G, Donati ME, Sudanese A, Zanotti C, Toni A. Cytokines and osteolysis around total hip prostheses. *Cytokine*. 2000;12:1575-1579.
15. Trindade MC, Nakashima Y, Lind M, Sun DH, Goodman SB, Maloney WJ, Schurman DJ, Smith RL. Interleukin-4 inhibits granulocyte-macrophage colony-stimulating factor, interleukin-6, and tumor necrosis factor-alpha expression by human monocytes in response to polymethylmethacrylate particle challenge in vitro. *Journal of orthopaedic research : official publication of the Orthopaedic Research Society*. 1999;17:797-802.
16. Wang CT, Lin YT, Chiang BL, Lee SS, Hou SM. Over-expression of receptor activator of nuclear factor-kappaB ligand (RANKL), inflammatory cytokines, and chemokines in periprosthetic osteolysis of loosened total hip arthroplasty. *Biomaterials*. 2010;31:77-82.
17. Wang Y, Wu NN, Mou YQ, Chen L, Deng ZL. Inhibitory effects of recombinant IL-4 and recombinant IL-13 on UHMWPE-induced bone destruction in the murine air pouch model. *The Journal of surgical research*. 2013;180:e73-81.
18. Weinblatt ME, Keystone EC, Furst DE, Moreland LW, Weisman MH, Birbara CA, Teoh LA, Fischkoff SA, Chartash EK. Adalimumab, a fully human anti-tumor necrosis factor alpha monoclonal antibody, for the treatment of rheumatoid arthritis in patients taking concomitant methotrexate: the ARMADA trial. *Arthritis and rheumatism*. 2003;48:35-45.
19. Weinblatt ME, Kremer JM, Bankhurst AD, Bulpitt KJ, Fleischmann RM, Fox RI, Jackson CG, Lange M, Burge DJ. A trial of etanercept, a recombinant tumor necrosis factor receptor:Fc fusion protein, in patients with rheumatoid arthritis receiving methotrexate. *The New England journal of medicine*. 1999;340:253-259.
20. Xu JW, Konttinen YT, Lassus J, Natah S, Ceponis A, Solovieva S, Aspenberg P, Santavirta S. Tumor necrosis factor-alpha (TNF-alpha) in loosening of total hip replacement (THR). *Clinical and experimental rheumatology*. 1996;14:643-648.
21. Xu JW, Konttinen YT, Waris V, Patiala H, Sorsa T, Santavirta S. Macrophage-colony stimulating factor (M-CSF) is increased in the synovial-like membrane

- of the periprosthetic tissues in the aseptic loosening of total hip replacement (THR). *Clinical rheumatology*. 1997;16:243-248.
22. Yue JJ, Bertagnoli R, McAfee PC, Howard S. *Motion Preservation Surgery of the Spine: Advanced Techniques and Controversies*: Saunders; 2008.

Appendix

1. Relevant MATLAB Scripts

1-1. Polarized Light Input File

```

%polyprocess.m

%% Automated Selection of DAB-labeled Tissue
% By SYV

%script to segment polyethylene from background
%read the fully polarized and brightfield images
iorig = imread('filename.jpg');
ibf = imread('filename.jpg');

%part1: polarized particle masking
%select the 'blue' channel
p1 = iorig(:,:,3);

%threshold the blue channel
%note: the .2 is image dependent, seems to work ok. Range is from 0 to
1
pth = im2bw(p1,1.0);

%remove 'small objects' that are camera noise
%NOTE, 'nthresh' is camera/imaging dependent!
%When you correctly perform Black/White References, this value can be
set
%to 0.
nthresh = 00;
apth = bwareaopen(pth,nthresh);

%build new RGB image for displaying only poly particles
for i=1:3, nap(:,:,i) = uint8(apth).*iorig(:,:,i);end

%display poly segmented image
%here is your chance to change nthresh accordingly
%imshow(nap); inactivate this line to get rid of the first image

%count poly pixels (area of poly)
inap = rgb2gray(nap);
ppix = sum(sum(apth));

%part2: brightfield masking
gibf = rgb2gray(ibf);

%threshold, note: must select value, 0.75 seems to work

```

```

%the ~ inverts the image to make tissue white
gibfth = ~im2bw(gibf,.8);

%count 'tissue' pixels
tpix = sum(sum(gibfth));

%easy to compute poly vs. tissue region ratio and display result
ratiopoly = ppix / tpix;

%display poly and tissue maps
%figure,imshow(apth*29 + gibfth*61,colorcube);

[L,num] = bwlabel(apth,8);

pnum = num;

%Enable these two command lines if you want to look at original
polarized
%light an brightfield.
%figure,imshow(L);
%figure,imshow(iorig);

imwrite(L, 'filename.jpg');
imwrite(apth*29 + gibfth*61,colorcube, 'filename.jpg');

subplot(2,2,1), subimage(iorig)
subplot(2,2,2), subimage(L)
%subplot(2,2,3), subimage(ibf)
%subplot(2,2,4), subimage(apth*29 + gibfth*61,colorcube)

```

1-2. DAB Quantification Input File

```

% DAB.m

%% Automated Selection of DAB-labeled Tissue
% By SYV

close all

%% Load in images and process
files = dir('filename.jpg');
for k = 1:(numel(files))
    OrigImg=imread(files(k).name);
    % Splitting the image into R, G, and B matrices
    R=OrigImg(:,:,1); % The first page is red
    G=OrigImg(:,:,2); % The second page is green
    B=OrigImg(:,:,3); % The third page is blue
    BN=(255*((B)./(0.9*(R+G+B)))); % Normalizing (see Ref. Brey et
al.,2003); Use 80-90% RGB if tissue is over-stained; Use 90-99% B if
tissue is under-stained, but stay consistent between stains
    %BNinv=sum(255-BN,3); % Inverted image to highlight DAB-labeling

```

```

    %Save processed image
    imwrite(BN,[ 'filename.jpg' files(k).name]);
end

%% To view a processed image

%ProcImg = imread('filename.jpg');
%figure,hold on
%imshow(ProcImg);
%hold off

```

2. Relevant ImageJ Macros

2-1. Macro for Area Analysis of Transmitted Light Images

```

run("8-bit");

run("Set Scale...", "distance=3.887 known=1 pixel=1 unit=µm");

setThreshold(100, 200);

//run("Threshold...");

run("Measure");

```

2-2. Macro for Particle Analysis of Processed Polarized Light Images

```

//Run only on 20X Polarized Light Images post-Matlab.
run("8-bit");

//run("Threshold...");
setAutoThreshold("Default");
//run("Threshold...");
run("Convert to Mask");

```

//The following commands set the appropriate scales of pixels/ μm . The default distance=3.887 for 20X images. Then a second threshold is performed to prepare for the particle analysis.

```
run("Set Scale...", "distance=3.887 known=1 pixel=1 unit= $\mu\text{m}$ ");
```

```
//run("Threshold...");
```

```
setAutoThreshold("Default dark");
```

```
run("Set Measurements...", "area centroid standard perimeter fit shape area_fraction display redirect=None decimal=3");
```

//To use the right analysis, remove the "//" from the beginning of the "run" command.

```
//Line for All Particles (ECD)
```

```
run("Analyze Particles...", "size=0.2298-Infinity circularity=0.00-1.00 show=Outlines display exclude summarize");
```

```
//Line for particles less than 1  $\mu\text{m}$  (ECD)
```

```
//run("Analyze Particles...", "size=0.2298-0.785 circularity=0.00-1.00 show=Outlines display exclude summarize");
```

```
//Line for particles less between 1 and 10  $\mu\text{m}$  (ECD)
```

```
//run("Analyze Particles...", "size=0.785-78.53 circularity=0.00-1.00 show=Outlines display exclude summarize");
```

```
//Line for particles greater than 10  $\mu\text{m}$  (ECD)
```

```
//run("Analyze Particles...", "size=78.53-Infinity circularity=0.00-1.00 show=Outlines display exclude summarize");
```

III. Relevant Image-Pro Plus Macro

3-1. Macro for Automated CD68+ DAB-Stained Cells

Sub macrophage()

```
Dim x As Integer
```

```
Dim DocId As Integer
```

```
For x = 1 To 50
```

```
ret = IpDocGet(GETACTDOC, 0, DocId)
```

```
    ret = IpCmChannelExtract(CM_RGB, CM_RGB, 2)
```

```
    ret = IpBlbShow(1)
```

```
    ret = IpSegSetRange(0, 0, 100)
```

```
    ret = IpSegPreview(CURRENT_C_T)
```

```
    ret = IpBlbEnableMeas(BLBM_ROUNDNESS, 1)
```

```
    ret = IpBlbSetFilterRange(BLBM_ROUNDNESS, 0.1, 7.0)
```

```
    ret = IpBlbSetFilterRange(BLBM_AREA, 50.0, 200000.0)
```

```
    ret = IpBlbCount()
```

```
    ret = IpBlbUpdate(0)
```

```
    ret = IpBlbSplitObjects(1)
```

```
    ret = IpDcShow(1)
```

```
    ret = IpDcShow(3)
```

```
    ret = IpDcSelect("Image", "Name", 0)
```

```
    ret = IpDcSelect("Count_Size", "Count", 0)
```

```
ret = IpDcShow(1)
```

```
ret = IpDcSet(DC_AUTO, 0)
```

```
ret = IpDcUpdate(DC_FETCH)
```

```
ret = IpDocClose()
```

```
ret = IpDocCloseEx(DocId)
```

```
Next x
```

```
End Sub
```